

AWARD NUMBER: W81XWH-16-1-0566

TITLE: Polycaprolactone-collagen Composite Biomaterials for Mandible Regeneration

PRINCIPAL INVESTIGATOR: Brendan Harley

RECIPIENT: UNIVERSITY OF ILLINOIS  
URBANA, IL 61801-3649

REPORT DATE: October 2018

TYPE OF REPORT: Annual

PREPARED FOR: U.S. Army Medical Research and Materiel Command  
Fort Detrick, Maryland 21702-5012

DISTRIBUTION STATEMENT: Approved for public release; distribution is unlimited.

The views, opinions and/or findings contained in this report are those of the author(s) and should not be construed as an official Department of the Army position, policy or decision unless so designated by other documentation.

# REPORT DOCUMENTATION PAGE

*Form Approved*  
*OMB No. 0704-0188*

Public reporting burden for this collection of information is estimated to average 1 hour per response, including the time for reviewing instructions, searching existing data sources, gathering and maintaining the data needed, and completing and reviewing this collection of information. Send comments regarding this burden estimate or any other aspect of this collection of information, including suggestions for reducing this burden to Department of Defense, Washington Headquarters Services, Directorate for Information Operations and Reports (0704-0188), 1215 Jefferson Davis Highway, Suite 1204, Arlington, VA 22202-4302. Respondents should be aware that notwithstanding any other provision of law, no person shall be subject to any penalty for failing to comply with a collection of information if it does not display a currently valid OMB control number. **PLEASE DO NOT RETURN YOUR FORM TO THE ABOVE ADDRESS.**

<b>1. REPORT DATE</b> OCT 2018			<b>2. REPORT TYPE</b> Annual		<b>3. DATES COVERED</b> 30SEP2017 - 29SEP2018	
<b>4. TITLE AND SUBTITLE</b>  Polycaprolactone-collagen Composite Biomaterials for Mandible Regeneration					<b>5a. CONTRACT NUMBER</b>	
					<b>5b. GRANT NUMBER</b> W81XWH-16-1-0566	
					<b>5c. PROGRAM ELEMENT NUMBER</b>	
<b>6. AUTHOR(S)</b>  Brendan Harley  E-Mail: bharley@illinois.edu					<b>5d. PROJECT NUMBER</b>	
					<b>5e. TASK NUMBER</b>	
					<b>5f. WORK UNIT NUMBER</b>	
<b>7. PERFORMING ORGANIZATION NAME(S) AND ADDRESS(ES)</b> UNIVERSITY OF ILLINOIS GRANTS AND CONTRACTS OFFICE 506 S WRIGHT ST STE 364 URBANA, IL 61801-3649					<b>8. PERFORMING ORGANIZATION REPORT NUMBER</b>	
<b>9. SPONSORING / MONITORING AGENCY NAME(S) AND ADDRESS(ES)</b>  U.S. Army Medical Research and Materiel Command Fort Detrick, Maryland 21702-5012					<b>10. SPONSOR/MONITOR'S ACRONYM(S)</b>	
					<b>11. SPONSOR/MONITOR'S REPORT NUMBER(S)</b>	
<b>12. DISTRIBUTION / AVAILABILITY STATEMENT</b>  Approved for public release; distribution is unlimited						
<b>13. SUPPLEMENTARY NOTES</b>						
<b>14. ABSTRACT</b> Our primary objective is to demonstrate approaches to create mechanically robust, patient-customized biomaterials for large, load-bearing maxillofacial bone defects. To do this, we are developing approaches to integrate a biomolecule decorated collagen scaffold with micro-scale porosity into a mechanically-robust polymeric frame generated via 3D-printing with macro-porosity. Through the second year of this project we have completed the design, fabrication, as well as mechanical and in vitro osteogenesis testing of multiple elements of the final composite biomaterial design. We identified a PLA-collagen composite that could support robust mesenchymal stem cell (MSC) viability, osteogenic differentiation, and new mineral synthesis while rendering it shape-fitting to improve conformal contact with the wound margin. We have advanced multiple strategies to incorporate biomolecular signals into the collagen scaffold via transient sequestration, covalent attachment, and through included zinc ions that enhance osteogenic activity. Ongoing efforts are completing biomolecule incorporation and release experiments to facilitate long-term (>7 day) biomolecule bioavailability via mineral-based factor sequestration chemistries. Our efforts are essential for our goal to identify a shelf-stable, patient customizable biomaterial that can be seeded with autologous MSCs to regenerate large CMF bone defects.						
<b>15. SUBJECT TERMS</b> Biomaterial, composite, collagen, growth factor release, osteogenesis						
<b>16. SECURITY CLASSIFICATION OF:</b>				<b>17. LIMITATION OF ABSTRACT</b>	<b>18. NUMBER OF PAGES</b>	<b>19a. NAME OF RESPONSIBLE PERSON</b> USAMRMC
<b>a. REPORT</b>	<b>b. ABSTRACT</b>	<b>c. THIS PAGE</b>	<b>19b. TELEPHONE NUMBER</b> (include area code)			
Unclassified	Unclassified	Unclassified	Unclassified	87		

## Table of Contents

	<u>Page</u>
1. Introduction	4
2. Keywords	4
3. Overall Project Summary	5
4. Key Research Accomplishments	12
5. Conclusion	13
6. Publications, Abstracts, and Presentations	14
7. Inventions, Patents and Licenses	17
8. Reportable Outcomes	18
9. Other Achievements	19
10. References	20
11. Appendices	22

## **INTRODUCTION:**

Severe craniomaxillofacial (CMF) injuries are prevalent after a wide range of acute and chronic injuries, are typically large in size, and are characterized by significant loss of hard and soft tissue. Our primary objective is to demonstrate a novel approach for creating mechanically robust, patient-customized biomaterials for large, load-bearing maxillofacial bone defects. We address a fundamental bottleneck in CMF biomaterial design. Constructs must balance very real considerations regarding mechanical competence and load bearing, the need to fit complex defect geometries unique to each patient, and biotransport of nutrients within the construct during healing. To do this, we are developing approaches to integrate a biomolecule decorated collagen scaffold with micro-scale porosity into a mechanically-robust polymeric frame generated via 3D-printing with macro-porosity. We are first validating the osteogenic potential of growth factor decorated composite (Aim 1). We are evaluating the influence of composite structural properties on mesenchymal stem cell (MSC) osteogenesis in vitro and will subsequently establish whether, and to what extent, selective incorporation and release of the growth factors BMP-2/VEGF, the mineral zinc, or modifications to scaffold glycosaminoglycan (GAG) content enhances osteogenesis. Next, we will examine the quality and kinetics of mandible bone regeneration using the composite in critically-sized mandibular ramus defects in the Yorkshire pig (Aim 2). The larger goal of this program is to identify a shelf-stable, patient customizable biomaterial that can be seeded with autologous MSCs intraoperatively and immediately implanted in order to regenerate large, load-bearing CMF bone defects.

## **KEYWORDS:**

Biomaterial, composite, collagen, growth factor release, osteogenesis

## OVERALL PROJECT SUMMARY:

Through the second year of this project, we have made significant progress in addressing tasks and milestones associated with Major Tasks 1 and 2. Our efforts are on track to meet the goals of the entire research project, which are to validate the osteogenic potential of the biomolecule decorated collagen composites via tiered in vitro and in vivo assays.

### MAJOR TASK 1: Composite Fabrication

#### *The primary goals associated with Major Task 1 are:*

- Fabricate PCL cages for collagen-PCL composites
- Fabricate library of collagen-PCL composites and growth factor modified composites for in vitro testing

#### *Key Milestones associated with Major Task 1 are:*

- Biophysical characterization of mineralized collagen scaffolds and PCL-collagen composites
- Biophysical and functional characterization of growth factor loading/elution
- IACUC approval (U. Illinois) for growth factor modified collagen-PCL composites

#### *Summary of Results, Progress and Accomplishments with Discussion:*

**SUPPORTING WORK (separate from USAMRMC funding). Mineralized collagen scaffolds support MSC osteogenesis.** In work separate from this project, we have continued to refine a model CaP nanocrystallite mineralized collagen-GAG scaffold fabricated via lyophilization that promotes MSC osteogenic differentiation in the absence of osteogenic supplements (no BMP-2, osteogenic media). These efforts have focused on mechanistic investigations, where we showed these scaffolds promote osteogenesis via activation of endogenous BMP-2 receptor paths and that they promote enhanced regenerative healing of bone defects in vivo in small animal models (rabbit, rat) [1-5]. However, the compressive modulus of these scaffolds is far too low for application in CMF bone repair and necessitated the composite designs developed by this project. Further, there are opportunities to expand the scope of bone repair via the inclusion of growth factors release technologies.

**SUPPORTING WORK (From Year 1 of USMRMC funding). Composite biomaterials for CMF repair.** A significant challenge to improving the quality and speed of craniomaxillofacial bone regeneration are competing design requirements for a biomaterial platform: porosity required for cell recruitment and adequate biotransport; mechanical strength that is significantly reduced by the inclusion of pores; shape-fitting to improve conformal contact and osseointegration between the implant and the defect. Over the course of Year 1 of this funding, we developed a new class of collagen composite biomaterial. We leveraged 3D printing tools to create macro-scale poly (lactic acid) (PLA) reinforcement frames that can be integrated into the collagen suspension prior to lyophilization, resulting in a multiscale scaffold-fiber composite. A critical advance associated with this work was demonstrating an approach to render the composite shape-fitting to address an unmet clinical need: the need for close conformal contact between biomaterial implant and the surrounding wound site. We showed selective removal of circumferential fiber segments from the PLA frame could yield a composite that was deformable radially yet retained sufficient spring-back capacity to increase the required push-out force. These findings confirm that the addition of even small volume fractions (~10% v/v) of polymeric mechanical reinforcement are sufficient to increase composite mechanical strength and address

the current translational limitation of the mineralized collagen scaffold (compressive moduli < 1MPa). While the biophysical characterization was completed and reported in the Year 1 Annual Report, during Year 2 we have completed in vitro characterization of MSC osteogenic activity within these composites, with results reported under in a manuscript currently under review (Dewey et al., manuscript; Appendix) [6].

*NOTIFICATION: As a result of these findings, we have chosen a shape fitting fiber reinforcement design for future use in in vivo studies and are working to translate the fabrication of the PLA design to the original mineralized PCL chemistry.*

### **Finding 1.1. Modification of growth factor bioavailability to improve osteogenesis.**

Biomaterial implants for craniomaxillofacial bone regeneration likely require controlling bioavailability of biomolecular cues such as growth factors to promote desired cell responses. Over the past year we reported (in quarterly reports) result from a project to exploit transient interactions as a means to concentrate growth factor activity. We reported incorporation of  $\beta$ -cyclodextrin into a model collagen-GAG scaffold to passively sequester and release growth factors via guest-host interactions in order to alter mesenchymal stem cell differentiation. We incorporated  $\beta$ -cyclodextrins within the scaffold to improve sequestration as well as extend retention and release of TGF-  $\beta$ 1. We also showed extended retention and release of BMP-2 from  $\beta$ -cyclodextrin modified scaffolds was sufficient to influence the metabolic activity and proliferation of mesenchymal stem cells as well as differential activation of Smad 1/5/8 pathways associated with osteogenic differentiation. Together, this work established a defined method to incorporate and retain growth factors within collagen scaffolds via supramolecular interactions. This work has been accepted for publication during the past calendar year [7].

**Finding. 1.2. Addition of zinc sulfate into mineralized collagen scaffolds.** Efforts described during quarterly reports over the past year have reported efforts to augment the mineral content of the mineralized collagen scaffolds in this project for craniomaxillofacial bone regeneration via the inclusion of zinc ions. Zinc is an essential trace element in skeletal tissue and bone, with soluble zinc being shown to promote osteogenic differentiation of porcine adipose derived stem cells. Zinc functionalized scaffolds are fabricated by adding zinc sulfate to a mineralized collagen-glycosaminoglycan precursor suspension that is then freeze dried to form a porous biomaterial. We have completed extended biophysical and in vitro osteogenic characterization of zinc functionalized scaffolds. These scaffolds exhibit zinc release kinetics on the order of days to weeks, with ICP-MS analyses used to reveal steady release of zinc ions through 28 days in culture (37°C) into a model culture media (PBS + 1% BSA) (**Fig. 1**). Release was

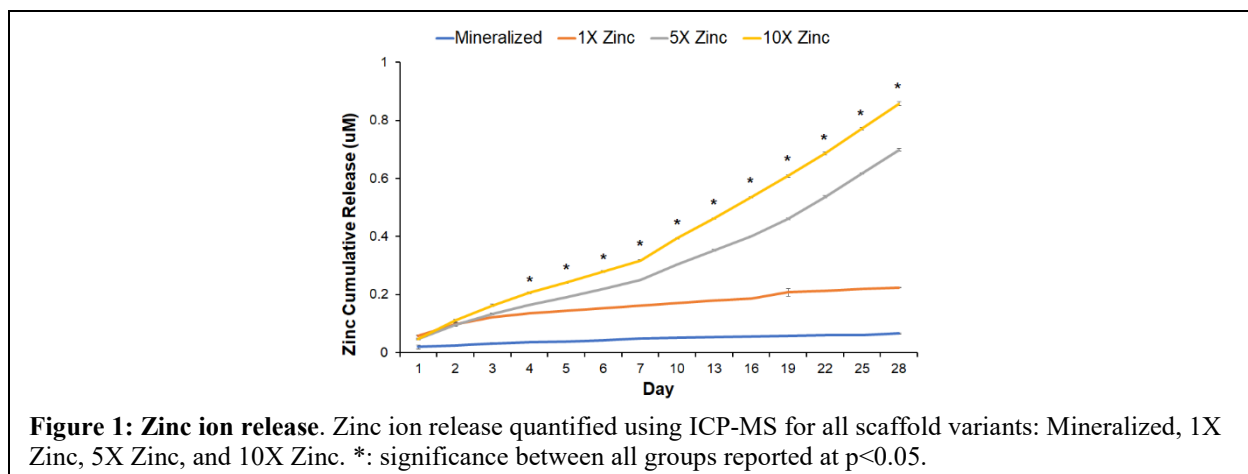


**Figure 1: Zinc ion release.** Zinc ion release quantified using ICP-MS for all scaffold variants: Mineralized, 1X Zinc, 5X Zinc, and 10X Zinc. \*: significance between all groups reported at  $p < 0.05$ .

dependent on dose of zinc incorporated into the scaffold, with significant differences between groups beginning at Day 4.

We have completed additional biophysical analysis of zinc functionalized scaffolds via imaging (SEM), mechanical testing (compression), and compositional (x-ray diffraction, inductively coupled plasma mass spectrometry analyses). Notably, zinc-functionalized scaffolds display morphological changes to the mineral phase and altered elastic modulus. Incorporation of zinc ions leads to the formation of elongated, needle-like mineral precipitates, with crystal elongation increasing with increasing concentrations of zinc sulfate added to the precursor suspension (results shown in Yr1Q4 annual report). XRD analysis of zinc functionalized scaffolds reveals patterns different from those of pure zinc sulfate, suggesting successful incorporation of zinc ions into the scaffold. Further, unit cell analysis of brushite crystals within the scaffolds revealed the brushite lattice parameters (a, b, and c) as well as the beta angle of brushite ( $\beta=116.4^\circ$ ) do not deviate with increasing amounts of zinc sulfate. Hence, zinc can be incorporated within the mineralized collagen scaffolds without substantially altering the brushite phase of the mineral component or the micro-scale pore morphology of the scaffold (**Fig. 2**).

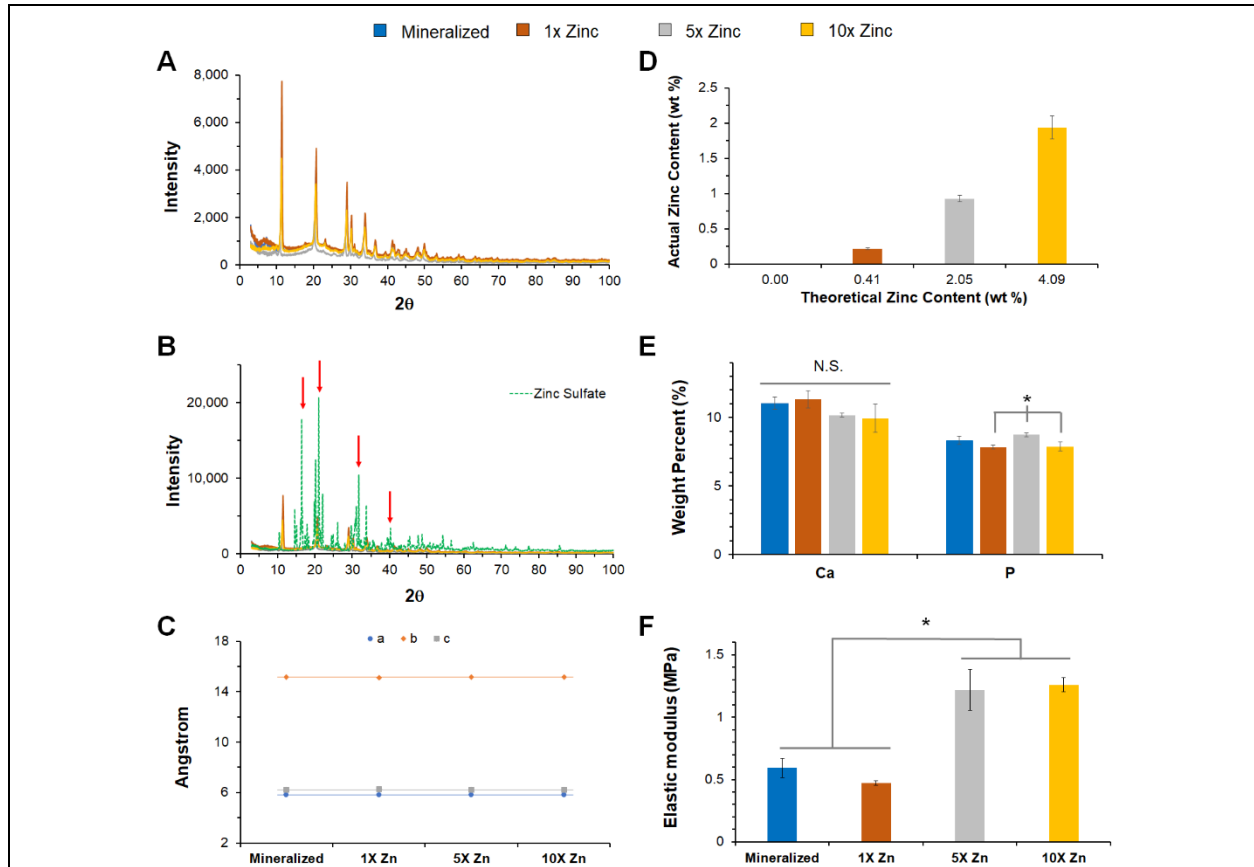


**Figure 2: Compositional and mechanical analysis of zinc-functionalized mineralized scaffolds.** (A) X-ray diffraction patterns of mineralized and zinc functionalized scaffolds indicate brushite is present in all variants. (B) X-ray diffraction data from 2A overlaid with zinc sulfate diffraction pattern. Additional peaks present in zinc sulfate are not present in zinc functionalized scaffolds (red arrows). (C) Unit cell analysis of brushite within each scaffold variant, indicating that increasing zinc concentration does not change unit cell parameters. (D) ICP-MS analysis of zinc in scaffolds. Approximately 50% of zinc added into slurry is in scaffolds. (E) ICP-OES analysis of calcium and phosphorus content in each scaffold demonstrate no relationship between inclusion of zinc and the overall amount of calcium phosphate in the scaffold. (F) Elastic modulus for each scaffold variant. \*: significance reported at  $p < 0.05$ .

Results from ongoing efforts to characterize long-term growth, osteogenic differentiation and mineral deposition/remodeling via porcine adipose derived stem cells, and activation of zinc transporters are reported later in this report (MAJOR TASK 2).

**Ongoing Work 1.3. Biomolecule retention within the mineralized collagen scaffold.** A central effort within this project is to demonstrate methods to incorporate growth factors within the collagen scaffold as a means to enhance adMSC bioactivity and osteogenic differentiation. A key challenge is the ability to control availability of growth factors over multiple time scales. Results here (Y2Q4 Finding 1.1) detailed recent efforts to employ transient incorporation of growth factors within the scaffold. These efforts parallel previous work (outside the scope of this project) where we alter scaffold GAG chemistry in non-mineralized scaffolds [8] to leverage transient interactions to enhance growth factor activity.

Our effort are also examining the impact of the immobilized growth factors on adMSC osteogenic lineage specification. We are working to expand preliminary efforts reported last year to incorporate a model growth factor (fluorescent Bovine Serum Albumin, fBSA) into the collagen scaffolds via carbodiimide crosslinking. We found ~63% of loaded fBSA was retained within the scaffold, with subsequent retention of ~77% of fBSA over 30 days in simulated culture (PBS, 37°C). However, the use of a carbodiimide crosslinker to retain growth factors within the scaffold did not lead to across the board enhanced cell response (data not shown) due to the common need for cell-receptor complexes to be internalized into the cell for activity. As a result, we are modifying these efforts to exploit the mineral phase of the mineralized collagen scaffold to retain growth factors. This effort is inspired by work using mineral coatings on nanoparticles to stabilize proteins and prolong their release and activity *in vitro* and *in vivo* [9,10]. These effort coated microparticles with a mineral layer using modified simulated body fluid (i.e. water with ions) and showed mineral coatings were able to sequester as well as maintain the conformational structure and bioactivity of bound proteins over long periods of culture (in vitro, in vivo). We hypothesize the mineral content of the mineralized collagen scaffolds provides an equivalent surface that may support extended growth factor retention and bioactivity. Those experiments are ongoing and will be reported in the subsequent quarterly reports.

## **MAJOR TASK 2: In vitro osteogenesis assays**

### ***The primary goals associated with Major Task 2 are:***

- Assess the native osteogenic potential of adMSCs within the collagen-PCL composite versus the PCL cage and collagen scaffold alone. Metrics: metabolic health, gene expression, histology, mechanics,  $\mu$ CT, bone densitometry)
- Determine the enhanced osteogenic potential of adMSCs within biomolecule modified (BMP-2, VEGF, Zinc) collagen scaffolds.
- Evaluate the effect of selective addition of growth factor sequestering chemistries (GAGs, cyclodextrin) on osteogenic activities.

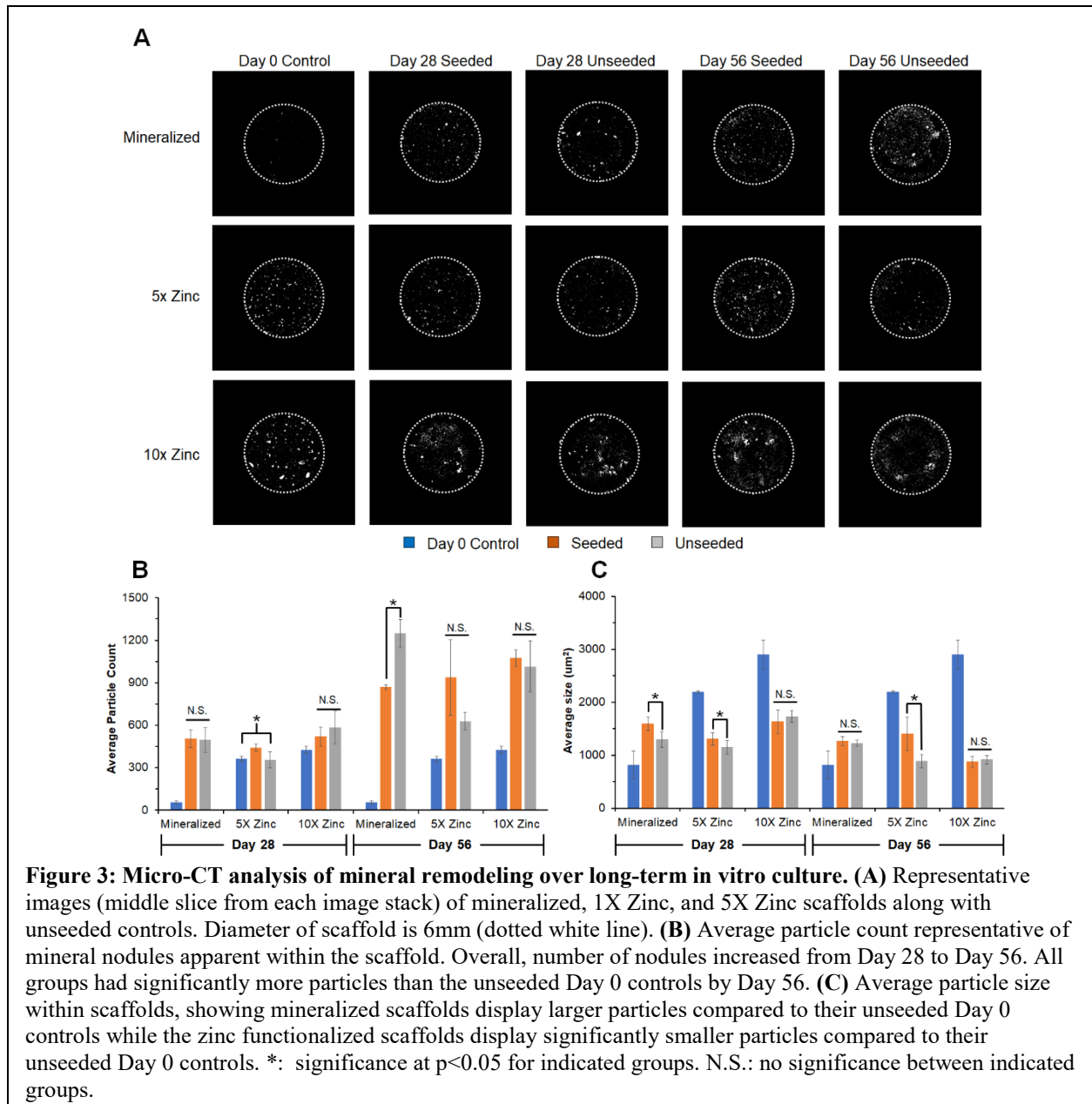
### ***Key Milestones associated with Major Task 2 are:***

- Identify the degree to which BMP-2, VEGF, and growth factor sequestering chemistries incorporated within the collagen scaffolds increase MSC osteogenic differentiation.
- Finalize design criteria for collagen-PCL composites for subsequent in vivo studies (Aim 2).

### ***Summary of Results, Progress and Accomplishments with Discussion:***

**Finding 2.1. MSC bioactivity in composite PLA-collagen biomaterials.** In addition to prior analysis of mechanical properties and conformal fitting potential of PLA-collagen scaffolds, we have also completed expanded MSC bioactivity (proliferation) and osteogenesis (gene expression patterns, matrix biosynthesis). Elements of this work have been reported during quarterly reports over the past year, but the totality of the results are included here as a manuscript now in review (Dewey et al., manuscript; Appendix) [6].

**Finding 2.2. Zinc-functionalized scaffolds support new mineral deposition.** Zinc is an important mediator of bone development and growth [11,12]. *In vitro* studies have shown that zinc ions improve stem cell osteogenesis and increase mineral deposition *in vitro* [13,14]. Recent work by Bertels *et al.* identified a critical dose range (0.04 – 0.08 mM) of zinc sulfate that when added to osteogenic media enhanced adipose derived stem cell mineral nodule formation

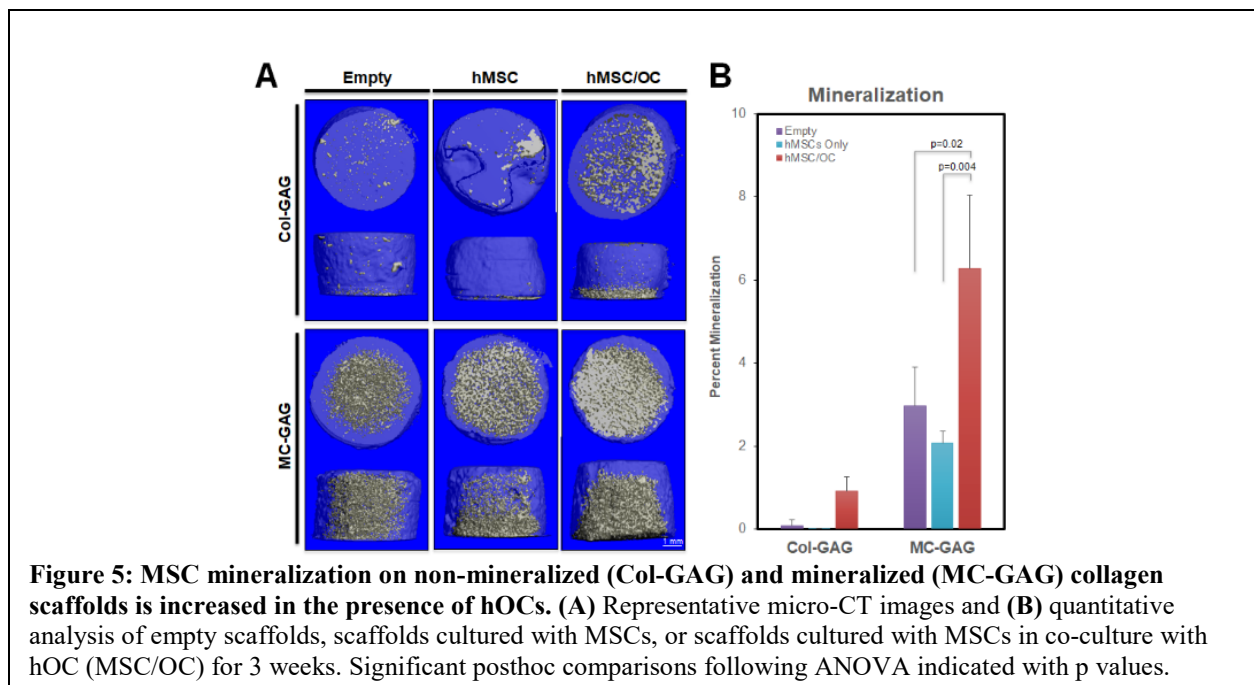


in two-dimensional culture [15]. These findings have motivated our efforts over the last project year to incorporate zinc into the mineralized collagen scaffold and evaluate adMSC osteogenesis. In previous quarterly reports (Y2Q3) we reported adMSC proliferation and metabolic health over an 8-week in vitro experiment, with adMSC-seeded zinc functionalized scaffolds maintained in growth (not osteogenic) media. All scaffolds supported adMSC proliferation and metabolic health, with the 5X Zinc variant showing the greatest adMSC expansion and highest metabolic activity by Day 56.

We have now completed evaluation of the extent of mineral remodeling in adMSC seeded scaffolds over the course of the 56-day in vitro experiment (**Fig. 3**). The mineral content of mineralized collagen vs. zinc-functionalized mineralized collagen scaffolds was assessed via micro-computed tomography (Zeiss MicroXCT-400; Oberkochen, Germany), with analyses comparing new mineral formation in cell-seeded scaffolds to unseeded controls. New mineral formation was evaluated as the number and size of mineral formations (particles) observed within the scaffold microstructure with time. All scaffold variants displayed more mineral particles at Day 28 and 56 compared to Day 0 controls (except for 5X Day 28 unseeded group), suggesting significant mineral remodeling is taking place. We observed significantly more mineral particles present in all scaffolds at Day 56 vs. to 28, showing mineral deposition over time. Further, 5X and 10X Zinc scaffolds contained more particles than unseeded controls by Day 56, though the particles were significantly smaller compared to Day 0 controls. This suggests that zinc functionalized mineralized collagen scaffolds support robust mineral remodeling within the mineralized scaffolds.

Ongoing analyses are examining zinc transporter signaling pathways as a means to explore potential routes by which zinc functionalized scaffolds enhance adMSC proliferation and metabolic health.

**Finding 2.3. Mineralized collagen scaffolds alter osteoclast activity.** A major effort in this project has been validating the osteogenic potential of mineralized collagen-GAG scaffolds. To complement efforts that have focused primarily on MSC osteogenesis, we have begun to



examine interactions between these scaffolds and primary human osteoclasts (hOCs) responsible for bone resorption. While components of the extracellular matrix are known to direct changes in osteoclast activity, the role of the mineralized scaffold on OC activity have been largely unknown but may offer the opportunity to address large CMF bone defects. We are therefore evaluating mineralization events for MSC seeded scaffolds undergoing osteogenic differentiation in the presence of primary human osteoclasts (hOCs). Empty scaffolds, scaffolds seeded with MSCs, or co-cultures with MSCs on scaffolds in Transwell inserts with hOCs in the lower chamber were evaluated with micro-CT after 3 weeks of culture in osteogenic (10 mM  $\beta$ -glycerophosphate, 50  $\mu$ g/mL ascorbic acid, and 0.1  $\mu$ M dexamethasone) and osteoclastogenic (Osteoclast Precursor Basal Medium, Lonza, supplemented with 33 ng/mL macrophage-colony stimulating factor, 66 ng/mL RANKL, 10 mM  $\beta$ -glycerophosphate, 50  $\mu$ g/mL ascorbic acid, 0.1  $\mu$ M dexamethasone) differentiation media. Preliminary data suggest a significant increase in new mineral formation in mineralized collagen scaffolds in the presence of hOCs (**Fig. 4**). These effects are not as robustly observed for cultures in non-mineralized collagen scaffolds. These data suggest that hOCs may increase MSC osteogenic differentiation in mineralized scaffolds via soluble factors in a paracrine fashion, suggesting opportunities to identify these factors and then deliver them from the scaffold via the soluble factor immobilization, sequestration, and release strategies developed during this project to further accelerate CMF bone healing.

**Ongoing Work 2.4. Modification of the organic phase of the mineralized collagen scaffold via amniotic membrane matrix.** The goal of this project is to develop degradable biomaterials that actively instruct, rather than passively permit, MSC osteogenic differentiation and subsequent bone regeneration. However, the severity of host inflammatory response post-injury can severely limit implant osseointegration and regenerative healing. As a result, there is an unmet clinical need for biomaterials that promote MSC osteogenic differentiation but also modulate the host inflammatory response following injury. The amniotic membrane (AM) is an allograft tissue with immunomodulatory and anti-scarring properties underutilized in tissue engineering [16,17]. We showed modifying the organic phase of non-mineralized collagen scaffold via incorporation of AM-matrix could alter the inflammatory phenotype of MSCs and macrophages (M $\phi$ ) exposed to inflammatory biomolecules [18]. We are testing the hypothesis a mineralized collagen-AM composite will improve osseointegrative activity via immunomodulatory effects, with ongoing experiments examining MSC osteogenesis and macrophage polarization in the mineralized collagen scaffolds as a function of AM matrix incorporation.

## KEY RESEARCH ACCOMPLISHMENTS (cumulative):

- Demonstrating multi-scale composite reinforcement paradigm for mineralized collagen scaffolds to address acute clinical needs for biomaterials with improved macro-scale compressive strength and conformal fitting within the defect margins [6].
- Confirming incorporation of a polymeric reinforcement frame does not negatively influence the osteogenic capabilities of porcine adipose stem cells within the multi-scale composite.
  - NOTE: This finding extends beyond previous publications that examined the activity of human and rabbit bone marrow derived MSCs in the mineralized collagen scaffold alone [1,3] or that only confirmed adMSC viability in one design variant of a collagen-PCL composite [19].
- Developing and characterizing a novel zinc-functionalized variant of the mineralized collagen scaffold at the core of this CMF bone regeneration project. We confirmed zinc can be incorporated into and released from the scaffold microstructure. We showed incorporation of zinc improved scaffold mechanical properties, and that while zinc incorporation alters microscale mineral morphology of the scaffold it does not affect the Brushite phase of the calcium phosphate deposits. We showed zinc-functionalized scaffolds accelerate adMSC proliferation and metabolic health while maintaining osteogenic differentiation and mineral deposition capacity [20].
- We demonstrated the use of cyclodextrin-based transient sequestration of growth factors within the scaffold could enhance BMP-2 mediated osteogenic differentiation [7]. While short term growth factor retention may accelerate cell recruitment, cyclodextrin studies are now motivating current exploration of mineral-linked growth factor retention as an alternative means to delivery growth factors within the collagen scaffold.
- In addition to long standing analysis of MSC-osteogenesis within mineralized collagen scaffolds, we have showed the mineralized collagen scaffold may also alter activity of osteoclasts, and motivates ongoing efforts to better investigate scaffold-osteoclast-MSC interactions in the context of matrix remodeling.

## **CONCLUSION:**

Successful biomaterial implants to improve regenerative healing must meet a number of design requirements that are often in conflict with each other. They must be biocompatible, meet micro-scale mechanical needs to promote osteogenesis as well as macro-scale requirements for a mechanically robust implant, be bioresorbable, and conformal fitting within irregular defects to improve osseointegration. Through the second year of this project we have completed the design, fabrication, as well as mechanical and in vitro osteogenesis testing of a conformal fitting mineralized composite for CMF defect repair applications. We have demonstrated multiple means to incorporate and release growth factors from the scaffold. And we have shown incorporation of zinc ions into the scaffold mineral phase is a powerful stimulus to increase MSC proliferation and metabolic health. The ability to increase close contact between the biomaterial implant and the host bone as well as incorporate pro-osteogenic factors (i.e., zinc) is particularly important for improving cell recruitment and subsequent osseointegration between host and implant. Ongoing efforts are completing mineral-based sequestration of growth factors and evaluating the resultant change in MSC activity in biomolecule and mineral (VEGF, BMP-2, zinc) decorated collagen scaffolds.

Data and intellectual property generated during the course of this period will be critical for future translation events. As a result we have submitted two intellectual property disclosures to campus. We expect this work to generate significant enthusiasm in the regenerative medicine and biomaterials community regarding a new paradigm for orthogonally manipulating multiple design criteria to create biomaterials for large, load bearing craniofacial defects. Impact will be primarily in basic sciences associated with the design of regenerative biomaterials.

## **PUBLICATIONS, ABSTRACTS, AND PRESENTATIONS:**

### **a. List all manuscripts submitted for publication during the period covered by this report resulting from this project.**

#### **(1) Lay Press:**

Nothing to report

#### **(2) Peer-Reviewed Scientific Journals:**

Accepted/Published:

W.K. Grier\*, A.S. Tiffany\*, M.D. Ramsey, B.A.C. Harley, 'Incorporating  $\beta$ -cyclodextrin into collagen scaffolds to sequester growth factors and modulate MSC activity,' *Acta Biomater.*, 76:116-25, 2018. \* co-first authors.

Under review/revision

M.J. Dewey, E.M. Johnson, D.W. Weisgerber, M.B. Wheeler, B.A.C. Harley, 'Shape-fitting collagen-PLA composite promotes osteogenic differentiation of porcine adipose stem cells,' in review, *J. Mech. Behav. Biomed. Mater.*, 2018.

In preparation

X. Ren, Q. Zhou, D. Foulad, M.J. Dewey, T.A. Miller, D.T. Yamaguchi, D. Bischoff, B.A.C. Harley, J.C. Lee, 'Nanoparticulate mineralized collagen glycosaminoglycan materials alter osteoclast activation in the presence of mesenchymal stem cells,' in preparation, 2018.

A.S. Tiffany, D.L. Gray, T.J. Woods, K. Subedi, B.A.C. Harley, 'The inclusion of zinc into mineralized collagen scaffolds for craniofacial bone repair applications,' in preparation, 2018.

#### **(3) Invited Articles:**

Nothing to report

#### **(4) Abstracts:**

M. Dewey (poster and podium), E. Johnson, D. Weisgerber, M. Wheeler, B. A. C. Harley. 'Shape-fitting Mineralized Collagen-PLA Composite for Craniomaxillofacial Bone Regeneration,' *Society for Biomaterials Conference*, 2018, Atlanta, GA.

A. Tiffany (poster), B. Harley, 'Additive effects of biomolecular supplementation in mineralized collagen scaffolds for bone regeneration,' *Society for Biomaterials Annual Meeting*, 2018, Atlanta, GA.

M. Dewey (poster), E. Johnson, D. Weisgerber, S. Slater, M. Wheeler, B. A. C. Harley. 'Addition of shape-fitting poly(lactic acid) mechanical supports and immunomodulatory amniotic membrane to enhance mineralized collagen scaffolds for craniofacial bone repair,' *Musculoskeletal Biology and Bioengineering Gordon Research Conference*, 2018, Andover, NH.

R.A. Sun Han Chang (poster and GRS podium), C.-W. Lee, S. Rogers, B.A.C. Harley, 'Triphasic biomaterial for enhanced toughness and regenerative healing of the osteotendinous junction,' *Musculoskeletal Biology and Bioengineering Gordon Research Conference*, 2018, Andover, NH.

A. Tiffany, M. Dewey, D. Milner, M. Wheeler, B. Harley (poster), 'Fiber-reinforced collagen scaffold for craniomaxillofacial regeneration,' 2018 Military Health System Research

Symposium, Orlando, FL.

M. Dewey, E. Johnson, S. Slater, D. Slater, B. A. C. Harley. 'The Addition of the Amniotic Membrane to Mineralized Collagen Scaffolds for Immunomodulatory Bone Regeneration,' Submitted, *Society for Biomaterials Annual Meeting*, 2019, Seattle, WA.

R.A. Sun Han Chang, C.-W. Lee, S. Rogers, B.A.C. Harley, 'Biomimetic triphasic scaffolds for osteotendinous junction regeneration,' Submitted, *Society for Biomaterials Annual Meeting*, 2019, Seattle, WA.

**b. List presentations made during the last year (international, national, local societies, military meetings, etc.).**

B.A.C. Harley, 'A composite biomaterial for osteotendinous insertion repair,' TERMIS-AM Annual Meeting, Charlotte, NC, 12/2017.

B.A.C. Harley, '*Engineering the niche – biomaterials for tissue engineering*,' Lehigh University, Depts. of Materials Science & Engineering and Bioengineering, 1/2018.

B.A.C. Harley, '*Engineering complexity via biomaterial design*,' Duke University, Depts. of Biomedical Engineering and Orthopaedic Surgery, 2/2018.

B.A.C. Harley, '*Engineering complexity via biomaterial design*,' Harvard University, School of Engineering and Applied Sciences, 2/2018.

B.A.C. Harley, '*Engineering complexity via biomaterial design*,' Keynote, 5th International Conference on Cellular and Molecular Bioengineering, Nanyang Technological University, Singapore, 3/2018.

B.A.C. Harley, '*Engineering complexity via biomaterial design*,' University of Massachusetts at Amherst, Dept. of Chemical Engineering, 3/2018.

M. Dewey (poster and podium), E. Johnson, D. Weisgerber, M. Wheeler, B. A. C. Harley. 'Shape-fitting Mineralized Collagen-PLA Composite for Craniomaxillofacial Bone Regeneration,' *Society for Biomaterials Conference*, 2018, Atlanta, GA.

A. Tiffany (poster), B. Harley, 'Additive effects of biomolecular supplementation in mineralized collagen scaffolds for bone regeneration,' *Society for Biomaterials Annual Meeting*, 2018, Atlanta, GA.

B.A.C. Harley, '*Engineering complexity via biomaterial design*,' Rensselaer Polytechnic Institute, Dept. of Biomedical Engineering, 4/2018.

B.A.C. Harley, '*Dynamic remodeling of a biomaterial niche alters hematopoietic stem cell lineage specification*,' Keynote: Bone Marrow Properties and Mechanobiology symposium, World Congress of Biomechanics, Dublin, Ireland, 6/2018.

B.A.C. Harley, '*Biomaterial motifs to address complexity in regenerative medicine*,' National Academy of Science, Forum on Regenerative Medicine, Washington, DC, 10/2018.

M. Dewey (poster), E. Johnson, D. Weisgerber, S. Slater, M. Wheeler, B. A. C. Harley. 'Addition

of shape-fitting poly(lactic acid) mechanical supports and immunomodulatory amniotic membrane to enhance mineralized collagen scaffolds for craniofacial bone repair,' *Musculoskeletal Biology and Bioengineering Gordon Research Conference*, 2018, Andover, NH.

R.A. Sun Han Chang (poster and GRS podium), C.-W. Lee, S. Rogers, B.A.C. Harley, 'Triphasic biomaterial for enhanced toughness and regenerative healing of the osteotendinous junction,' *Musculoskeletal Biology and Bioengineering Gordon Research Conference*, 2018, Andover, NH.

A. Tiffany, M. Dewey, D. Milner, M. Wheeler, B. Harley (poster), 'Fiber-reinforced collagen scaffold for craniomaxillofacial regeneration,' 2018 Military Health System Research Symposium, Orlando, FL.

B.A.C. Harley, '*Engineering complexity via biomaterial design*,' Brown University, Dept. of Biomedical Engineering, 10/2018.

## **INVENTIONS, PATENTS AND LICENSES:**

Marley Dewey, Brendan Harley, Daniel Weisgerber, 'Adaptable PLA fiber reinforcement for conformal fitting,' submitted, Nov. 2017.

Marley Dewey, Brendan Harley, Rebecca Hortensius, Simona Slater, 'Mineralized Collagen Scaffolds combined with the Amniotic Membrane derived from placentas to address inflammation in Craniomaxillofacial Bone Regeneration,' submitted, July, 2018.

## REPORTABLE OUTCOMES:

**Multiscale composite supports adMSC osteogenesis.** We have integrated a millimeter-scale reinforcing poly(lactic acid) (PLA) frame fabricated via 3D-printing into the mineralized collagen scaffold to form a multi-scale mineralized collagen-PLA composite. We have described modifications to the PLA frame design to increase the compressive strength (Young's Modulus, ultimate stress and strain). We also developed modifications to the frame architecture to render the composite with increased compressive strength in one axis but radial compressibility and conformal fitting capabilities in an orthogonal axis. We completed *in vitro* comparison of the bioactivity of porcine adipose derived stem cells (adMSCs) in the composite versus the mineralized collagen scaffold. We found incorporation of the reinforcing frame does not negatively influence the bioactivity and osseoinductive nature of the mineralized collagen scaffold. These findings represent the first key element of this project, a composite design to address competing bioactivity, mechanical strength, and shape-fitting design requirements for biomaterials for craniomaxillofacial bone regeneration.

**Inclusion of zinc ions into mineralized collagen scaffolds.** We have integrated zinc ions into the mineralized collagen scaffold. We have described biophysical properties (porosity, mechanics, mineral content) of the resultant scaffolds. We showed inclusion of zinc accelerated MSC proliferation and metabolic activity. We showed inclusion of zinc does not negatively influence osteogenic differentiation or mineral biosynthesis *in vitro*. These findings represent a key biomolecular adaptation of the mineralized scaffold with the goal of improving craniomaxillofacial bone regeneration.

**Alteration of growth factor bioavailability via cyclodextrin chemistry.** We have used cyclodextrin functionalized collagen scaffolds as a means to exploit the passive sequestration and release of growth factors (TGF- $\beta$ 1 and BMP-2) via guest-host interactions to control mesenchymal stem cell differentiation. BMP-2 sequestrations confers pro-osteogenic advantages for the scaffold. we report the incorporation of  $\beta$ -cyclodextrin into a model collagen-GAG scaffold. These findings suggest a design framework to selectively alter the bioavailability of multiple biomolecules within a three-dimensional collagen-GAG scaffold to intensify cell response to exogenously added or endogenously produced growth factors for a range of musculoskeletal regenerative medicine applications.

### Future reportable outcomes:

1. Expansion of studies of MSC-osteoclast activity and the role of scaffold microstructure in mediating these interactions.
2. Completion of mineral based growth factor tethering and release studies, followed by *in vitro* adMSC bioactivity and osteogenesis in response to incorporated BMP-2 and VEGF
3. Initiation and completion of tiered *in vivo* craniomaxillofacial bone regeneration studies

**OTHER ACHIEVEMENTS:**

**Degrees obtained by personnel supported by this award:**

Nothing to report this year.

**Fellowships awarded to personnel supported by this award:**

Marley Dewey

National Science Foundation Graduate Research Fellowship, 2018 – 2021.

**Additional honors awarded to personnel supported by this award:**

Marley Dewey

2018 STAR award (top 10% of all trainee abstracts), Orthopaedic Biomaterials Special Interest Group (SIG), Society for Biomaterials 2018 Annual Meeting.

2018 Dow Chemical Soft Materials Seminar Silver Medal, Dept. of Materials Science and Engineering, University of Illinois.

Raul Sun Han Chang

Invited oral presentation, Musculoskeletal Biology and Bioengineering Gordon Research Seminar, (Proctor Academy, NH).

## REFERENCES:

1. Weisgerber DW, Caliarì SR, Harley BAC, Mineralized collagen scaffolds induce hMSC osteogenesis and matrix remodeling. *Biomater Sci*, 3(3):533-42, 2015.
2. Lee JC, Pereira CT, Ren X, Huang W, Weisgerber DW, Yamaguchi DT, Harley BAC, Miller TA, Optimizing collagen scaffolds for bone engineering: effects of crosslinking and mineral content on structural contraction and osteogenesis. *J Craniofac Surg*, 26(6):1992-6, 2015.
3. Ren X, Bischoff D, Weisgerber DW, Lewis MS, Tu V, Yamaguchi DT, Miller TA, Harley BA, Lee JC, Osteogenesis on nanoparticulate mineralized collagen scaffolds via autogenous activation of the canonical BMP receptor signaling pathway. *Biomaterials*, 50:107-14, 2015.
4. Caliarì SR, Harley BAC, Structural and biochemical modification of a collagen scaffold to selectively enhance MSC tenogenic, chondrogenic, and osteogenic differentiation. *Adv Healthc Mater*, 3(7):1086-96, 2014.
5. Ren X, Tu V, Bischoff D, Weisgerber DW, Lewis MS, Yamaguchi DT, Miller TA, Harley BAC, Lee JC, Nanoparticulate mineralized collagen scaffolds induce in vivo bone regeneration independent of progenitor cell loading or exogenous growth factor stimulation. *Biomaterials*, 89:67-78, 2016.
6. Dewey MJ, Johnson EM, Weisgerber DW, Wheeler MB, Harley BAC, Shape-fitting collagen-PLA composite promotes osteogenic differentiation of porcine adipose stem cells. *J Mech Behav Biomed Mater*, in review 2018.
7. Grier WK, Tiffany AS, Ramsey MD, Harley BAC, Incorporating  $\beta$ -cyclodextrin into collagen scaffolds to sequester growth factors and modulate mesenchymal stem cell activity. *Acta Biomaterialia*, 76:116-125, 2018.
8. Hortensius RA, Harley BA, The use of bioinspired alterations in the glycosaminoglycan content of collagen-GAG scaffolds to regulate cell activity. *Biomaterials*, 34(31):7645-52, 2013.
9. Clements AEB, Leiferman EM, Chamberlain CS, Vanderby R, Murphy WL, Addition of Mineral-Coated Microparticles to Soluble Interleukin-1 Receptor Antagonist Injected Subcutaneously Improves and Extends Systemic Interleukin-1 Inhibition. 1(7):1800048, 2018.
10. Yu X, Biedrzycki AH, Khalil AS, Hess D, Umhoefer JM, Markel MD, Murphy WL, Nanostructured Mineral Coatings Stabilize Proteins for Therapeutic Delivery. 29(33):1701255, 2017.
11. Hojyo S, Fukada T, Shimoda S, Ohashi W, Bin BH, Koseki H, Hirano T, The zinc transporter SLC39A14/ZIP14 controls G-protein coupled receptor-mediated signaling required for systemic growth. *PLoS One*, 6(3):e18059, 2011.
12. Prasad AS SA, Miale A Jr, Farid Z, Sandstead HH., Zinc and Iron Deficiencies in Male Subjects with Dwarfism and Hypogonadism but Without Ancylostomiasis, Schistosomiasis or Severe Anemia. *American Journal of Clinical Nutrition*, 12:8, 1963.
13. Yusa K, Yamamoto O, Iino M, Takano H, Fukuda M, Qiao Z, Sugiyama T, Eluted zinc ions stimulate osteoblast differentiation and mineralization in human dental pulp stem cells for bone tissue engineering. *Arch Oral Biol*, 71:162-169, 2016.
14. An S, Gong Q, Huang Y, Promotive Effect of Zinc Ions on the Vitality, Migration, and Osteogenic Differentiation of Human Dental Pulp Cells. *Biol Trace Elem Res*, 175(1):112-121, 2017.
15. Bertels JC, Rubessa M, Schreiber SR, Wheeler MB, The effect of zinc on the differentiation of adipose-derived stem cells into osteoblasts. *Reprod Fertil Dev*, 29(1):207, 2016.
16. Kubo M, Sonoda Y, Muramatsu R, Usui M, Immunogenicity of human amniotic membrane in experimental xenotransplantation. *Invest Ophthalmol Vis Sci*, 42(7):1539-1546, 2001.

17. Niknejad H, Peirovi H, Jorjani M, Ahmadiani A, Ghanavi J, Seifalian AM, Properties of the amniotic membrane for potential use in tissue engineering. *Eur Cell Mater*, 15:88-99, 2008.
18. Hortensius RA, Ebens JH, Dewey MJ, Harley BAC, Incorporation of amniotic membrane as an immunomodulatory design element in collagen scaffolds for tendon repair. *ACS Biomater Sci Eng*, 4(12):4367-77, 2018.
19. Weisgerber DW, Erning K, Flanagan C, Hollister SJ, Harley BAC, Evaluation of multi-scale mineralized collagen-polycaprolactone composites for bone tissue engineering. *J Mech Behav Biomed Mater*, 61:318-327, 2016.
20. Tiffany AS, Gray DL, Woods TJ, Subedi K, Harley BAC, The inclusion of zinc into mineralized collagen scaffolds for craniofacial bone repair applications. in preparation, 2018.

## **APPENDICES:**

Please find appended original copies of the following work:

### ***Quad Chart:***

Year 2 Quarter 4 Quad Chart

### ***Abstracts:***

The Addition of the Amniotic Membrane to Mineralized Collagen Scaffolds for Immunomodulatory Bone Regeneration

Marley J. Dewey, Eileen M. Johnson, Simona Slater, Brendan A.C. Harley  
Society for Biomaterials Annual Conference, 2019, Seattle, WA (submitted).

Biomimetic triphasic scaffolds for osteotendinous junction regeneration

Raul A. Sun Han Chang, Ching-Wei Lee, Simon Rogers, Brendan A.C. Harley  
Society for Biomaterials Annual Conference, 2019, Seattle, WA (submitted).

### ***Campus intellectual property disclosures applications:***

Marley Dewey, Brendan Harley, Daniel Weisgerber, 'Adaptable PLA fiber reinforcement for conformal fitting,' submitted, Nov. 2017.

Marley Dewey, Brendan Harley, Rebecca Hortensius, Simona Slater, 'Mineralized Collagen Scaffolds combined with the Amniotic Membrane derived from placentas to address inflammation in Craniomaxillofacial Bone Regeneration,' submitted, July, 2018.

### ***Peer-Reviewed Scientific Journals:***

W.K. Grier\*, A.S. Tiffany\*, M.D. Ramsey, B.A.C. Harley, 'Incorporating  $\beta$ -cyclodextrin into collagen scaffolds to sequester growth factors and modulate MSC activity,' Acta Biomater., 76:116-25, 2018. \* co-first authors.

M.J. Dewey, E.M. Johnson, D.W. Weisgerber, M.B. Wheeler, B.A.C. Harley, 'Shape-fitting collagen-PLA composite promotes osteogenic differentiation of porcine adipose stem cells,' in review, J. Mech. Behav. Biomed. Mater., 2018.

# Polycaprolactone-collagen composite biomaterials for mandible regeneration

USAMRMC 1464004

W81XWH-16-1-0566



PI: **Brendan Harley**

Org: University of Illinois at Urbana-Champaign

Award Amount: \$800,000

## Study/Product Aim(s)

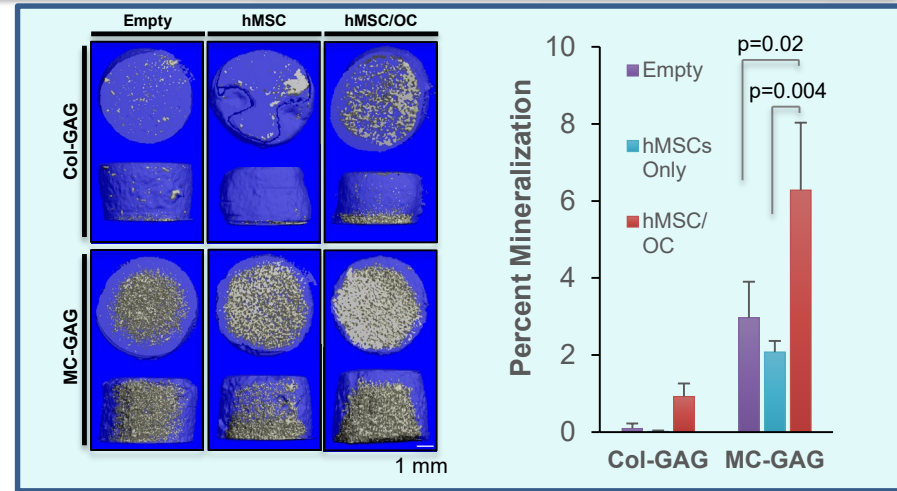
Our goal is to demonstrate that integrating a mineralized collagen scaffold within a macroporous PCL construct will generate a multi-scale composite that enhances adipose-derived MSC osteogenesis and subsequent bone regeneration. Our aims:

**Aim 1:** Validate the osteogenic potential of growth factor decorated collagen-PCL composites.

**Aim 2:** Examine the quality and kinetics of mandible bone regeneration using the collagen-PCL composite.

## Approach

We a polycaprolactone (PCL) support cage into a mineralized collagen scaffold to form a PCL-collagen composite. We will define the improvement in adipose-derived mesenchymal stem cell osteogenesis in response to the release of growth factors (BMP-2 and VEGF) from the collagen scaffold, as well as regenerative potential of the growth factor decorated collagen-PCL composite in a porcine model of mandibular defect.



**Accomplishments:** We have validated a multi-scale polymer-scaffold composite with enhanced strength and shape-fitting capabilities, showed inclusion of zinc ions enhances bioactivity, identified methods for growth factor retention, and identified MSC-osteoclast (OC) crosstalk as an avenue by which the mineralized scaffold improves osteogenic activity.

## Timeline and Cost

Activities	CY	16	17	18	19
Fabrication, biophysical characterization of growth-factor decorated collagen-PCL composites					
In vitro osteogenic activity of growth-factor decorated collagen-PCL composites					
Determine kinetics of mandibular healing via growth-factor decorated collagen-PCL composites					
Define improved quality of mandibular healing using growth-factor decorated collagen-PCL composites					
<b>Estimated Budget (\$K)</b>		<b>\$30k</b>	<b>\$200k</b>	<b>\$340k</b>	<b>\$230k</b>

## Goals/Milestones

**CY16 Goal** – Collagen-PCL composite fabrication

- Fabricate initial library of collagen-PCL composites
- Finalize campus IACUC approval for growth factor modified composites

**CY17 Goal** – In vitro osteogenesis assessment

- Biophysical characterization of composites
- Define growth factor elution from collagen-PCL composites

**CY18 Goal** – In vivo bone regeneration assays

- Quantify degree of enhanced osteogenic potential of adMSCs within BMP-2 and VEGF decorated collagen-PCL composites
- Finalize design criteria for collagen-PCL composites for *in vivo* implantation and initiate subcritical and critical defect models

**CY19 Goal** – Quantify quality and kinetics of mandible regeneration

- Identify collagen-PCL variant that displays the highest quality of mandibular bone repair.

## Comments/Challenges/Issues/Concerns

- No concerns.

## Budget Expenditure to Date

Projected Expenditure: \$485,000

Actual Expenditure: \$454,125.38

Updated: 20 October 2018

# The Addition of the Amniotic Membrane to Mineralized Collagen Scaffolds for Immunomodulatory Bone Regeneration

Marley J. Dewey, Eileen M. Johnson, Simona Slater, Brendan A.C. Harley  
University of Illinois at Urbana-Champaign

**Statement of Purpose:** Cranio-maxillofacial (CMF) defects often are comprised of critical sized bone defects that will not heal without surgical intervention. Examples of CMF defects extend from birth defects, to post-oncologic treatment and high-energy impacts, with billions spent on repair. Due to the overwhelmingly large portion of bone missing in these defects, there is a high chance for infection and a high probability of chronic inflammation occurring. This leaves a crucial niche for developing a bone regenerative material that can modulate the immune response to aid healing. Efforts in our lab have recently developed a mineralized collagen-GAG scaffold to induce MSC osteogenic differentiation and CMF bone regeneration in the absence of traditional pro-osteogenic signals [1]. Here we describe the incorporation of the amniotic membrane, known for its anti-inflammatory, anti-scarring, and anti-microbial properties, into mineralized collagen scaffolds for immunomodulatory applications. We examine the mechanical properties and pore size upon the addition of the amniotic membrane, as well as the response of porcine adipose derived stem cells (pASCs) seeded on these scaffolds in both normal media and high inflammatory media. We evaluate the metabolic activity, cell number, gene expression, protein activity, and mineralization of these scaffolds *in vitro*. Current work explores the bacterial response on the amniotic membrane and macrophage polarization.

**Methods:** Amniotic membranes were obtained from a collaboration with Carle Foundation Hospital Tissue Repository (Urbana, IL) after having met uncomplicated vaginal birth standards [2]. Mineralized collagen scaffolds and mineralized collagen-amnion scaffolds were fabricated by lyophilizing a mineralized collagen-GAG precursor suspension [3]. Mechanical compression testing was performed with an Instron 5943 mechanical tester. Pore size was evaluated via stereology from histology sections [4]. *In vitro* testing employed scaffolds seeded with pASCs for up to 28 days in normal growth media and inflammatory media (supplemented with 1ng/mL of IL-1 $\beta$ ). Metabolic activity, Hoechst, Western Blot, RT-PCR, micro-CT, and histology were used to investigate osteogenesis and mineralization of constructs. Statistical analysis was performed via ANOVA followed by Tukey post-hoc test. Error reported as mean  $\pm$  standard dev.

**Results:** ESEM images of mineralized collagen and mineralized collagen-amnion scaffolds demonstrated an open pore structure still remained with the addition of the amniotic membrane in a 5:1 ratio of collagen to amnion. Mechanical compression testing revealed that the mineralized collagen-amnion scaffolds had significantly ( $p < 0.05$ ) increased compressive properties and smaller pore size than the mineralized collagen, indicating successful incorporation of the amnion. Metabolic activity and cell number was significantly ( $p < 0.05$ ) greater in the

mineralized collagen scaffold and high inflammatory media negatively affected the activity and cell number in both scaffold variants. There was no difference in protein activity, with osteogenic proteins such as AKT being near 100% active at all timepoints and p38 at 100% activity in the early timepoints. The presence of inflammatory media affected the two scaffolds protein activity differently. AKT activity increased in the mineralized collagen-amnion scaffold in inflammatory media at one timepoint. Osteogenic gene expression demonstrated a high *RUNX2* fold change in mineralized collagen scaffolds, but similar *COL1A2* and *BMP2* fold change between the two groups. Once again, increased fold change of *RUNX2* was observed for mineralized collagen-amnion scaffolds in response to inflammatory media. Micro-CT showed mineral crystals in mineralized collagen scaffolds but was not present in mineralized collagen-amnion scaffolds, and similar trends followed for histological staining with alizarin red and Von Kossa staining.

**Conclusions:** We show that the amniotic membrane

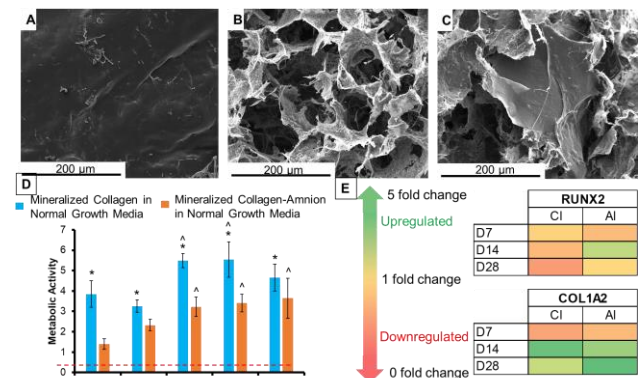


**Figure 1:** (A) ESEM of amnion. (B) ESEM of mineralized collagen. (C) ESEM of mineralized collagen-amnion. (D) Metabolic activity of mineralized collagen and mineralized collagen-amnion scaffolds in normal growth media. (E) Gene expression of mineralized collagen and mineralized collagen-amnion scaffolds in inflammatory media normalized to the same groups in normal growth media.

matrix can be incorporated into a mineralized collagen scaffold under development for CMF bone repair applications. AM-modified scaffolds show increased mechanical properties along with markers of osteogenesis and cell proliferation over the course of 28 days even in the presence of challenge with inflammatory cytokines. Ongoing work is examining bacterial response as well as the kinetics of macrophage polarization in the presence of the amniotic membrane.

## References:

1. Ren, X., *Biomaterials*, 2015. 50: p. 107-14
2. Hortensius, R.A., *J Biomed Mater Res A*, 2016. 104(6): p. 1332-42
3. Weisgerber, D.W., *Biomater Sci*, 2015. 3(3): p. 533-42
4. Caliarì, S.R., *Biomaterials*, 2011. 32(23): p. 5330-40

## Biomimetic triphasic scaffolds for osteotendinous junction regeneration

Raul A. Sun Han Chang, Ching-Wei Lee, Simon Rogers, Brendan A.C. Harley  
University of Illinois at Urbana-Champaign

**Statement of Purpose:** The osteotendinous junction links tendon to bone via a continuous fibrocartilaginous interface (enthesis) that reduces interfacial strain and decreases the risk of failure between highly elastic tendon and 100-fold stiffer bone.<sup>1</sup> Osteotendinous injuries can take place via acute (e.g. overload) or degradative (e.g. aging) processes. Surgical interventions that mechanically fix the torn tendon to bone result in poor healing of the native enthesis and high re-failure rates.<sup>2</sup> Functional reintegration of the torn tissues requires regeneration of the compliant fibrocartilaginous interface. Progress towards regenerating the tendon-to-bone enthesis is hampered by an inability for biomaterials to present spatially continuous interface zones or to overcome high levels of local strain that form at the interface between dissimilar tissues. We describe a triphasic biomaterial comprising osseous and tendinous collagen-GAG (CG) scaffold zones integrated via a compliant polyethylene glycol (PEG) hydrogel seam. We report tuning biomaterial properties by varying the gelation rate and stiffness of the hydrogel seam to control the topology of the interface and resultant mechanical properties and deformation under tensile load. The flanking CG zones promote region-specific osteogenic and tenogenic behavior in human mesenchymal stem cells (hMSCs)<sup>3</sup>, and the interfacial hydrogel seam grants a platform to explicitly address interface remodeling. Individually, these compartments address local cell response using tissue-relevant matrix structural cues, and together form a continuous scaffold that mimics the physical behavior of osteotendinous tissue.

**Methods:** PEG hydrogels are formed via horseradish peroxidase (HRP) polymerization of 4-arm PEG-Thiol.<sup>4</sup> Triphasic hydrogel-CG scaffolds were fabricated by adding the hydrogel precursor suspension between non-mineralized (CG) and mineralized (CGCaP) collagen-GAG suspensions prior to lyophilization. Gelation of hydrogels was measured using small-amplitude oscillatory shear (SAOS) rheology (2% strain, 0.8 rad/s) to identify gel point and equilibrium storage modulus.<sup>5</sup> We employed tensile testing (Instron 5943) and digital image correlation (DIC) methods to quantify bulk mechanical performance (toughness, elastic modulus) and map strain profiles across the scaffold. In vitro studies aim to map hMSC fibrocartilagenous differentiation profiles across triphasic scaffolds under physiological loads using a custom bioreactor. Statistical analysis will be performed via ANOVA and Tukey post-hoc tests. Error will be reported as mean  $\pm$  standard error.

**Results:** We developed a lyophilization approach that generates structurally continuous CG-PEG-CGCaP scaffolds. SAOS rheology elucidated HRP-crosslinked hydrogel variants with gel points spanning 3-12 minutes and storage moduli between 1-16kPa. Hydrogel variants were categorized based on gel point (fast 3-4 min, slow 12 min) and equilibrium storage modulus (soft 1-5 kPa,

stiff 10-15 kPa). Fast gelling hydrogels were more uniformly incorporated into the scaffold in distinct, monolithic layers, whereas slow gelling hydrogels were distributed within the collagen fibers (Fig. 1A). Bulk scaffold toughness (area under stress-strain curve) increased two-fold in triphasic scaffolds containing fast gelling hydrogels compared to biphasic scaffolds with no hydrogel between osseous and tendinous compartments. Furthermore, hydrogel rigidity contributed to significant changes in bulk scaffold elastic modulus, with a two-fold increase in scaffolds containing stiff versus soft hydrogels. Critically, triphasic scaffolds containing hydrogel seams that exhibited increased toughness also effectively blunted strain concentrations away from the interface (Fig. 1B). These constructs failed at more than double the applied strain compared to biphasic scaffolds, which had strain concentrated at the material interface.

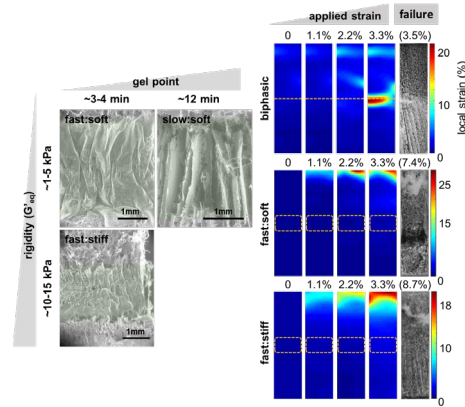


Figure 1. A) ESEM of triphasic scaffolds show extent of incorporation and topology of hydrogel seam. B) Heat maps localize strain in biphasic, triphasic fast:stiff and triphasic fast:soft scaffolds.

**Conclusions:** We describe fabrication and characterization of a triphasic biomaterial that mimics structural and physical elements of the native osteotendinous junction. Inclusion of a compliant hydrogel zone between tendon and bone scaffold compartments significantly reduces interfacial strain levels, increases construct toughness, and provides a local environment conducive to enthesis-specific fibrocartilagenous differentiation. Current work aims to exploit mechanical tuning of the hydrogel zone to enhance fibrocartilage activity of seeded hMSCs and to validate that variants able to temper interfacial strain enhance fibrocartilage differentiation and matrix remodeling. Ongoing efforts also employ crosslinking chemistries to locally add biomolecules involved in enthesis development.

### References:

1. Yamaguchi. JBJS. 2006; 88:1699-1704.
2. Genin. Biophys J. 2009; 97:976-85.
3. Caliarì. Adv Healthc Mater. 2015; 4:976-85.
4. Moriyama. Chem Commun. 2014; 50:5895-8.
5. Chambon. J Rheol. 1987; 31:683-97.
6. Tellado. Adv Drug Deliv Rev. 2015; 94:126-40.



## General Instructions for the Office of Technology Management Invention Disclosure Form

Thank you for disclosing your technology to the Office of Technology Management (OTM). The Invention Disclosure Form is the first step in a process that could potentially lead to commercialization of your technology. Completion of the form assists the OTM in two important ways:

- First, it serves as a written, dated record of your invention.
- Second, it provides the OTM with basic information which helps to evaluate, subsequently protect and potentially commercialize the intellectual property associated with your invention.

**It is not necessary to answer every question in order to submit this disclosure form. If you do not know an answer, if you have any questions, or would like assistance completing the form, please contact the OTM at (217) 333-7862 (Phone); (217) 265-5530 (Fax), or email OTM@uiuc.edu.**

Use the following guidelines while filling out the form:

- Provide as much detailed information about the technology as possible, citing all relevant sponsorship and publication information. This enables the OTM and its outside patent counsel to determine if the technology is patentable as well as identify possible opportunities for commercialization of the technology.
- When identifying inventors, use the broadest spectrum possible; OTM, assisted by outside patent counsel, will work to determine legal inventorship.

**Return the original, signed Disclosure Form along with any supporting documentation to:**

Office of Technology Management  
319 Ceramics Building, MC-243  
105 South Goodwin Avenue  
Urbana, Illinois 61801-2901

In addition to sending the original to the OTM, please distribute additional copies to:

- o each Inventor
- o Unit Executive Officer(s)

Upon receipt of the completed disclosure form, the OTM will assign it to a technology manager who will arrange a meeting. The purpose of this meeting will be to acquaint you with the OTM process, gain a more comprehensive understanding of the technology and define next steps.

### 1. TITLE OF INVENTION

The title should describe what the invention does, but not how it is made or how it works.

Adaptable PLA fiber reinforcement for conformal fitting

### 2. SEARCH TERMS (up to 10)

The OTM uses the Internet as a research tool when searching databases and markets. To make our searches efficient, please provide a short list of words, common industry phrases and/or categories.

Shape-fitting, conformal fitting, Poly(lactic acid), PLA, mechanical support

### 3. BRIEF OVERVIEW OF THE INVENTION (3-4 paragraphs)

- Provide a short, general layperson's overview of the invention and how it works.
- What is the purpose of the invention? For example, "What problem does it solve?"
- Is it a new product, process, or composition of matter? Or is it a new use for or improvement to an existing product, process or composition of matter?
- What are the features and benefits of the invention?

This invention is a 3D extrusion printed PLA support that provides mechanical stability and conformal fitting. It is combined with existing mineralized collagen slurry to provide a composite with shape-fitting character as well as increased mechanical properties over the mineralized collagen alone. Its shape-fitting character comes from being able to squeeze the support radially and on release it expands back to its original shape due to its angular design.

The purpose of the invention is to provide a biomaterial for bone-regeneration in cranio-maxillofacial (CMF) defects. These are defects of the skull that require surgical intervention and bone replacement due to the overwhelming size of the defect. Mineralized collagen has been used previously for CMF defects and bone regeneration, but has poor mechanical properties and no shape-fitting behavior. This invention will be combined with this mineralized collagen to offer an increase in mechanical properties as well as conformal fitting in the form of a composite material. This composite will be a biomaterial to replace the missing bone in these large defects and provide the proper mechanical support needed for these defects. By adding conformal fitting to the biomaterial through the use of this invention it will provide a better fit to the host bone to better allow new bone growth into the biomaterial.

This invention is a new design for a mechanical support and with this design it offers advantages over other mechanical supports, by providing conformal fitting. It is created by the use of a 3D printer, extrusion printing PLA, and is combined with existing mineralized collagen to make an innovative composite.

The benefits of this invention include increased mechanical properties over mineralized collagen alone, and conformal fitting behavior. By having both of these the invention creates a biomaterial that can regenerate bone in CMF defects better by offering mechanical properties more closely similar to bone than mineralized collagen, as well as a tighter fit to the bone defect to allow for closer contact of the bone-regenerative mineralized collagen and the host bone.

### 4. TECHNICAL DESCRIPTION, DETAILS AND SUPPORTING DATA

Provide results, data or other evidence demonstrating how the invention works. Any papers or visual material that you may already have, published or unpublished, can be attached as answer to this question.

Attached documents:

- Paper in progress utilizing this invention
- Powerpoint presentation of images of the invention and graphical results

*It is not necessary to answer every question in order to submit this disclosure form. If you do not know an answer, if you have any questions, or would like assistance completing the form, please contact the OTM at (217) 333-7862 (Phone); (217) 265-5530 (Fax), or email OTM@uiuc.edu.*



## 5. PRIOR METHODS, APPARATUS, DEVELOPMENTS AND PUBLICATIONS

- a) Provide a complete description of the closest known methods or apparatus in existence and the disadvantages or problems of each that are solved by the present invention.
- b) Cite any of your own publications and patents, and those of anyone else believed by you to disclose ideas most closely related to the invention.

Please attach all relevant publications, patents, advertisements, etc, if available.

1. Mineralized collagen: this has been used as a biomaterial to heal CMF defects and has shown good results of mineralization and osteogenesis. However, this lacks the proper mechanical support needed for bone replacement applications [1-4].
  2. 3D laser sintered printing of PCL with mineralized collagen: this provided an increase in mechanical properties well beyond that of mineralized collagen, and sufficient mechanical properties for CMF defect repair. However, this has no conformal fitting behavior [5].
1. Ren, X., et al., *Nanoparticulate mineralized collagen scaffolds induce in vivo bone regeneration independent of progenitor cell loading or exogenous growth factor stimulation*. Biomaterials, 2016. **89**: p. 67-78.
  2. Weisgerber, D.W., S.R. Caliarì, and B.A. Harley, *Mineralized collagen scaffolds induce hMSC osteogenesis and matrix remodeling*. Biomater Sci, 2015. **3**(3): p. 533-42.
  3. Harley, B.A., et al., *Design of a multiphase osteochondral scaffold. II. Fabrication of a mineralized collagen-glycosaminoglycan scaffold*. J Biomed Mater Res A, 2010. **92**(3): p. 1066-77.
  4. Ren, X., et al., *Osteogenesis on nanoparticulate mineralized collagen scaffolds via autogenous activation of the canonical BMP receptor signaling pathway*. Biomaterials, 2015. **50**: p. 107-14.
  5. Weisgerber, D.W., et al., *Evaluation of multi-scale mineralized collagen-polycaprolactone composites for bone tissue engineering*. J Mech Behav Biomed Mater, 2016. **61**: p. 318-27.

None of these directly relate to the incorporation of a reinforcement frame designed to enhance conformal fitting between biomaterial and defect. This is the unique contribution of this concept.

## 6. STAGE OF DEVELOPMENT (2-3 paragraphs)

Describe the development status (concept only, laboratory tested, prototype, etc) and briefly indicate what further development may be necessary to commercialize it.

We have deonstrated the concept (see attached manuscript draft). We have completed mechanical compression tests as well as "push-out" tests (described in paper). We anticipate modifications to the design as part of future IP that would refine the concept for unique defect sites in the skull. Such design could be further tested via more advanced "push-out" tests utilizing roughness similar to bone and additional slight manipulations may be done to the design to increase compression testing properties (Young's modulus, ultimate stress and strain). However, we feel the current stage of the IP covers all such modifications.

## 7. POTENTIAL LICENSEES

Identify companies that you think could benefit from the use of this technology.

Collagen Solutions

Also: DePuy Synthes Companies, Botiss, Novadip.

*It is not necessary to answer every question in order to submit this disclosure form. If you do not know an answer, if you have any questions, or would like assistance completing the form, please contact the OTM at (217) 333-7862 (Phone); (217) 265-5530 (Fax), or email OTM@uiuc.edu.*



**8. PUBLICATIONS/PRESENTATIONS/AND OTHER FORMS OF PUBLIC COMMUNICATION (DISCLOSURE)**

Please identify all past and future seminars, talks, abstracts, publications, and web postings describing the invention. These may affect the scope of patent protection and the timing of filing. **Disclosure to Others** is the oral, written, or electronic dissemination of the invention to a person outside the University of Illinois that would enable someone working in the field to practice the invention or repeat its development. Note: any communication with colleagues and students within the University of Illinois community do not count as disclosures.

Type of disclosure (i.e. publications, seminars, etc)	Date(s)
Dewey, M., E. Johnson, B.A. Harley, <i>Shape-fitting PLA-collagen composite biomaterial promotes osteogenic differentiation of porcine adipose stem cells</i> . In Progress	11/24/17
Society for Biomaterials Conference Presentation	04/2018

**9. DATES OF CONCEPTION AND REDUCTION TO PRACTICE**

It is important for us to document these dates should any challenges to the patent ever arise. Conception is the formulation in the mind of the inventors of the ultimate working invention. Reduction to practice can be accomplished either "actually" or "constructively." **Actual reduction to practice** is the physical creation of the invention. **Constructive reduction to practice** is a detailed written description that demonstrates the invention will work as conceived. Describe the circumstances and dates surrounding development of your invention:

	Details	Date
Conception of invention. Is this date documented in writing? If so, where?	Conception, documented on Fusion 360 model design	03/08/17
First reduction to practice.	Actual reduction to practice	03/18/17

**10. SPONSORSHIP**

Identify all grants, contracts, and other sources of funds contributing to the research that led to the invention. You should list all agencies that you would acknowledge in a publication. Be liberal in the interpretation. The OTM will take care of the contractual reporting obligations associated with your funding.

Agency or Sponsor	Grant/Contract/Other Number	BANNER/UFAS No.
U.S. Army Medical Research and Materiel Command	W81XWH-16-1-0566	

**11. OTHER AGREEMENTS AND INTERACTIONS**

Identify any agreements or interactions that you have entered into that are related to the invention and might grant rights to a company or other party outside of the University (material transfer agreements, commercially sponsored research agreements, consortia agreements, consulting agreements, etc.)

Did this invention use any materials which were obtained from a company or another institution? NO  YES  (Please provide details, and indicate if there is a Materials Transfer Agreement.)

Did you transfer to any researcher outside of your institution any new Materials (DNA, peptides, cell lines, vectors, catalysts, alloys, etc) related to the invention? NO  YES  (Please provide details)

*It is not necessary to answer every question in order to submit this disclosure form. If you do not know an answer, if you have any questions, or would like assistance completing the form, please contact the OTM at (217) 333-7862 (Phone); (217) 265-5530 (Fax), or email OTM@uiuc.edu.*

**12. INVENTORS**

List all those who helped contribute to the conception of the ultimate working invention. The people you include ultimately may or may not be legal inventors. Please place an asterisk (\*) next to the name of the inventor to whom correspondence should be sent. If any person holds a sole or joint appointment with any other university, company or governmental agency, please note that fact.

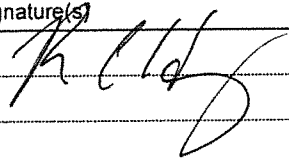
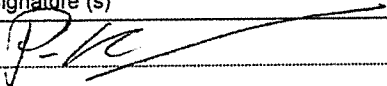
INVENTOR: Marley Dewey      Dept/Affiliation: Materials Science and Engineering, UIUC  
Home Address: 11 Little Brook Drive, Falmouth, ME      Citizenship: United States

INVENTOR: Brendan Harley      Dept/Affiliation: Chemical and Biomolecular Engineering, UIUC  
Home Address: 1009 S. Douglas Ave, Urbana, IL 61801      Citizenship: USA

INVENTOR: Daniel Weisgerber      Dept/Affiliation: Department of Bioengineering and Therapeutic Sciences, University of California, San Francisco (Currently). Was post-doctoral research associate, Materials Science and Engineering, UIUC, when contribution made.  
Home Address: 1390 White Eagle Ranch Road, Hickory, NC      Citizenship: United States

(If more, please list on last page.)

The CORRESPONDING INVENTOR should sign and date, along with his/her UNIT EXECUTIVE OFFICER. (Note: If that inventor is not the head of the laboratory, the signature of his/her faculty advisor or supervisor is required.)

Corresponding Inventor printed name	Signature(s)	Date
Brendan Harley		11/27/2017
Unit Executive Officer(s) Printed name & Unit	Signature (s)	Date
Paul J.A. Kenis		11/27/2017

*It is not necessary to answer every question in order to submit this disclosure form. If you do not know an answer, if you have any questions, or would like assistance completing the form, please contact the OTM at (217) 333-7862 (Phone), (217) 265-5530 (Fax), or email OTM@uiuc.edu*



## General Instructions for the Office of Technology Management Invention Disclosure Form

Thank you for disclosing your technology to the Office of Technology Management (OTM). The Invention Disclosure Form is the first step in a process that could potentially lead to commercialization of your technology. Completion of the form assists the OTM in two important ways:

- First, it serves as a written, dated record of your invention.
- Second, it provides the OTM with basic information which helps to evaluate, subsequently protect and potentially commercialize the intellectual property associated with your invention.

**It is not necessary to answer every question in order to submit this disclosure form. If you do not know an answer, if you have any questions, or would like assistance completing the form, please contact the OTM at (217) 333-7862 (Phone); (217) 265-5530 (Fax), or email [OTM@uiuc.edu](mailto:OTM@uiuc.edu).**

Use the following guidelines while filling out the form:

- Provide as much detailed information about the technology as possible, citing all relevant sponsorship and publication information. This enables the OTM and its outside patent counsel to determine if the technology is patentable as well as identify possible opportunities for commercialization of the technology.
- When identifying inventors, use the broadest spectrum possible; OTM, assisted by outside patent counsel, will work to determine legal inventorship.

**Return the original, signed Disclosure Form along with any supporting documentation to:**

Office of Technology Management  
319 Ceramics Building, MC-243  
105 South Goodwin Avenue  
Urbana, Illinois 61801-2901

In addition to sending the original to the OTM, please distribute additional copies to:

- o each Inventor
- o Unit Executive Officer(s)

Upon receipt of the completed disclosure form, the OTM will assign it to a technology manager who will arrange a meeting. The purpose of this meeting will be to acquaint you with the OTM process, gain a more comprehensive understanding of the technology and define next steps.



### 1. TITLE OF INVENTION

The title should describe what the invention does, but not how it is made or how it works.

Mineralized Collagen Scaffolds combined with the Amniotic Membrane derived from placentas to address inflammation in Craniomaxillofacial Bone Regeneration

### 2. SEARCH TERMS (up to 10)

The OTM uses the Internet as a research tool when searching databases and markets. To make our searches efficient, please provide a short list of words, common industry phrases and/or categories.

Amniotic Membrane, Mineralized Collagen, Scaffolds, Porous, Craniomaxillofacial, Bone Regeneration, Inflammation

### 3. BRIEF OVERVIEW OF THE INVENTION (3-4 paragraphs)

- a) Provide a short, general layperson's overview of the invention and how it works.
- b) What is the purpose of the invention? For example, "What problem does it solve?"
- c) Is it a new product, process, or composition of matter? Or is it a new use for or improvement to an existing product, process or composition of matter?
- d) What are the features and benefits of the invention?

This invention is a modification of the mineralized collagen scaffolds used for craniomaxillofacial bone regeneration, by incorporating the amniotic membrane to address inflammation. A common issue with large bone replacements using biomaterials is chronic inflammation, which can lead to the biomaterial being walled off by the patient. We modified these naturally bioactive scaffolds with the amniotic membrane due to its anti-inflammatory and anti-microbial properties. This is an improvement on an existing product, mineralized collagen scaffolds. By combining the amniotic membrane with mineralized collagen we avoid the use of drugs and antibiotics to control inflammation and bacterial infection, and provide a scaffold that could regenerate bone as well as resist inflammation.

### 4. TECHNICAL DESCRIPTION, DETAILS AND SUPPORTING DATA

Provide results, data or other evidence demonstrating how the invention works. Any papers or visual material that you may already have, published or unpublished, can be attached as answer to this question.

We have data that involves the use and characterization of mineralized collagen-amnion scaffolds. A paper will be started soon.

### 5. PRIOR METHODS, APPARATUS, DEVELOPMENTS AND PUBLICATIONS

- a) Provide a complete description of the closest known methods or apparatus in existence and the disadvantages or problems of each that are solved by the present invention.
- b) Cite any of your own publications and patents, and those of anyone else believed by you to disclose ideas most closely related to the invention.

Please attach all relevant publications, patents, advertisements, etc, if available.

The closest known method is the use of mineralized collagen scaffolds and non-mineralized collagen-amnion scaffolds. Mineralized collagen scaffolds have no anti-inflammatory response and non-mineralized collagen-amnion scaffolds have no mineral content, so they are not as effective at regenerating bone as their mineralized collagen counterparts. To our knowledge, the assembly of this composite is completely novel and not immediately obvious.

*It is not necessary to answer every question in order to submit this disclosure form. If you do not know an answer, if you have any questions, or would like assistance completing the form, please contact the OTM at (217) 333-7862 (Phone); (217) 265-5530 (Fax), or email OTM@uiuc.edu.*



CITE RELEVANT PATENTS AND PAPERS:

Previous research in NON-mineralized biomaterials:

(1) Hortensius RA, Ebens JH, Harley BA. Immunomodulatory effects of amniotic membrane matrix incorporated into collagen scaffolds. *J Biomed Mater Res A*. 2016;104(6):1332-42.

6. STAGE OF DEVELOPMENT (2-3 paragraphs)

Describe the development status (concept only, laboratory tested, prototype, etc) and briefly indicate what further development may be necessary to commercialize it.

A first design of a mineralized collagen-amnion scaffold has been fabricated and mechanically tested as well as tested *in vitro*. Other designs will be created with different amounts of amniotic membrane incorporated into them, as well as the addition of GAG. These designs will be tested with macrophages to determine phenotype and with bacteria to determine antimicrobial effects. In the future, these will be tested *in vivo*.

7. POTENTIAL LICENSEES

Identify companies that you think could benefit from the use of this technology.

We have had discussions with the company Collagen Solutions about biomaterials for craniofacial regeneration, but have not to date discussed this specific technology with them.



**8. PUBLICATIONS/PRESENTATIONS/AND OTHER FORMS OF PUBLIC COMMUNICATION (DISCLOSURE)**

Please identify all past and future seminars, talks, abstracts, publications, and web postings describing the invention. These may affect the scope of patent protection and the timing of filing. **Disclosure to Others** is the oral, written, or electronic dissemination of the invention to a person outside the University of Illinois that would enable someone working in the field to practice the invention or repeat its development. Note: any communication with colleagues and students within the University of Illinois community do not count as disclosures.

Type of disclosure (i.e. publications, seminars, etc)	Date(s)
Poster presentation at the Gordon Research Conference (considered off-the-record)	August 4-10, 2018
Paper in early stages of preparation	Fall 2018 submission

**9. DATES OF CONCEPTION AND REDUCTION TO PRACTICE**

It is important for us to document these dates should any challenges to the patent ever arise. **Conception** is the formulation in the mind of the inventors of the ultimate working invention. **Reduction to practice** can be accomplished either "actually" or "constructively." **Actual reduction to practice** is the physical creation of the invention. **Constructive reduction to practice** is a detailed written description that demonstrates the invention will work as conceived. Describe the circumstances and dates surrounding development of your invention:

	Details	Date
Conception of invention. Is this date documented in writing? If so, where?	Yes, as an ISUR proposal (word document)	8/11/17
First reduction to practice.	Yes, written in lab notebook	10/31/17

**10. SPONSORSHIP**

Identify all grants, contracts, and other sources of funds contributing to the research that led to the invention. You should list all agencies that you would acknowledge in a publication. Be liberal in the interpretation. The OTM will take care of the contractual reporting obligations associated with your funding.

Agency or Sponsor	Grant/Contract/Other Number	BANNER/UFAS No.
U.S. Army Medical Research and Materiel Command	W81XWH-16-1-0566	

**11. OTHER AGREEMENTS AND INTERACTIONS**

Identify any agreements or interactions that you have entered into that are related to the invention and might grant rights to a company or other party outside of the University (material transfer agreements, commercially sponsored research agreements, consortia agreements, consulting agreements, etc.)

Did this invention use any materials which were obtained from a company or another institution? NO \_\_ YES X (Please provide details, and indicate if there is a Materials Transfer Agreement.)

*It is not necessary to answer every question in order to submit this disclosure form. If you do not know an answer, if you have any questions, or would like assistance completing the form, please contact the OTM at (217) 333-7862 (Phone); (217) 265-5530 (Fax), or email OTM@uiuc.edu.*



Placentas obtained from Carle Hospital (we isolated amniotic membrane from the placentas within our laboratory)

Did you transfer to any researcher outside of your institution any new Materials (DNA, peptides, cell lines, vectors, catalysts, alloys, etc) related to the invention? NO  YES  (Please provide details)

12. INVENTORS

List all those who helped contribute to the conception of the ultimate working invention. The people you include ultimately may or may not be legal inventors. Please place an asterisk (\*) next to the name of the inventor to whom correspondence should be sent. If any person holds a sole or joint appointment with any other university, company or governmental agency, please note that fact.

INVENTOR: Brendan A.C. Harley \_\_\_\_\_ Dept/Affiliation: Chemical & Biomolecular Engineering

Home Address: \_1009 S Douglas Ave, Urbana, IL 61801 \_\_\_\_\_ Citizenship: \_\_\_ USA \_\_\_\_\_

INVENTOR: Marley Dewey \_\_\_\_\_ Dept/Affiliation: Materials Science and Engineering

Home Address: 600 S Mathews Ave, Urbana, IL 61801 \_\_\_\_\_ Citizenship: \_\_\_ USA \_\_\_\_\_

(If more, please list on last page.)

The CORRESPONDING INVENTOR should sign and date, along with his/her UNIT EXECUTIVE OFFICER. (Note: If that inventor is not the head of the laboratory, the signature of his/her faculty advisor or supervisor is required.)

Corresponding Inventor printed name	Signature(s)	Date
Brendan Harley		7/19/2018
Marley Dewey		7/10/18

Unit Executive Officer(s) Printed name & Unit	Signature (s)	Date
Paul J. A. Kenis		7/19/2018

*It is not necessary to answer every question in order to submit this disclosure form. If you do not know an answer, if you have any questions, or would like assistance completing the form, please contact the OTM at (217) 333-7862 (Phone); (217) 265-5530 (Fax), or email OTM@uiuc.edu.*



**Additional Inventors**

INVENTOR: Rebecca Hortensius \_\_\_\_\_

Dept/Affiliation: Bioengineering

Home Address: \_\_ 1399 Albert Street North, Saint Paul, MN 55108

Citizenship: \_\_ USA \_\_\_\_\_

INVENTOR: Simona Slater \_\_\_\_\_

Dept/Affiliation: Chemical & Biomolecular Engineering

Home Address: 901 Plymouth Ct, Algonquin, IL 60102

Citizenship: \_\_ USA \_\_\_\_\_

*It is not necessary to answer every question in order to submit this disclosure form. If you do not know an answer, if you have any questions, or would like assistance completing the form, please contact the OTM at (217) 333-7862 (Phone); (217) 265-5530 (Fax), or email OTM@uiuc.edu.*



Full length article

## Incorporating $\beta$ -cyclodextrin into collagen scaffolds to sequester growth factors and modulate mesenchymal stem cell activity



William K. Grier<sup>a,1</sup>, Aleczandria S. Tiffany<sup>a,1</sup>, Matthew D. Ramsey<sup>b</sup>, Brendan A.C. Harley<sup>a,c,\*</sup>

<sup>a</sup> Department of Chemical and Biomolecular Engineering, University of Illinois at Urbana-Champaign, Urbana, IL 61801, United States

<sup>b</sup> Department of Bioengineering, University of Illinois at Urbana-Champaign, Urbana, IL 61801, United States

<sup>c</sup> Carl R. Woese Institute for Genomic Biology, University of Illinois at Urbana-Champaign, Urbana, IL 61801, United States

### ARTICLE INFO

#### Article history:

Received 15 June 2017

Received in revised form 21 June 2018

Accepted 22 June 2018

Available online 23 June 2018

#### Keywords:

Collagen scaffold

Beta-cyclodextrin

Guest-host interactions

Growth factors

Mesenchymal stem cell

### ABSTRACT

The development of biomaterials for a range of tissue engineering applications increasingly requires control over the bioavailability of biomolecular cues such as growth factors in order to promote desired cell responses. While efforts have predominantly concentrated on covalently-bound or freely-diffusible incorporation of biomolecules in porous, three-dimensional biomaterials, opportunities exist to exploit transient interactions to concentrate growth factor activity over desired time frames. Here, we report the incorporation of  $\beta$ -cyclodextrin into a model collagen-GAG scaffold as a means to exploit the passive sequestration and release of growth factors via guest-host interactions to control mesenchymal stem cell differentiation. Collagen-GAG scaffolds that incorporate  $\beta$ -cyclodextrin show improved sequestration as well as extended retention and release of TGF- $\beta$ 1. We further show extended retention and release of TGF- $\beta$ 1 and BMP-2 from  $\beta$ -cyclodextrin modified scaffolds was sufficient to influence the metabolic activity and proliferation of mesenchymal stem cells as well as differential activation of Smad 2/3 and Smad 1/5/8 pathways associated with differential osteo-chondral differentiation. Further, gene expression analysis showed TGF- $\beta$ 1 release from  $\beta$ -cyclodextrin CG scaffolds promoted early chondrogenic-specific differentiation. Ultimately, this work establishes a novel method for the incorporation and display of growth factors within CG scaffolds via supramolecular interactions. Such a design framework offers opportunities to selectively alter the bioavailability of multiple biomolecules within a three-dimensional collagen-GAG scaffold to enhance cell activity for a range of musculoskeletal regenerative medicine applications.

#### Statement of Significance

We describe the incorporation of  $\beta$ -cyclodextrin into a model CG-scaffold under development for musculoskeletal tissue engineering applications. We show  $\beta$ -cyclodextrin modified scaffolds promote the sequestration of soluble TGF- $\beta$ 1 and BMP-2 via guest-host interactions, leading to extended retention and release. Further,  $\beta$ -cyclodextrin modified CG scaffolds promote TGF- $\beta$ 1 or BMP-2 specific Smad signaling pathway activation associated with divergent osseous versus chondrogenic differentiation pathways in mesenchymal stem cells.

© 2018 Acta Materialia Inc. Published by Elsevier Ltd. All rights reserved.

### 1. Introduction

Collagen-glycosaminoglycan (CG) materials are composed of natural extracellular matrix (ECM) components and have shown

great promise as tissue engineering scaffolds. Initially developed for skin regeneration applications, these porous CG scaffolds are produced by the lyophilization of an acidic suspension of type I collagen and glycosaminoglycans [1]. One of the major advantages of CG scaffolds is the ease in which the microstructure, composition, or bioactivity can be adapted to meet the functional demands of a wide variety of tissue engineering applications. For instance, the freezing kinetics can be manipulated to produce anisotropic scaffolds composed of aligned tracks of ellipsoidal pores for tendon repair applications [2–4]. Calcium phosphate nanocrystallites have

\* Corresponding author at: Dept. of Chemical and Biomolecular Engineering, Carl R. Woese Institute for Genomic Biology, University of Illinois at Urbana-Champaign, 110 Roger Adams Laboratory, 600 S. Mathews Ave., Urbana, IL 61801, United States.

E-mail address: [bharley@illinois.edu](mailto:bharley@illinois.edu) (B.A.C. Harley).

<sup>1</sup> These authors contributed equally to this work.

been incorporated during lyophilization to enhance mesenchymal stem cell (MSC) osteogenic differentiation and bone regeneration [5–10]. These structural modifications have also shown to bias MSC differentiation down chondrogenic vs. osteogenic lineages in the presence of mixed media supplementation [11]. The desire to promote increasingly specific cell behaviors (e.g., proliferation, MSC lineage specification) has motivated efforts to incorporate design elements that alter the bioavailability of growth factors within the scaffold network itself. In addition to covalent immobilization of growth factors to the scaffold via carbodiimide [12] and benzophenone [13] crosslinking chemistries, growth factors have also been covalently bound to polymeric reinforcing cages fabricated by 3D printing that can be incorporated into the scaffold during lyophilization to generate a composite with enhanced mechanical and biomolecular properties [14]. However, while covalent immobilization offers benefits in the form of extended bioavailability, this process is only applicable to biomolecular signals that do not require receptor internalization. Exciting opportunities therefore exist in the space of non-covalent presentation of biomolecular signals. Recently, Hortensius et al. adapted charge-based transient sequestration concepts previously demonstrated in heparin-modified hydrogels [15] and 2D culture surfaces [16], and showed the glycosaminoglycan content of the CG scaffold itself could be manipulated to transiently sequester and release growth factors from the media [17,18]. However, we examine alternative chemistries to transiently sequester activity-inducing growth factors within the CG scaffold network.

Recently, a series of investigation have explored the use of chemical modifications to a biomaterial to enhance growth factor

sequestration or release kinetics. Notably, efforts such as Benoit et al. exploiting the incorporation of heparin into PEG hydrogels [19,20], Borselli et al. exploiting VEGF functionalization [21], and Martino et al. exploiting the use of fibronectin fragments for cytokine sequestration [22]. However here we explore an alternative promising method for the selective incorporation of growth factors into biomaterial constructs is the use of supramolecular interactions such as those achievable with cyclodextrins. These six, seven, and eight member D-glucopyranose rings ( $\alpha$ -cyclodextrin,  $\beta$ -cyclodextrin, and  $\gamma$ -cyclodextrin respectively) [23,24] are commonly used in pharmaceutical applications to increase drug solubility. Cyclodextrins are known for their ability to form cyclodextrin inclusion complexes (CDIC), where guest-host interactions enable the adsorption of hydrophobic guest molecules into the central cavity (Fig. 1A) [25]. The ability of cyclodextrins to form guest-host complexes is determined by the size of the cyclodextrin cavity (6.0–6.5 Å) and the size of the guest molecule or key functional groups within the guest molecule [26]. It is suggested that cyclodextrins can interact with proteins via interactions with hydrophobic amino acids [27,28]. Thus, cyclodextrins can bind and interact with a variety of molecules, proteins, and peptides. Cyclodextrin chemistries have been demonstrated as a means to generate dynamic, adaptable hydrogel environments [29–33]. Cyclodextrins have also been incorporated into porous biomaterials as a means to alter the release of drug molecules [34,35]. While cyclodextrins have been shown to have a strong affinity for various growth factors [36], the ability for these molecules to regulate growth factor sequestration and display within porous scaffold biomaterials has not been deeply exploited.

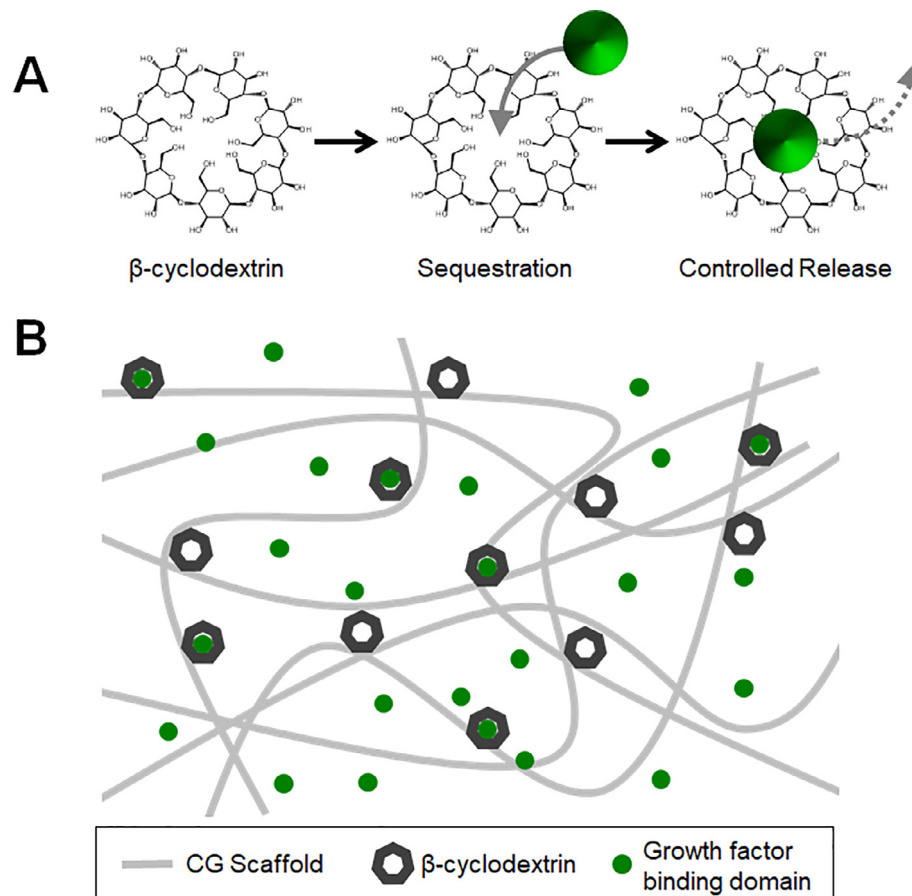


**Fig. 1.**  $\beta$ -cyclodextrin guest-host interactions and incorporation into CG scaffolds. (A) Seven-membered ring structure of  $\beta$ -cyclodextrin and spontaneous formation of inclusion complexes. (B) Representation of  $\beta$ -cyclodextrin incorporation into CG scaffold for transient sequestration of growth factors from solution.

Here, we describe the incorporation of  $\beta$ -cyclodextrin into a CG scaffold variant under development for musculoskeletal repair applications. We hypothesized that incorporation of cyclodextrin into the CG scaffold network would facilitate the formation of CDICs with exogenously added soluble growth factors, leading to growth factor sequestration and enhanced activity on MSCs within the scaffold. We examine sequestration and subsequent release of a model growth factor, transforming growth factor-beta 1 (TGF- $\beta$ 1), within the scaffold network. We then examine the capacity for cyclodextrin modified CG scaffolds (CGcyclo) to enhance the activity of the chondrogenic growth factor TGF- $\beta$ 1 or the osteogenic growth factor bone morphogenetic protein-2 (BMP-2) to influence MSC fate. We examine MSC osteo-chondral lineage specification via activation of the Smad 1/5/8 and Smad 2/3 pathways as well as changes in gene expression profiles.

## 2. Materials and methods

All materials and chemicals were purchased from Sigma-Aldrich (St. Louis, MO) unless otherwise specified.

### 2.1. Scaffold fabrication

Scaffolds were fabricated via lyophilization from a precursor collagen suspension. The standard collagen-GAG (CG) suspension was produced from type I collagen from bovine Achilles tendon and chondroitin sulphate from shark cartilage were homogenized in 0.05 M acetic acid at a ratio of collagen to glycosaminoglycan of 11.25:1 [1,37]. A cyclodextrin-modified suspension (CGcyclo) were prepared by adding  $\beta$ -cyclodextrin (from a 10 mg/mL stock solution in deionized water) directly to the CG slurry at a final concentration of 37  $\mu$ g/mL. Scaffolds were fabricated after pipetting 200  $\mu$ L of degassed CG or CGcyclo suspension into wells (6 mm diameter, 7 mm deep), of a polysulfone mold that was subsequently placed on a freeze-dryer shelf (VirTis, Gardner, NY). The CG or CGcyclo suspensions were frozen at  $-10$  °C for 2 h and then sublimated at 0 °C and 200 mTorr to remove the ice crystals, resulting in a dry porous scaffold.

Scaffolds were then hydrated by immersion in 200 proof ethanol overnight followed by a 24 h rinse in sterile phosphate-buffered saline (PBS) replacing the PBS three times. Each scaffold was then crosslinked using carbodiimide chemistry by immersion in a solution of 1-ethyl-3-[3-dimethylaminopropyl] carbodiimide hydrochloride (EDC) and N-hydroxysulfosuccinimide (NHS) for 2 h at room temperature in a 5:2:1 molar ratio (EDC:NHS:COOH) in sterile PBS with gentle shaking. After crosslinking, the scaffolds were washed twice with sterile PBS and stored at 4 °C.

### 2.2. SEM imaging of the scaffold microstructure

Critical point drying (CPD) was used to prepare hydrated and cell-seeded scaffolds for SEM imaging. CPD was performed using a Samdri-PVT-3D (Tousimis, Rockville, MD), where the aqueous media in the scaffold was sequentially replaced with ethanol and then liquid CO<sub>2</sub>. Liquid CO<sub>2</sub> was allowed to infiltrate the scaffolds and was then held above 6.895 kPa and 31 °C in order to remove the CO<sub>2</sub> as a gas with minimal structural deformation. Samples were then mounted on carbon tape, sputter coated with a gold/palladium mixture, and imaged with a Philips XL30 ESEM-FEG (FEI Company, Hillsboro, OR) at 5 kV with a secondary electron detector.

### 2.3. Biomolecule sequestration and release

The ability for the conventional CG or CGcyclo scaffolds to sequester and release two model biomolecules, TGF- $\beta$ 1 and

BMP-2, was assessed via ELISA. Briefly, scaffolds were incubated in 5 ng/mL recombinant TGF- $\beta$ 1 or 5 ng/mL BMP-2 (R & D Systems, Minneapolis, MN) in sterile PBS with 1% bovine serum albumin (BSA) for 1 h on a gentle shaker; solution without scaffolds were used as controls. Following incubation, scaffolds were removed from the TGF- $\beta$ 1 or BMP-2 solutions, and the amount of TGF- $\beta$ 1 or BMP-2 remaining in the seeding solution was determined via DuoSet<sup>®</sup> ELISA (R&D Systems) in order to calculate the fraction of TGF- $\beta$ 1 or BMP-2 sequestered by the scaffold variants themselves [17].

The elution of TGF- $\beta$ 1 or BMP-2 from the CG and CGcyclo scaffold variants was subsequently traced over 6 days. Briefly, scaffolds were transferred to fresh PBS with 1% bovine serum albumin media and maintained in the incubator (37 °C, 5% CO<sub>2</sub>) for up to 6 days. Samples of the media were removed after 1, 6, 12, 24, 72, and 144 h for analysis of TGF- $\beta$ 1 or BMP-2 release via DuoSet<sup>®</sup> ELISA. Results are reported as the fraction of the total TGF- $\beta$ 1 or BMP-2 retained by the scaffold at each time point.

### 2.4. Human mesenchymal stem cell culture and scaffold seeding

Human bone marrow-derived mesenchymal stem cells were purchased from Lonza (Walkersville, MD). Cells from multiple lots, originating from separate donors, were combined to account for any donor-specific responses. The MSCs were cultured at 37 °C and 5% CO<sub>2</sub> in a complete MSC growth medium, consisting of low-glucose DMEM with 10 vol% MSC-qualified, USDA-approved fetal bovine serum and 1 vol% antibiotic-antimycotic (Thermo Fisher, Waltham, MA), fed every three days and used at passage 6.

Selected CG and CGcyclo scaffolds were incubated in 5 ng/mL human recombinant BMP-2 or human recombinant TGF- $\beta$ 1 (ProSpec-Tany, Ness-Ziona, Israel) for 1 h in sterile PBS in the same manner as previously described. The scaffolds were then moved into 5% FBS MSC Media for 2 h as cells were lifted and centrifuged in preparation for seeding using a previously established static method [38]. Scaffolds were partially dried with Kimwipes and seeded with  $1.0 \times 10^5$  MSCs per 24  $\mu$ L medium (one 10  $\mu$ L drop on opposite sides of the scaffold) in six well plates, with six scaffolds per well. Cells were allowed to attach for 1 h before submerging in 6 mL of low-serum MSC media, containing 5% FBS, per well. Cell-seeded scaffolds were cultured at 37 °C and 5% CO<sub>2</sub> and fed every three days with the low-serum media.

### 2.5. Cell number and metabolic activity assays

DNA quantification was performed using a previously described method to determine the number of cells present on each scaffold [39,40]. Briefly, scaffolds to be terminated were washed three times in warmed, sterile PBS to remove dead and unbound cells and placed in papain solution (2.4 mg/mL PBS) for digestion of the scaffold overnight at 60 °C. Lysates were then incubated with Hoechst 33,258 dye (Invitrogen, Carlsbad, CA) to fluorescently label double-stranded DNA. Fluorescent intensity (352/461 nm excitation/emission) from each sample was read using a fluorescent spectrophotometer (Tecan Infinite F200 Pro, Männedorf, Switzerland) and translated in cell counts through a standard curve of known MSC numbers.

Mitochondrial metabolic activity of the MSCs bound to each scaffold was quantified using the non-destructive alamarBlue<sup>®</sup> assay as previously described [41]. Cell-seeded scaffolds were incubated in 0.75 mL of alamarBlue (Invitrogen, Carlsbad, CA) (1:20 5% FBS MSC Media) and incubated at 37 °C for 90 min on a gentle shaker. The reduction of resazurin to resorufin by metabolically active cells was quantified on a fluorescent spectrophotometer through differential absorbance. Relative cell metabolic activity was determined from a standard curve generated with known MSC

concentrations and reported as a fraction of initial seeding cell count.

### 2.6. Protein isolation, SDS-PAGE, and immunoblotting

Upon reaching each time point, (day 1, 3, 6) scaffolds to be terminated were washed three times in warmed, sterile PBS to remove dead and unbound cells. The scaffolds were then blotted briefly and placed in a cold 1:100 dilution each of protease inhibitor cocktail, phosphatase inhibitor cocktail II and phosphatase inhibitor cocktail III in RIPA buffer and placed back on ice for thirty minutes with agitation. The scaffolds were then removed and lysates were frozen [42]. Protein concentrations were quantified with the Pierce BCA Protein Assay Kit (Thermo Fisher, Waltham, MA) and prepared for gel electrophoresis by diluting 10 µg of protein from each sample with an equal volume of Laemmli buffer. Samples were heated at 90 °C for 10 min and loaded into 4–20% polyacrylamide gels (Bio-Rad Laboratories, Hercules, CA) in duplicate for both Smad 2/3 and 1/5/8 imaging. The gel electrophoresis was run at 150 V for 90 min in 1 L of tris-glycine running buffer (25 mM NaCl, 192 mM glycine, 0.1% SDS, pH ~ 8.3 in DI water) and immediately transferred onto nitrocellulose membranes (GE Healthcare, Little Chalfont, UK) at 300 mV for 2 h in 1 L of Towbin's transfer buffer (2.5 M Tris base, 19.2 mM glycine, 20% methanol in DI water). The nitrocellulose membranes were then cut and blocked in 5% milk in tris-buffered-saline + 0.1% tween 20 (TBST). Membranes were incubated in primary antibody at 4 °C overnight in 5% BSA in TBST, washed three times in TBST, incubated in secondary antibody at RT for 1 h, washed and imaged using the SuperSignal West Pico or Femto Chemiluminescent Substrate (Thermo Fisher, Waltham, MA) and an ImageQuant LAS 4010 system (GE Healthcare, Little Chalfont, UK). Primary antibodies were purchased from Cell Signaling (Danvers, MA): pSmad 2/3 (8828), Smad 2/3 (8685), pSmad 1/5/8 (9511), Smad 1 (6944), β-actin (4967). Secondary antibody used was HRP-linked goat anti-rabbit IgG (1:5000 in TBST). Membranes were stripped using the OneMinute® Western Blot Stripping Buffer (GM Biosciences, Rockville, MD) and re-imaged two additional times, repeating the above procedure. ImageJ was used for band intensity quantification. Results were reported as the ratio of phosphorylated to total protein for each pathway.

### 2.7. RNA isolation and target gene expression characterization

RNA was extracted from the MSC-seeded scaffolds at D1, D3, D6 using an RNeasy Plant MiniKit (Qiagen, Valencia, CA) and frozen. The isolated RNA was then reverse transcribed to cDNA in a Bio-Rad S1000 thermal cycler, using the QuantiTect Reverse Transcription Kit (Qiagen, Valencia, CA) [2,43]. Real-time PCR reactions were carried out in triplicate, using 10 ng of cDNA and QuantiTect SYBR Green PCR kit (Qiagen, Valencia, CA) in a 7900HT Fast Real-Time PCR system (Applied Biosystems, Carlsbad, CA). The primers used were consistent with previous studies and were synthesized by Integrated DNA Technologies (Coralville, IA). The expression level of the following markers was quantified: proteoglycan aggrecan (ACAN), cartilage oligomeric matrix protein (COMP), SRY-Box9 (SOX9), and glyceraldehyde 3-phosphate dehydrogenase (GAPDH), which was used as a house keeping gene (Table 1). Results were generated using the  $\Delta\Delta C_t$  method and expressed as fold changes, normalized to the expression levels of MSCs at the time of seeding, D0.

### 2.8. Statistical analysis

Analysis of ELISA experiments (growth factor sequestration and elution) was performed using a Kruskal-Wallis test (due to

**Table 1**  
PCR primer sequences.

Transcript	Sequence	Reference
ACAN	Forward: 5'-TGCATTCCACGAAGCTAACCTT-3' Reverse: 5'-GACGCCTCGCCTTCTTGA-3'	[62]
COMP	Forward: 5'-GCAACACGGACGAGGACAAG-3' Reverse: 5'-CGCCATCACTGTCTTCTGG-3'	[63]
SOX9	Forward: 5'-AGCGAACGCACATCAAGAC-3' Reverse: 5'-GCTGTAGTGTGGAGGTTGAA-3'	[62]
GAPDH	Forward: 5'-CCATGAGAAGTATGACAACAGCC-3' Reverse: 5'-CCTTCCACGATACCAAGTTG-3'	[64]

non-normal data). Two-way ANOVA was performed on western blot, metabolic activity, cell number and gene expression data sets (independent variables: β-cyclodextrin loading and growth factor incubation), followed by Tukey-honest significant difference *post hoc* tests. For cell experiments, scaffolds at each time point were analyzed for all metrics, however, no statistical analyses was performed between time points. Significance was set at  $p < 0.05$ . Error is reported in figures as the standard error of the mean, unless otherwise noted.

## 3. Results

### 3.1. Scaffold pore microstructure

The pore microstructure of CG and CGcyclo scaffolds was examined by SEM. Both CG and CGcyclo scaffold variants showed an open porous structure, consistent with our previous studies, without any signs of differences as a result of cyclodextrin incorporation (Fig. 2A). Closer examination of CGcyclo scaffolds after carbodiimide crosslinking and subsequent CPD preparation reveals the CGcyclo scaffolds retained characteristic banding pattern of the collagen through the fabrication and SEM preparation processes (Fig. 2B). Additional images were acquired 72 h after MSC seeding show MSCs spreading out along the struts of the CG scaffolds (Fig. 2C).

### 3.2. β-cyclodextrin modified scaffolds sequester and retain TGF-β1 and BMP-2 more efficiently than conventional CG scaffolds

We first examined the retention of TGF-β1 within the CG vs. CGcyclo scaffold variants from a 5 ng/mL loading solution. Initial sequestration within all variants ranged between 45 and 50% of TGF-β1 in the loading solution, with CGcyclo scaffolds retaining significantly more TGF-β1 at all time points than standard CG scaffolds (Fig. 3A). We subsequently examined the retention of BMP-2 within the CG vs. CGcyclo scaffold variants from a 5 ng/mL loading solution. Initial sequestration within all variants was higher, ranging between 55 and 60% of the BMP-2 in the loading solution. Again, CGcyclo scaffolds retained significantly more BMP-2 within the scaffold network vs. CG scaffolds at all time points (Fig. 3B).

### 3.3. TGF-β1-β-cyclodextrin inclusion complexes increase metabolic activity and proliferation

After establishing the binding efficacy of CGcyclo scaffolds, the growth factor's presentation and effect on MSC response was explored. Specifically, the effect of TGF-β1 on cell number, metabolic activity and protein expression was examined. TGF-β1 had no effect on cellular proliferation (Fig. 4A) with all four experimental groups increasing from day 1 to day 3 and essentially

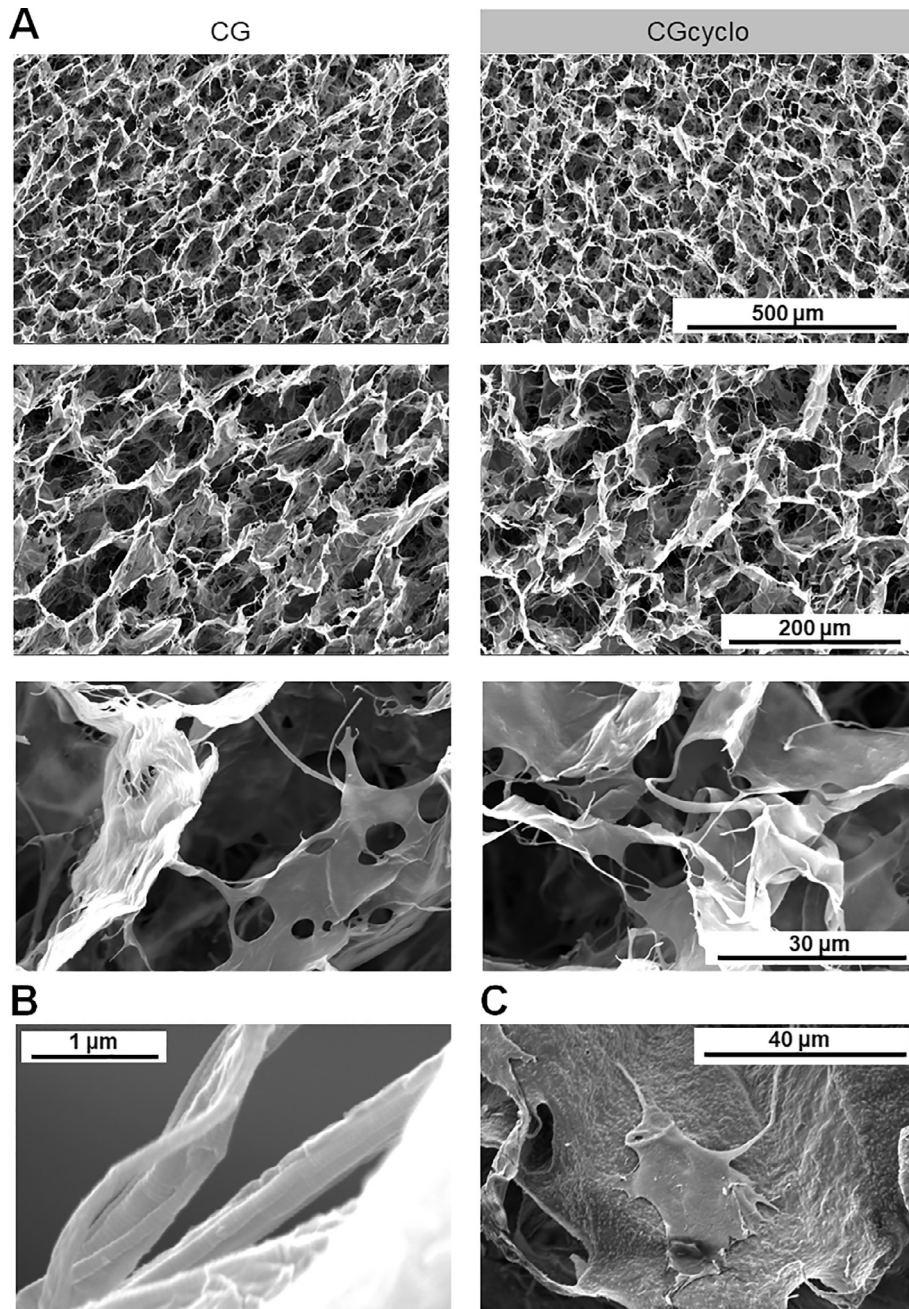


**Fig. 2.** CG and CGcyclo scaffold microstructure. (A) Comparative SEM images of the porous CG vs. CGcyclo scaffolds at 200 $\times$  (scale bar: 500  $\mu$ m), 400 $\times$  (scale bar: 200  $\mu$ m), and 3000 $\times$  (scale bar: 30  $\mu$ m). (B) High-magnification image of an individual collagen fiber banding within the CGcyclo scaffold microstructure. Scale bar: 1  $\mu$ m. (C) SEM image of hMSC spreading along CG scaffold surface. Scale bar: 40  $\mu$ m.

remaining constant to day 6. Conversely, there was a significant upregulation in cellular metabolic activity in the CGcyclo group with TGF- $\beta$ 1 at all three time points ( $p < 0.05$ ). Accounting for this equal cell count between all four groups, the distinct upregulation of cellular metabolic activity can be attributed to the enhanced initial retention of TGF- $\beta$  within the CGcyclo scaffolds (Fig. 4B).

#### 3.4. BMP-2- $\beta$ -cyclodextrin inclusion complexes increase metabolic activity and proliferation

In parallel with TGF- $\beta$ 1, the effect of BMP-2 on cell number and metabolic activity was also examined. It was found that BMP-2 has minor effects on cellular proliferation (Fig. 5A). Slightly lower cell numbers on the CGcyclo scaffolds with BMP-2 compared to the

CG scaffolds with no BMP-2 on day 1, while this trend was reversed on day 6. While significant, ( $p < 0.05$ ) the magnitudes of these changes are small compared to the significantly lower metabolic activity observed in the CGcyclo scaffolds with BMP-2 compared to the three other groups at all time points. (Fig. 5B).

#### 3.5. TGF- $\beta$ 1- $\beta$ -cyclodextrin inclusion complexes activate the Smad 2/3 pathway

The effect of TGF- $\beta$ 1 inclusion into CGcyclo scaffolds on the activation of the Smad 2/3 and Smad 1/5/8 pathways was evaluated by SDS-PAGE and western blot on days 1 and 3. Samples showed an increased activation of the Smad 2/3 pathway on day 3 when exposed to TGF- $\beta$ 1 (Fig. 6A). The increased activation of Smad

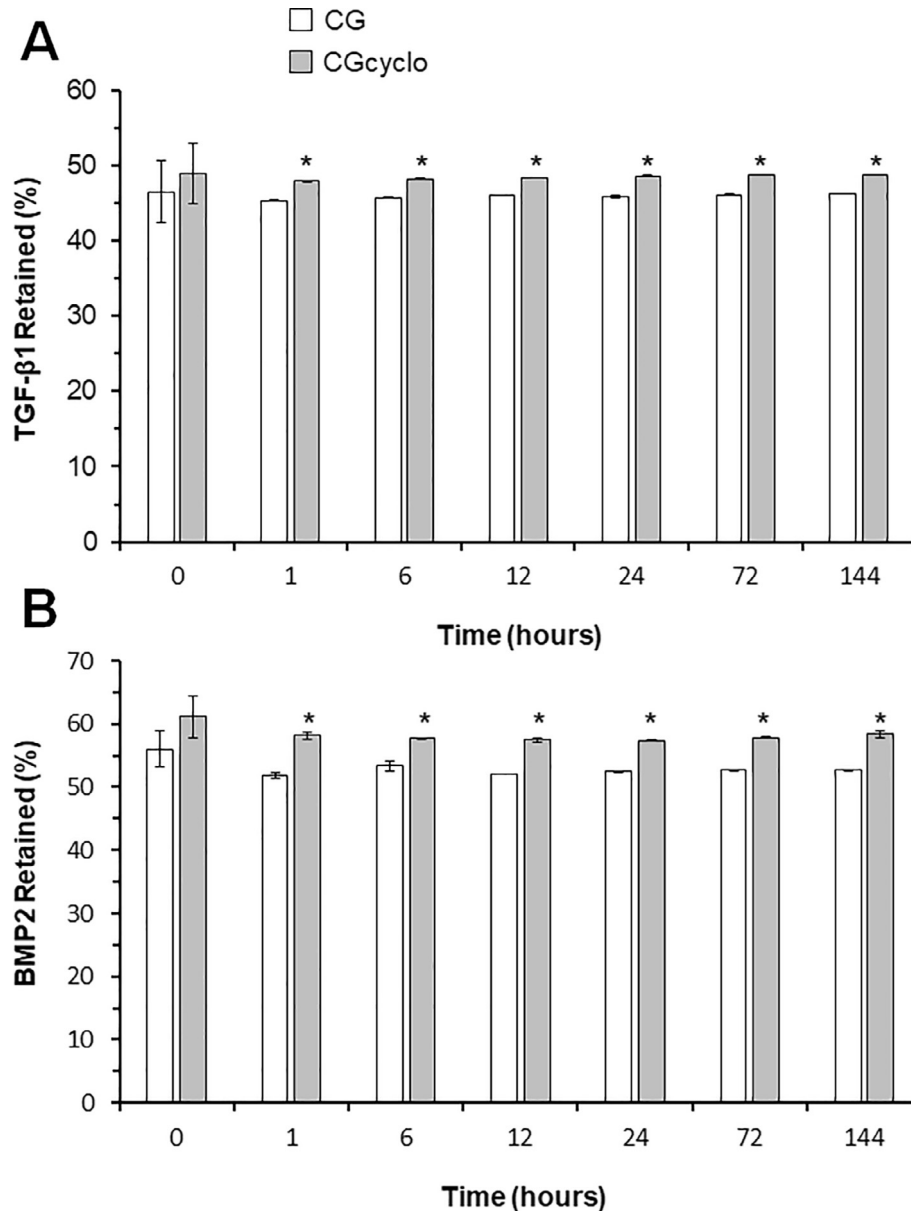


**Fig. 3.** Retention of TGF- $\beta$ 1 and BMP-2 within CG versus CGcyclo scaffolds. (A) Retention of TGF- $\beta$ 1 in CG vs. CGcyclo scaffolds for up to 6 days *in vitro* (5 ng/mL loading density). (B) Retention of BMP-2 in CG vs. CGcyclo scaffolds for up to 6 days *in vitro* (5 ng/mL loading density). \*:  $p < 0.05$ .

2/3 was significantly higher in the CGcyclo group with TGF- $\beta$ 1 compared to both the CG and CGcyclo groups without growth factor ( $p < 0.05$ ). The Smad 1/5/8 pathway was also examined to determine the non-targeted MSC cellular response to TGF- $\beta$ 1. No significant effects of the incorporation of  $\beta$ -cyclodextrin or TGF- $\beta$ 1 were observed on the activation of Smad 1/5/8 (Fig. 6B).

### 3.6. BMP-2- $\beta$ -cyclodextrin inclusion complexes activate the Smad 1/5/8 pathway

The effect of BMP-2 inclusion into CGcyclo scaffolds on the activation of the Smad 2/3 and Smad 1/5/8 pathways was also evaluated on days 1 and 3. Significant upregulation of Smad 2/3 activation was seen in the CGcyclo scaffolds with BMP-2 compared to the other three groups on day 1 (Fig. 7A) ( $p < 0.05$ ). Additionally, while not significant, there was a general trend of increased activation of the Smad 1/5/8 pathway in the CGcyclo group with BMP-2 compared to the other three groups (Fig. 7B).

### 3.7. TGF- $\beta$ 1- $\beta$ -cyclodextrin inclusion complexes increase tenogenic gene expression

The resultant effect of TGF- $\beta$ 1 inclusion into CGcyclo scaffolds on MSC chondrogenic gene expression was evaluated on days 1, 3 and 6 (Fig. 8A–C). While the expression levels for ACAN were quite low, large increases in expression of COMP and SOX9 were observed in the CGcyclo group with TGF- $\beta$ 1. The expression levels for ACAN were considerably lower throughout the experiment and were found to be significantly downregulated in both the CG and CGcyclo groups with TGF- $\beta$ 1 on day 6 ( $p < 0.05$ ). Conversely, expression levels for COMP were significantly higher in the groups with TGF- $\beta$ 1 compared to the unsupplemented CG and CGcyclo groups on days 1 and 3, while the CGcyclo group with TGF- $\beta$ 1 was significantly higher than all three other groups on day 6 ( $p < 0.05$ ). By day 6, the expression levels of SOX9 were significantly higher in just the CGcyclo group with TGF- $\beta$ 1 compared to all three other groups ( $p < 0.05$ ).

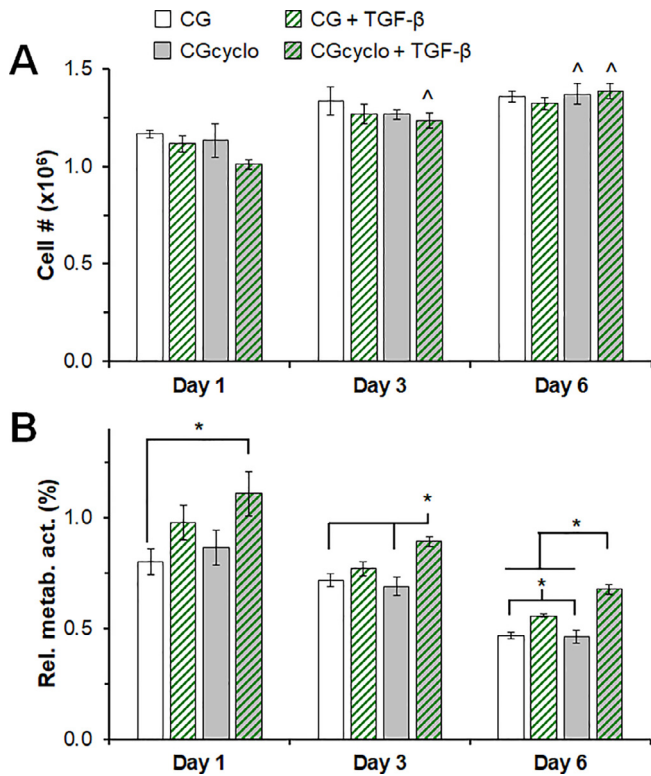


**Fig. 4.** MSC viability in CG scaffolds exposed to TGF- $\beta$ 1. (A) Number of cells and (B) normalized metabolic activity (versus the cells originally seeded into the scaffold) in unmodified CG or  $\beta$ -cyclodextrin CG scaffolds with and without TGF- $\beta$ 1 on days 1, 3, and 6 after seeding. Data expressed as mean  $\pm$  SEM ( $n = 6$ ). \*:  $p < 0.05$ . ^:  $p < 0.05$  versus day 1 within each scaffold group.

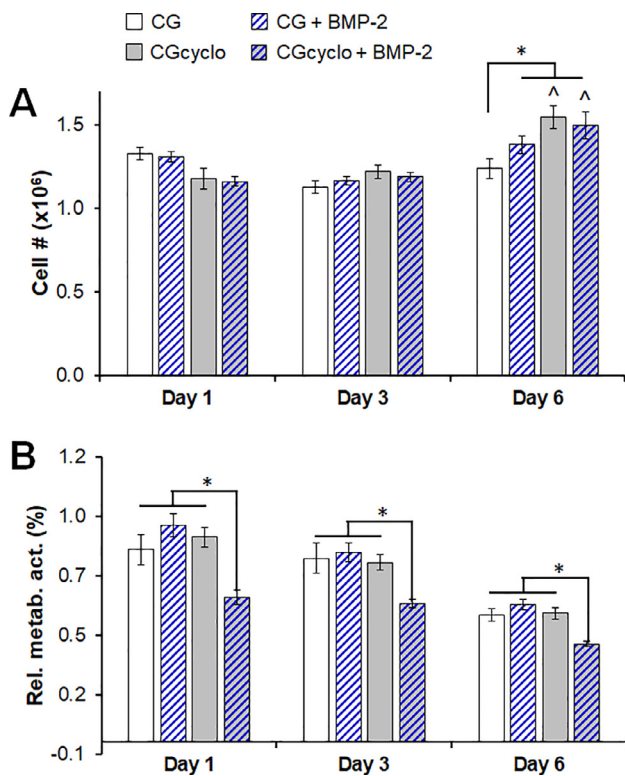


**Fig. 5.** MSC viability in CG scaffolds exposed to BMP-2. (A) Number of cells and (B) normalized metabolic activity (versus the cells originally seeded into the scaffold) in unmodified CG and  $\beta$ -cyclodextrin CG scaffolds with and without BMP-2 on days 1, 3, and 6 after seeding. Data expressed as mean  $\pm$  SEM ( $n = 6$ ). \*:  $p < 0.05$  between groups. ^:  $p < 0.05$  versus day 1 within each scaffold group.

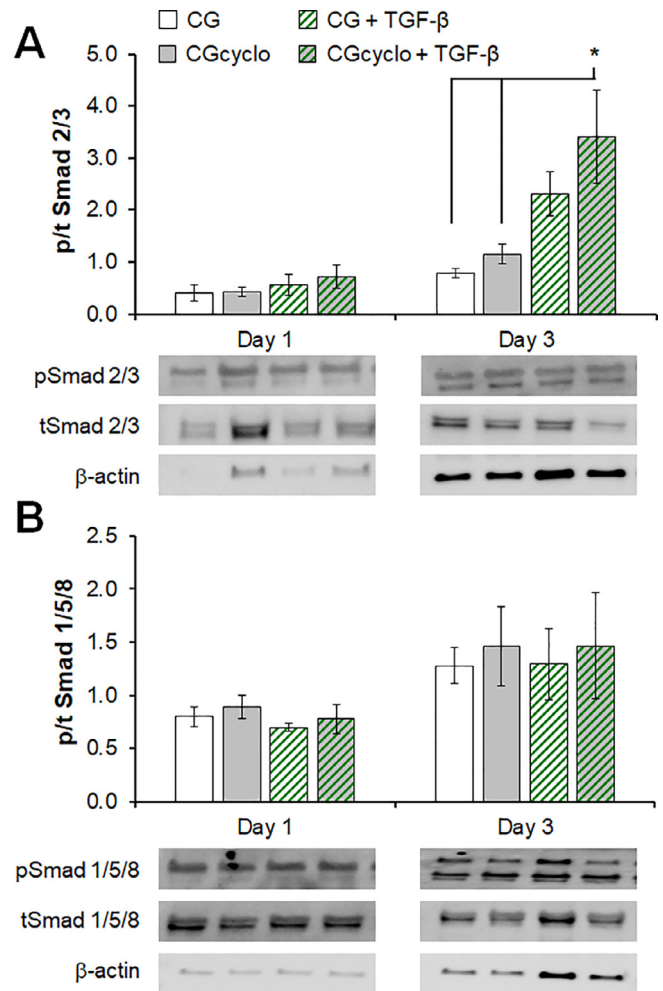


**Fig. 6.** Smad pathway activation in CG scaffolds exposed to TGF- $\beta$ 1. Relative levels of phosphorylated/total (p/t) (A) Smad 2/3 and (B) Smad 1/5/8 in scaffolds with and without TGF- $\beta$ 1 as determined by immunoblot on days 1 and 3 after seeding. Data expressed as mean  $\pm$  SEM ( $n = 3$ ). \*:  $p < 0.05$ .

#### 4. Discussion

Previous research from our group has shown that porous CG scaffolds serve as robust supports for both the stable culture of MSCs and their subsequent differentiation to tendon, cartilage, and osteogenic phenotypes [11,40,42,44]. Here, we examined a novel approach to accelerate this differentiation through the more efficient loading and display of growth factors into the CG scaffolds via  $\beta$ -cyclodextrin sequestration. As previously stated, the driving force for  $\beta$ -cyclodextrin sequestration is hydrophobic interactions. Therefore, it is crucial that the host molecule contains hydrophobic moieties to interact with the interior of  $\beta$ -cyclodextrin. Examination of TGF- $\beta$ 1 reveals exposed hydrophobic regions through  $\beta$ -strands  $\beta$ -8 and  $\beta$ -9 that form the 'bow-tie' link of its two arm domains and through an extended loop connecting  $\alpha$ 1 and  $\alpha$ 2 helices rich in proline and aromatic residues [45]. It is this region, directly surrounding the  $\alpha$ 1 helix, that most likely binds the interior of  $\beta$ -cyclodextrin, as it is more exposed on the tip of the molecule and most extensively hydrophobic in character. BMP-2 has been found to contain hydrophobic residues throughout the molecule and in particular local density at the bottom of the growth factor's central cleft [46]. The fundamental mechanism for  $\beta$ -cyclodextrin sequestration is applicable to the two growth factors, as it is also

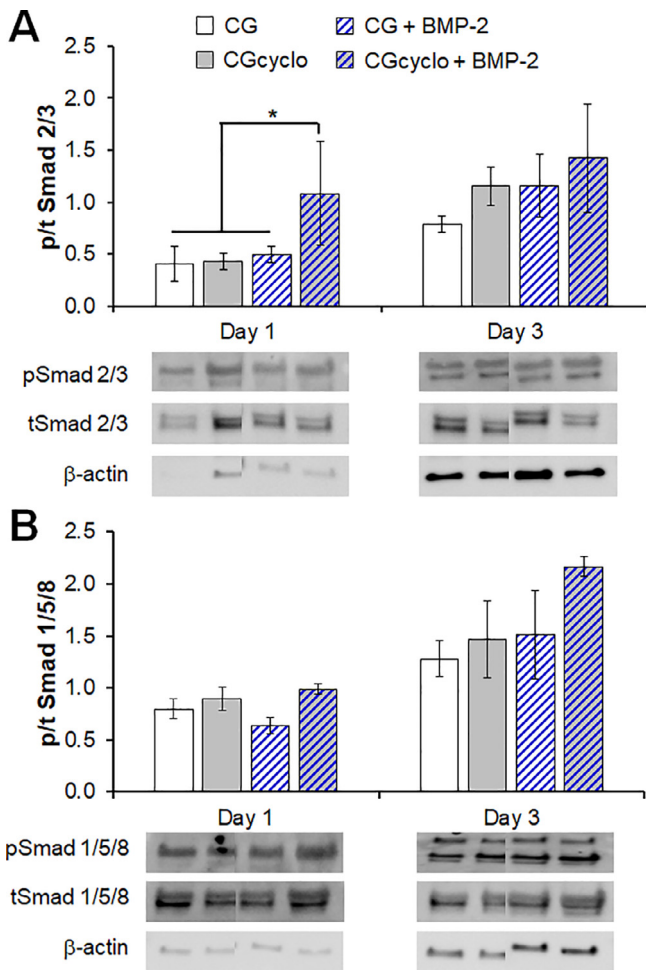


**Fig. 7.** Smad pathway activation in CG scaffolds exposed to BMP-2. Relative levels of phosphorylated/total (p/t) (A) Smad 2/3 and (B) Smad 1/5/8 in scaffolds with and without BMP-2 as determined by immunoblot on days 1 and 3 after seeding. Data expressed as mean  $\pm$  SEM ( $n = 3$ ). \*:  $p < 0.05$ .

known that BMPR-II:BMP-2 complex interactions are dominantly hydrophobic in nature, proven through residue mutations, and TGF- $\beta$  receptor:ligand complexes result from a combination of hydrophobic and electrostatic interactions [47,48].

Elucidating the sequestration mechanism for each growth factor to  $\beta$ -cyclodextrin clarifies the results of the work presented. The additional TGF- $\beta$ 1 and BMP-2 retained by the CGcyclo scaffolds compared to the CG scaffold over the course of the *in vitro* culture period can be attributed to  $\beta$ -cyclodextrin incorporation. The retention of TGF- $\beta$ 1 or BMP-2 in the CGcyclo scaffolds makes them an ideal candidate for the control of MSC fate as we have shown here, and also suggest that CGcyclo scaffolds may sequester a broader range of endogenously produced factors as well, which may also enhance cell activity. These results are similar to previous findings by our group using modification to the glycosaminoglycan content of the CG scaffolds (heparin sulfate vs. chondroitin sulfate), finding scaffolds incorporating more highly charged heparin sulfate were able to sequester model biomolecules more efficiently and that sequestration led to significant changes in cell bioactivity [49].

Bone morphogenetic proteins (BMPs) belong to the larger transforming growth factor  $\beta$  (TGF- $\beta$ ) superfamily, which regulate a wide array of cellular functions including cell migration, adhesion, division, and differentiation throughout the human life span [50]. TGF- $\beta$ 1 and BMP-2 are generally respectively associated with Smad

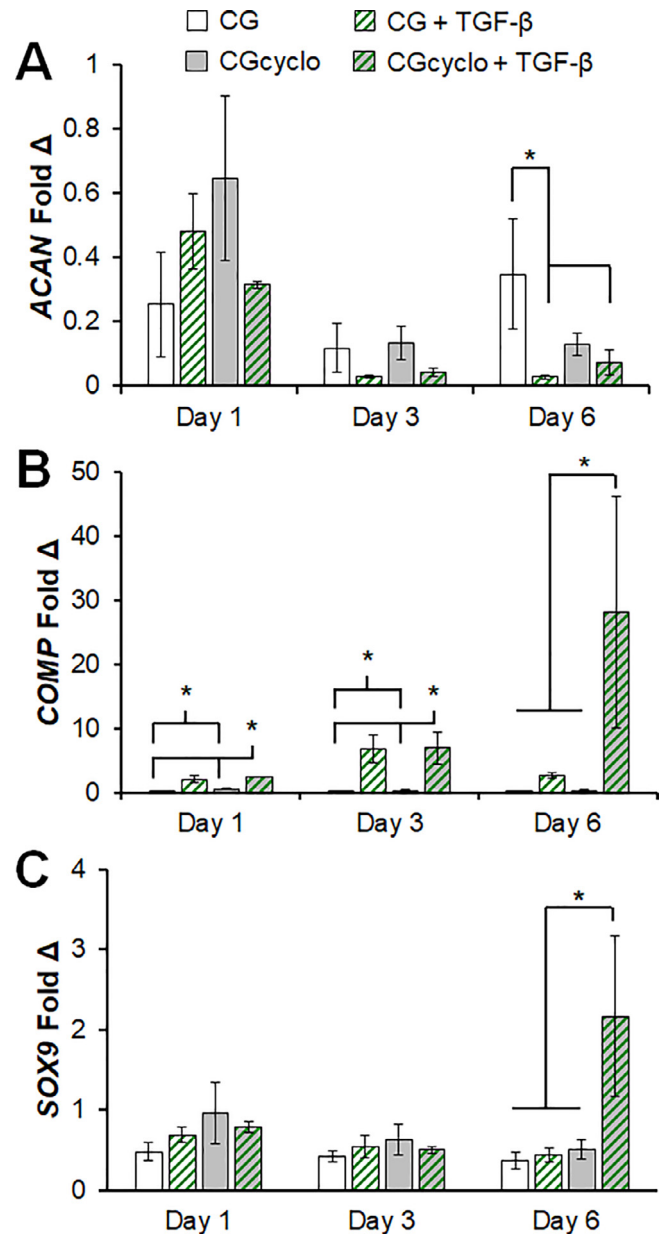


**Fig. 8.** Changes in pro-chondrogenic gene expression in response to TGF- $\beta$ 1. Expression levels of (A) ACAN, (B) COMP, and (C) SOX9 with and without TGF- $\beta$ 1 exposure on days 1, 3, and 6. Data expressed as mean  $\pm$  SEM ( $n = 6$ ). \*:  $p < 0.05$ .

2/3 and Smad 1/5/8 signaling [51]. Thus, cell metabolic activity and Smad pathway activation were consequently employed as the metrics for increased growth factor loading. Previous work has shown that the minimum effective concentrations for TGF- $\beta$ 1 and BMP-2 are 0.02–2.0 ng/mL and  $\sim$ 20 ng/mL respectively [52,53]. This difference in threshold concentration may help to explain the lower activity of BMP-2 compared to TGF- $\beta$ 1 in this study.

TGF- $\beta$ 1 functionalized CGCyclus scaffolds was found to increase cellular metabolic activity, Smad 2/3 pathway activation, and the expression of chondrogenic markers COMP and SOX9. This is consistent with previous work where TGF- $\beta$ 1 has been found to stimulate proliferation and self-renewal of MSCs and inhibit differentiation into osteocytic lineages through Smad 3 signaling [51]. TGF- $\beta$ 1 has also been found to co-stimulate Smad 2/3 through phosphorylation that collectively associates into a larger transcription factor complex [54,55]. Phosphorylated Smad 2/3 has then

been shown to stimulate tenogenic lineages in conjunction with *COMP*, *ACAN*, and *SOX9* expression [11,40,56].

Conversely, BMP-2 functionalized CGCyclo scaffolds was found to lead to a slight drop in cellular metabolic activity and simultaneously generally increase Smad 1/5/8 phosphorylation. The BMP II receptor-mediated phosphorylation of Smad 1/5/8 allows the activated isoforms to associate with Smad 4, translocate to the nucleus, and stimulate transcription of target genes related to bone deposition, making the 1/5/8 signaling pathway critical in MSC osteogenic signaling [57–59]. The upregulation of one such target gene, runt-related transcription factor 2 (*RUNX2*), has been found to lead to the subsequent expression of alkaline phosphatase (*ALP*) and osteocalcin (*OC*), genes critical for bone formation [53]. The activation of the Smad 1/5/8 osteogenic pathway strongly correlates with the metabolic activity data presented in Fig. 4, as MSCs in the early stages of osteoblastic differentiation rarely divided compared to the more immature MSCs [60,61].

One additional potential benefit to the incorporation of  $\beta$ -cyclodextrin into the CG scaffold is the possibility of non-specific sequestration of growth factors and other biomolecules from serum or factors that are produced endogenously by cells within the scaffold. Since the sequestration method of  $\beta$ -cyclodextrin is primarily through hydrophobic interactions, this could allow for unoccupied  $\beta$ -cyclodextrin entities within the scaffold to non-selectively sequester various factors from serum, resulting in increased availability within the scaffold and improved cell viability. This could account for the increased cell numbers noticed in the CGcyclo groups on day 6 in Fig. 5. Both CGcyclo groups displayed higher cell numbers than the CG scaffold groups regardless of growth factor treatment. Thus, in addition to using pre-culture exposure to specific growth factors to tailor cell responses, the incorporation of  $\beta$ -cyclodextrin into CG scaffolds could potentially be used to improve general cell viability and proliferation through the non-selective sequestration and presentation of serum factors. Here, efforts could also take advantage of the range of cyclodextrin variants (e.g.,  $\alpha$ -cyclodextrin,  $\beta$ -cyclodextrin,  $\gamma$ -cyclodextrin) [23,24] may provide increasing capacity to alter the availability of subsets of biomolecular signals.

## 5. Conclusions

The work presented demonstrates the ability for  $\beta$ -cyclodextrins to bind growth factors from solution prior to cell-seeding through cyclodextrin inclusion complexes formation as a means to accelerate MSC differentiation with lineage guidance dependent on growth factor bound. This mechanism can effectively lower the *in vitro* concentration of growth factors needed to induce cellular responses and can be potentially utilized for a variety of growth factors, cell types and applications in the hope of driving down patient related costs. This work establishes a new method for the successful incorporation and display of growth factors within CG scaffolds which, in combination with previously developed methods, has the potential to allow for more intricate designs for the selective display of multiple factors.

## Acknowledgements

The authors would like to acknowledge the Carl R. Woese Institute for Genomic Biology Core Facilities for assistance with real-time PCR system and immunoblotting. This research was carried out in part at the Imaging Technology Group within the Beckman Institute for Advanced Science and Technology at the University of Illinois at Urbana-Champaign. The authors would like to thank Scott Robinson and Cate Wallace for assistance with critical point drying and scanning electron microscopy. Research reported in this

publication was supported by the National Institute of Arthritis and Musculoskeletal and Skin Diseases of the National Institutes of Health under Award Number R21 AR063331. This work was also supported by the Office of the Assistant Secretary of Defense for Health Affairs Broad Agency Announcement for Extramural Medical Research through the Award No. W81XWH-16-1-0566. Opinions, interpretations, conclusions and recommendations are those of the authors and are not necessarily endorsed by the Department of Defense. Additional support was provided by the Chemical and Biomolecular Engineering Dept. and the Carl R. Woese Institute for Genomic Biology (BACH) at the University of Illinois at Urbana-Champaign.

## References

- I.V. Yannas, E. Lee, D.P. Orgill, E.M. Skrabut, G.F. Murphy, Synthesis and characterization of a model extracellular matrix that induces partial regeneration of adult mammalian skin, *Proc. Natl. Acad. Sci. U.S.A.* 86 (3) (1989) 933–937.
- S.R. Caliar, D.W. Weisgerber, M.A. Ramirez, D.O. Kelkhoff, B.A.C. Harley, The influence of collagen-glycosaminoglycan scaffold relative density and microstructural anisotropy on tenocyte bioactivity and transcriptomic stability, *J. Mech. Behav. Biomed. Mater.* 11 (2012) 27–40.
- S.R. Caliar, B.A.C. Harley, Composite growth factor supplementation strategies to enhance tenocyte bioactivity in aligned collagen-GAG scaffolds, *Tissue Eng. Part A* 19 (9–10) (2012) 1100–1112.
- S.R. Caliar, B.A.C. Harley, The effect of anisotropic collagen-GAG scaffolds and growth factor supplementation on tendon cell recruitment, alignment, and metabolic activity, *Biomaterials* 32 (23) (2011) 5330–5340.
- B.A. Harley, A.K. Lynn, Z. Wissner-Gross, W. Bonfield, I.V. Yannas, L.J. Gibson, Design of a multiphase osteochondral scaffold. II. Fabrication of a mineralized collagen-glycosaminoglycan scaffold, *J. Biomed. Mater. Res. Part A* 9999A (2009). NA–NA.
- E. Quinlan, A. Lopez-Noriega, E. Thompson, H.M. Kelly, S.A. Cryan, F.J. O'Brien, Development of collagen-hydroxyapatite scaffolds incorporating PLGA and alginate microparticles for the controlled delivery of rhBMP-2 for bone tissue engineering, *J. Control Release* 198 (2015) 71–79.
- X. Ren, V. Tu, D. Bischoff, D.W. Weisgerber, M.S. Lewis, D.T. Yamaguchi, T.A. Miller, B.A.C. Harley, J.C. Lee, Nanoparticulate mineralized collagen scaffolds induce *in vivo* bone regeneration independent of progenitor cell loading or exogenous growth factor stimulation, *Biomaterials* 89 (2016) 67–78.
- X. Ren, D.W. Weisgerber, D. Bischoff, M.S. Lewis, R.R. Reid, T.-C. He, D.T. Yamaguchi, T.A. Miller, B.A.C. Harley, J.C. Lee, Nanoparticulate mineralized collagen scaffolds and BMP-9 induce a long term bone cartilage construct in human mesenchymal stem cells, *Adv. Healthcare Mater.* 5 (14) (2016) 1821–1830.
- X. Ren, D. Bischoff, D.W. Weisgerber, M.S. Lewis, V. Tu, D.T. Yamaguchi, T.A. Miller, B.A. Harley, J.C. Lee, Osteogenesis on nanoparticulate mineralized collagen scaffolds via autogenous activation of the canonical BMP receptor signaling pathway, *Biomaterials* 50 (2015) 107–114.
- D.W. Weisgerber, S.R. Caliar, B.A.C. Harley, Mineralized collagen scaffolds induce hMSC osteogenesis and matrix remodeling, *Biomater. Sci.* 3 (3) (2015) 533–542.
- S.R. Caliar, B.A. Harley, Collagen-GAG scaffold biophysical properties bias MSC lineage choice in the presence of mixed soluble signals, *Tissue Eng. Part A* 20 (17–18) (2014) 2463–2472.
- J.M. Banks, L.C. Mozdzen, B.A.C. Harley, R.C. Bailey, The combined effects of matrix stiffness and growth factor immobilization on the bioactivity and differentiation capabilities of adipose-derived stem cells, *Biomaterials* 35 (32) (2014) 8951–8959.
- T.A. Martin, S.R. Caliar, P.D. Williford, B.A. Harley, R.C. Bailey, The generation of biomolecular patterns in highly porous collagen-GAG scaffolds using direct photolithography, *Biomaterials* 32 (16) (2011) 3949–3957.
- L.C. Mozdzen, A. Vucetic, B.A.C. Harley, Modifying the strength and strain concentration profile within collagen scaffolds using customizable arrays of poly-lactic acid fibers, *J. Mech. Behav. Biomed. Mater.* 66 (2017) 28–36.
- S.E. Sakiyama-Elbert, J.A. Hubbell, Controlled release of nerve growth factor from a heparin-containing fibrin-based cell ingrowth matrix, *J. Control Release* 69 (1) (2000) 149–158.
- G.A. Hudalla, N.A. Kouris, J.T. Koepsel, B.M. Ogle, W.L. Murphy, Harnessing endogenous growth factor activity modulates stem cell behavior, *Integr. Biol. (Camb.)* 3 (8) (2011) 832–842.
- R.A. Hortensius, B.A.C. Harley, The use of bioinspired alterations in the glycosaminoglycan content of collagen-GAG scaffolds to regulate cell activity, *Biomaterials* 34 (31) (2013) 7645–7652.
- R.A. Hortensius, J.H. Ebens, B.A.C. Harley, Immunomodulatory effects of amniotic membrane matrix incorporated into collagen scaffolds, *J. Biomed. Mater. Res. A* 104 (6) (2016) 1332–1342.
- D.S. Benoit, S.D. Collins, K.S. Anseth, Multifunctional hydrogels that promote osteogenic hMSC differentiation through stimulation and sequestering of BMP2, *Adv. Funct. Mater.* 17 (13) (2007) 2085–2093.

- [20] D.S. Benoit, A.R. Durney, K.S. Anseth, The effect of heparin-functionalized PEG hydrogels on three-dimensional human mesenchymal stem cell osteogenic differentiation, *Biomaterials* 28 (1) (2007) 66–77.
- [21] C. Borselli, H. Storrer, F. Benesch-Lee, D. Shvartsman, C. Cezar, J.W. Lichtman, H. H. Vandenberg, D.J. Mooney, Functional muscle regeneration with combined delivery of angiogenesis and myogenesis factors, *Proc. Natl. Acad. Sci.* 107 (8) (2010) 3287–3292.
- [22] M.M. Martino, J.A. Hubbell, The 12th–14th type III repeats of fibronectin function as a highly promiscuous growth factor-binding domain, *FASEB J.* 24 (12) (2010) 4711–4721.
- [23] P. Mura, Analytical techniques for characterization of cyclodextrin complexes in aqueous solution: a review, *J. Pharm. Biomed. Anal.* 101 (2014) 238–250.
- [24] C.D. Radu, O. Parteni, L. Ochiuz, Applications of cyclodextrins in medical textiles – review, *J. Control Release* 224 (2016) 146–157.
- [25] D.C. Bibby, N.M. Davies, I.G. Tucker, Mechanisms by which cyclodextrins modify drug release from polymeric drug delivery systems, *Int. J. Pharm.* 197 (1–2) (2000) 1–11.
- [26] E.M.M. Del Valle, Cyclodextrins and their uses: a review, *Process Biochem.* 39 (12) (2004) 1033–1046.
- [27] A. Cooper, Effect of cyclodextrins on the thermal stability of globular proteins, *J. Am. Chem. Soc.* 114 (1992) 2.
- [28] J. Horsky, J. Pitha, Inclusion complexes of proteins: interaction of cyclodextrins with peptides containing aromatic amino acids studied by competitive spectrophotometry, *J. Inclusion Phenom. Mol. Recognit. Chem.* 18 (1994) 10.
- [29] R. Machin, J.R. Isasi, I. Vélaz,  $\beta$ -Cyclodextrin hydrogels as potential drug delivery systems, *Carbohydr. Polym.* 87 (3) (2012) 2024–2030.
- [30] C. Liu, Z. Zhang, X. Liu, X. Ni, J. Li, Gelatin-based hydrogels with [small beta]-cyclodextrin as a dual functional component for enhanced drug loading and controlled release, *RSC Adv.* 3 (47) (2013) 25041–25049.
- [31] K.L. Liu, Z. Zhang, J. Li, Supramolecular hydrogels based on cyclodextrin-polymer polypseudorotaxanes: materials design and hydrogel properties, *Soft Matter* 7 (24) (2011) 11290–11297.
- [32] S.K. Osman, G.M. Soliman, S.A. El Rasoul, Physically cross-linked hydrogels of beta-cyclodextrin polymer and poly(ethylene glycol)-cholesterol as delivery systems for macromolecules and small drug molecules, *Curr. Drug Deliv.* 12 (4) (2015) 415–424.
- [33] C.B. Rodell, C.B. Highley, M.H. Chen, N.N. Dusaj, C. Wang, L. Han, J.A. Burdick, Evolution of hierarchical porous structures in supramolecular guest-host hydrogels, *Soft Matter* 12 (37) (2016) 7839–7847.
- [34] M. Soheilimoghaddam, G. Sharifzadeh, R.H. Pour, M.U. Wahit, W.T. Whye, X.Y. Lee, Regenerated cellulose/ $\beta$ -cyclodextrin scaffold prepared using ionic liquid, *Mater. Lett.* 135 (2014) 210–213.
- [35] M. Prabaharan, R. Jayakumar, Chitosan-graft- $\beta$ -cyclodextrin scaffolds with controlled drug release capability for tissue engineering applications, *Int. J. Biol. Macromol.* 44 (4) (2009) 320–325.
- [36] S.N. Yuen, J. Folkman, P.B. Weisz, M.M. Joullie, W.R. Ewing, Affinity of fibroblast growth factors for beta-cyclodextrin tetradecasulfate, *Anal. Biochem.* 185 (1) (1990) 108–111.
- [37] M. Madaghiele, A. Sannino, I.V. Yannas, M. Spector, Collagen-based matrices with axially oriented pores, *J. Biomed. Mater. Res. Part A* 85A (3) (2008) 757–767.
- [38] F.J. O'Brien, B.A. Harley, I.V. Yannas, L.J. Gibson, The effect of pore size on cell adhesion in collagen-GAG scaffolds, *Biomaterials* 26 (4) (2005) 433–441.
- [39] Y.-J. Kim, R.L.Y. Sah, J.-Y.H. Doong, A.J. Grodzinsky, Fluorometric assay of DNA in cartilage explants using Hoechst 33258, *Anal. Biochem.* 174 (1) (1988) 168–176.
- [40] W.G. Grier, A.S. Moy, B.A. Harley, Cyclic tensile strain enhances human mesenchymal stem cell Smad 2/3 activation and tenogenic differentiation in anisotropic collagen-glycosaminoglycan scaffolds, *Eur. Cell Mater.* 33 (2017) 227–239.
- [41] E.G. Tierney, G.P. Duffy, S.A. Cryan, C.M. Curtin, F.J. O'Brien, Non-viral gene-activated matrices-next generation constructs for bone repair, *Organogenesis* 9 (1) (2013).
- [42] S.R. Caliani, D.W. Weisgerber, W.K. Grier, Z. Mahmassani, M.D. Boppert, B.A.C. Harley, Collagen scaffolds incorporating coincident gradations of instructive structural and biochemical cues for osteotendinous junction engineering, *Adv. Healthcare Mater.* 4 (6) (2015) 831–837.
- [43] G.P. Duffy, T.M. McFadden, E.M. Byrne, S.L. Gill, E. Farrell, F.J. O'Brien, Towards in vitro vascularisation of collagen-GAG scaffolds, *Eur. Cells Mater.* 21 (2011) 15–30.
- [44] S.R. Caliani, E.A. Gonnerman, W.K. Grier, D.W. Weisgerber, J.M. Banks, A.J. Alsop, J.S. Lee, R.C. Bailey, B.A. Harley, Collagen scaffold arrays for combinatorial screening of biophysical and biochemical regulators of cell behavior, *Adv. Healthcare Mater.* 4 (1) (2015) 58–64.
- [45] M. Shi, J. Zhu, R. Wang, X. Chen, L. Mi, T. Walz, T.A. Springer, Latent TGF-beta structure and activation, *Nature* 474 (7351) (2011) 343–349.
- [46] C. Scheufler, W. Sebald, M. Hulsmeier, Crystal structure of human bone morphogenetic protein-2 at 2.7 Å resolution, *J. Mol. Biol.* 287 (1) (1999) 103–115.
- [47] J.P. Hinck, Structural studies of the TGF-betas and their receptors – insights into evolution of the TGF-beta superfamily, *FEBS Lett.* 586 (14) (2012) 1860–1870.
- [48] J.P. Yin, P. Fu, X.S. Xie, F. Liu, L. Zhou, Effects of piperazine ferulate on connective tissue growth factor and extracellular matrix in TGF-beta1 induced mesangial cells, *Sichuan Da Xue Xue Bao Yi Xue Ban* 39 (5) (2008) 732–735.
- [49] R.A. Hortensius, B.A. Harley, The use of bioinspired alterations in the glycosaminoglycan content of collagen-GAG scaffolds to regulate cell activity, *Biomaterials* 34 (31) (2013) 7645–7652.
- [50] J. Massague, Y.G. Chen, Controlling TGF-beta signaling, *Genes Dev* 14 (6) (2000) 627–644.
- [51] X. Guo, X.F. Wang, Signaling cross-talk between TGF-beta/BMP and other pathways, *Cell Res.* 19 (1) (2009) 71–88.
- [52] F. Zhang, M. Laiho, On and off: proteasome and TGF-beta signaling, *Exp. Cell Res.* 291 (2) (2003) 275–281.
- [53] H. Lysdahl, A. Baatrup, C.B. Foldager, C. Bunger, Preconditioning human mesenchymal stem cells with a low concentration of BMP2 stimulates proliferation and osteogenic differentiation in vitro, *Biores. Open Access* 3 (6) (2014) 278–285.
- [54] J. Massague, D. Wotton, Transcriptional control by the TGF-beta/Smad signaling system, *Embo J.* 19 (8) (2000) 1745–1754.
- [55] X. Xin, X.H. Li, J.Z. Wu, K.H. Chen, Y. Liu, C.J. Nie, Y. Hu, M.W. Jin, Pentamethylquercetin ameliorates fibrosis in diabetic Goto-Kakizaki rat kidneys and mesangial cells with suppression of TGF-beta/Smads signaling, *Eur. J. Pharmacol.* 713 (1–3) (2013) 6–15.
- [56] W.K. Grier, E.M. Iyoha, B.A.C. Harley, The influence of pore size and stiffness on tenocyte bioactivity and transcriptomic stability in collagen-GAG scaffolds, *J. Mech. Behav. Biomed. Mater.* 65 (2017) 295–305.
- [57] C. Chen, H. Uludag, Z. Wang, H. Jiang, Noggin suppression decreases BMP-2-induced osteogenesis of human bone marrow-derived mesenchymal stem cells in vitro, *J. Cell. Biochem.* 113 (12) (2012) 3672–3680.
- [58] C.S. Soltanoff, S. Yang, W. Chen, Y.P. Li, Signaling networks that control the lineage commitment and differentiation of bone cells, *Crit. Rev. Eukaryot. Gene. Expr.* 19 (1) (2009) 1–46.
- [59] M. Beederman, J.D. Lamplot, G. Nan, J. Wang, X. Liu, L. Yin, R. Li, W. Shui, H. Zhang, S.H. Kim, W. Zhang, J. Zhang, Y. Kong, S. Denduluri, M.R. Rogers, A. Pratt, R.C. Haydon, H.H. Luu, J. Angeles, L.L. Shi, T.C. He, BMP signaling in mesenchymal stem cell differentiation and bone formation, *J. Biomed. Sci. Eng.* 6 (8A) (2013) 32–52.
- [60] M. Westhrin, M. Xie, M.O. Olderooy, P. Sikorski, B.L. Strand, T. Standal, Osteogenic differentiation of human mesenchymal stem cells in mineralized alginate matrices, *PLoS One* 10 (3) (2015) e0120374.
- [61] L. Malaval, F. Liu, P. Roche, J.E. Aubin, Kinetics of osteoprogenitor proliferation and osteoblast differentiation in vitro, *J. Cell. Biochem.* 74 (4) (1999) 616–627.
- [62] J. Zhou, C. Xu, G. Wu, X. Cao, L. Zhang, Z. Zhai, Z. Zheng, X. Chen, Y. Wang, In vitro generation of osteochondral differentiation of human marrow mesenchymal stem cells in novel collagen-hydroxyapatite layered scaffolds, *Acta Biomaterialia* 7 (11) (2011) 3999–4006.
- [63] F. Klatte-Schulz, S. Pauly, M. Scheibel, S. Greiner, C. Gerhardt, J. Hartwig, G. Schmidmaier, B. Wildemann, Characteristics and stimulation potential with BMP-2 and BMP-7 of tenocyte-like cells isolated from the rotator cuff of female donors, *PLoS One* 8 (6) (2013) e67209.
- [64] S. Pauly, F. Klatte, C. Strobel, G. Schmidmaier, S. Greiner, M. Scheibel, B. Wildemann, Characterization of tendon cell cultures of the human rotator cuff, *Eur. Cell Mater.* 20 (2010) 84–97.

# Shape-fitting collagen-PLA composite promotes osteogenic differentiation of porcine adipose stem cells

Marley J. Dewey<sup>1</sup>, Eileen M. Johnson<sup>2</sup>, Daniel W. Weisgerber<sup>1</sup>, Matthew B. Wheeler<sup>2,4</sup>,  
Brendan A.C. Harley<sup>2,3,4</sup>

<sup>1</sup> Dept. of Materials Science and Engineering

<sup>2</sup> Dept. of Bioengineering

<sup>3</sup> Dept. of Chemical and Biomolecular Engineering

<sup>4</sup> Carl R. Woese Institute for Genomic Biology  
University of Illinois at Urbana-Champaign  
Urbana, IL 61801

## Corresponding Author:

B.A.C. Harley  
Dept. of Chemical and Biomolecular Engineering  
Carl R. Woese Institute for Genomic Biology  
University of Illinois at Urbana-Champaign  
110 Roger Adams Laboratory  
600 S. Mathews Ave.  
Urbana, IL 61801  
Phone: (217) 244-7112  
Fax: (217) 333-5052  
e-mail: [bharley@illinois.edu](mailto:bharley@illinois.edu)

## ABSTRACT

Craniomaxillofacial bone defects can occur as a result of congenital, post-oncologic, and high-energy impact conditions. The scale and irregularity of such defects motivate new biomaterials to promote regeneration of the damaged bone. We have recently described a mineralized collagen scaffold capable of instructing stem cell osteogenic differentiation and new bone infill in the absence of traditional osteogenic supplements. Herein, we report the integration of a millimeter-scale reinforcing poly (lactic acid) frame fabricated via 3D-printing into the mineralized collagen scaffold with micron-scale porosity to form a multi-scale mineralized collagen-PLA composite. We describe modifications to the PLA frame design to increase the compressive strength (Young's Modulus, ultimate stress and strain) of the composite. A critical challenge beyond increasing the compressive strength of the collagen scaffold is addressing challenges inherent with the irregularity of clinical defects. As a result, we examined the potential for modifying the frame architecture to render the composite with increased compressive strength in one axis or radial compressibility and shape-fitting capacity in an orthogonal axis. A library of mineralized collagen-PLA composites was mechanically characterized via compression testing and push-out test to describe mechanical performance and shape-fitting capacity. We also report *in vitro* comparison of the bioactivity of porcine adipose derived stem cells in the mineralized collagen-PLA composite versus the mineralized collagen scaffold via metabolic activity, gene expression, and functional matrix synthesis. The results suggest that incorporation of the PLA reinforcing frame does not negatively influence the osteoinductive nature of the mineralized collagen scaffold. Together, these findings suggest a strategy to address often competing bioactivity, mechanical strength, and shape-fitting design requirements for biomaterials for craniomaxillofacial bone regeneration.

**Abbreviations:** PLA: poly(lactic acid), CMF: cranio-maxillofacial, PCL: poly(caprolactone), pASC: porcine adipose derived stem cell

**Keywords:** collagen, poly lactic acid, stem cell, osteogenesis, conformal fitting

**Running Head:** Collagen-PLA composite for craniofacial bone repair

## 1. Introduction

Cranio-maxillofacial defects (CMF) are bone defects that will not heal without surgical intervention due to the defect being too large to heal naturally by the body (Spicer et al., 2012). CMF defects are associated with a range of trauma, from birth defects such as cleft palate to surgical resection of head and neck cancers and high energy impacts such as battlefield injuries. The gold standard for treating such defects remains either permanent implants or biologic grafts such as patient-derived autograft tissue or allograft tissue, typically from a cadaveric donor (Depeyre et al., 2016). Allografts offer advantages in terms of ready supply and do not require a second surgery, but can exhibit significantly different osteogenic capacity and the possibility of enhanced immune response (Elsalanty and Genecov, 2009). While autografts do not lead to enhanced immune response and are naturally osteoconductive, their limited availability, need for a secondary surgical defect, and reduced healing capacity with age motivate a range of tissue engineering efforts (Thompson et al., 2015). Biomaterial approaches seek to address these concerns via an implantable material that provides the appropriate signals to promote cell recruitment, bioactivity, and eventual regenerative repair of the CMF defect. However, biomaterial solutions are not without challenges. Successful implants to improve regenerative healing must be biocompatible, meet micro-scale mechanical needs to promote osteogenesis as well as macro-scale requirements for a mechanically robust implant, be bioresorbable, and fit irregular defect margins. Such materials must be porous and support cell recruitment and bioactivity, be osteoconductive or osteoinductive in nature, and promote remodeling and the formation of vascular networks (Bose et al., 2012; Cunniffe et al., 2010). A poorly integrated bone replacement material can result in graft resorption, limited osteointegration, and the possibility of the material being lost or actively ejected from the defect (Nail et al., 2015; Zhang et al., 2014a).

One class of biomaterial that has received recent attention have been collagen-based scaffolds

and mineralized collagen composites (Donzelli et al., 2007; Farrell et al., 2006; Harley et al., 2010b; Kanungo et al., 2008; Murphy et al., 2010; Tierney et al., 2008). Porous collagen scaffolds offer an open pore structure to facilitate rapid cell attachment and invasion (Harley et al., 2008; O'Brien et al., 2005), and while they are mechanically weak, they have been shown to promote osteogenic differentiation and new mineral formation, typically through the addition of exogenous stimuli such as osteogenic media or BMP-2 (Curtin et al., 2012; Farrell et al., 2007). Recently, efforts in our lab and a number of other investigators have begun to demonstrate the potential of collagen-mineral composites. Here, nanocrystallite calcium phosphate mineral can be incorporated into or coated onto the collagen scaffold network to more closely approximate the compositional features of bone (Al-Munajjed et al., 2009; Caliari and Harley, 2014; Cunniffe et al., 2010; Curtin et al., 2012; Harley et al., 2010a; Weisgerber et al., 2015b). We have recently described the development of a calcium phosphate mineralized collagen scaffold containing glycosaminoglycans for CMF bone regeneration (Lee et al., 2015; Ren et al., 2016a; Weisgerber et al., 2015a). Notably, the mineralized collagen scaffold can promote mesenchymal stem cell (MSC) osteogenic differentiation and mineral biosynthesis *in vitro* (Lee et al., 2015; Ren et al., 2015; Weisgerber et al., 2015b), as well as new bone formation *in vivo* in both rabbit calvarial and porcine mandibular defects (Ren et al., 2016b; Ren et al., 2016c; Weisgerber et al., 2018), all in the absence of supplementary BMP-2. However, while these mineralized collagen scaffolds provide appropriate pore size and endogenous signals to promote osteogenic differentiation and matrix biosynthesis, their porous nature results in sub-optimal mechanical properties as stand-alone implants. Recently, we described fabrication approaches to integrate macro-porous (millimeter scale) polycaprolactone (PCL) polymer frame to create a mineralized collagen-PCL composite (Weisgerber et al., 2016a). The mineralized collagen-PCL composite possessed enhanced mechanical stiffness 6000-fold and promoted both bone marrow mesenchymal stem cell and porcine adipose derived stem cell (pASC) osteogenic differentiation *in vitro* (Ren et al., 2015; Weisgerber et al., 2016a). Further, the collagen-PCL composite

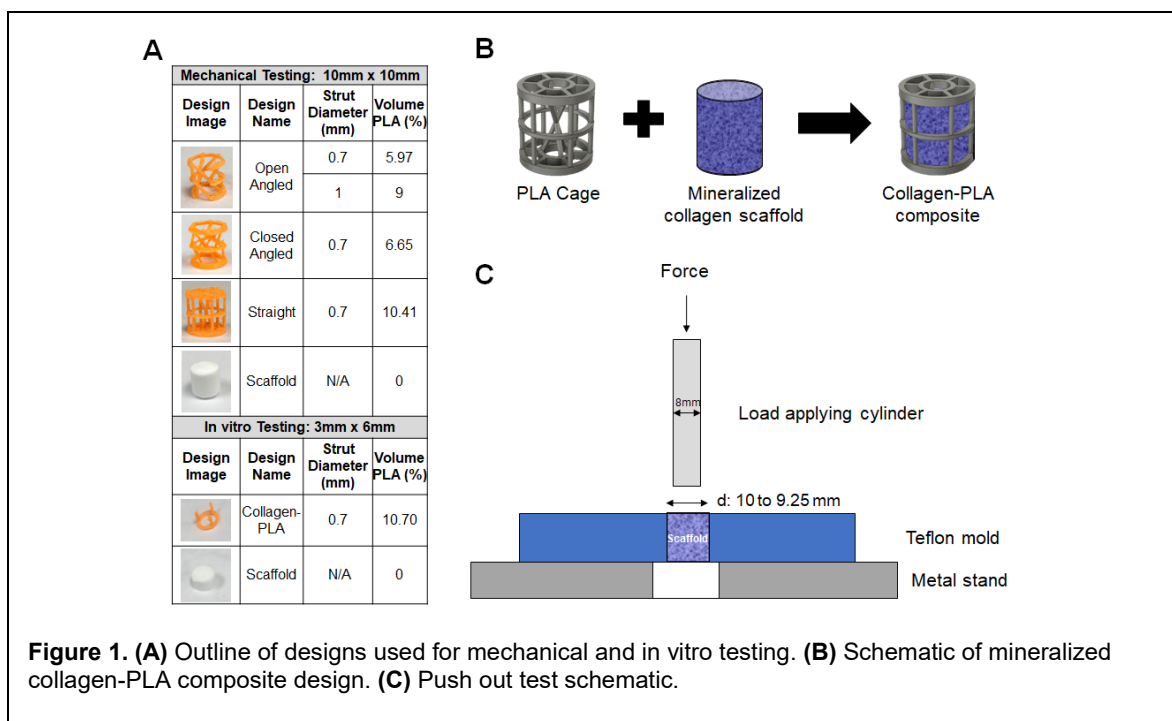
induced rapid bone in-fill *in vivo* in a large animal mandibular defect model in adolescent Yorkshire pigs (Weisgerber et al., 2018). However, two concerns noted with the current generation mineralized collagen-PCL composite was the slow degradation rate of the PCL polymer as well as the potential for poor fitting of the implant into an irregularly-shaped defect. Recent efforts by *Grunlan* et al. described an osteoconductive shape-memory biomaterial that possessed radial expansion capacity to improve conformal fitting between implant and defect margin (Nail et al., 2015; Zhang et al., 2014a), motivating efforts to redesign the polymeric reinforcement mesh of our mineralized collagen scaffold to improve the potential for conformal fitting within the defect margin.

In this manuscript, we describe the development and *in vitro* testing of a unique mineralized collagen-poly (lactic acid) (PLA) composite as a next-generation biomaterial for complex CMF defect repair that can support shape-fitting. PLA has been used extensively as a degradable polymeric biomaterial for a range of tissue engineering applications (Naderi et al., 2011), suggesting its use here to form a collagen-PLA composite biomaterial. We hypothesized that a low volume fraction frame architecture composed of mechanically-robust PLA could be incorporated into the mineralized collagen scaffold to form a composite with enhanced compressive strength. Further, this work seeks to demonstrate that modifications to the PLA frame geometry could render the collagen-PLA composite capable of returning to its original shape after being radially-compressed to enhance conformal fitting with defect margins. We first describe integration of the PLA frame into the mineralized collagen scaffold as well as the mechanical performance (ultimate stress, ultimate strain, elastic modulus, push-out strength) of the resultant mineralized collagen-PLA composite. We subsequently evaluate the functional capacity of the composite, examining attachment, proliferation, osteogenic differentiation, and mineral biosynthesis of porcine adipose derived stem cells in the mineralized collagen-PLA composite relative to the PLA cage or mineralized collagen scaffold alone.

## 2. Materials and Methods

### 2.1. 3D printing poly (lactic acid) cages

PLA cages were fabricated by extrusion printing of PLA filaments at 185°C using an Ultimaker 2+ 3D printer (Ultimaker, Geldermalsen, Netherlands) utilizing a 0.25 mm diameter nozzle. PLA cages were designed using the Fusion 360 (Autodesk, San Rafael, California) design program, with each design stored as a .stl file for fabrication. Two classes of collagen-PLA composites were used for this project. Mechanical testing was performed using cylindrical PLA cages (10 mm dia., 10 mm high) created in four distinct cage architectures of increasing complexity so as to examine the effect of PLA fiber thickness (0.7 mm vs. 1.0 mm) or the inclusion of design elements to alter compressive strength or space-fitting (angled vs. straight fibers; open vs. closed cage; **Fig. 1A**). These specimens are of the size used previously for *in vitro* testing of mineralized collagen scaffolds in a porcine mandibular defect model (10 mm dia., 10 mm thick cylindrical implants). However, the large volume of these implants made a comprehensive cell bioactivity study *in vitro* impractical in regards to the number of required adipose derived stem



cells. As a result, *in vitro* cell bioactivity and osteogenic assays to examine whether the inclusion of a PLA frame reduced the osteogenic capacity of the mineralized collagen scaffold were performed using a smaller cage design (6 mm dia., 6 mm high; **Fig. 1A**) fabricated with the same volume fraction of PLA (10.7% v/v) as in the larger composites tested mechanically (6 – 10.4% v/v PLA).

## **2.2 Fabrication of mineralized scaffolds and composites**

Scaffolds were fabricated by lyophilization of a mineralized collagen precursor suspension in a manner previously described (Weisgerber et al., 2015a). Briefly, the mineralized collagen suspension was prepared by homogenizing (1.9 w/v%) bovine type I collagen (Collagen Matrix, Oakland, NJ) and (0.84 w/v%) chondroitin-6-sulfate (Sigma-Aldrich, St. Louis, MO), and calcium salts ( $\text{Ca}(\text{OH})_2$ ,  $\text{Ca}(\text{NO}_3)_2 \cdot 4\text{H}_2\text{O}$ , Sigma-Aldrich), in phosphoric acid (Sigma-Aldrich). The mineralized collagen precursor suspension was then stored at 4°C and degassed before use. Scaffolds were then fabricated via lyophilization using a Genesis freeze-dryer (VirTis, Gardener, NY) (Harley et al., 2010a). The mineralized collagen suspension was pipetted into individual wells created in a polysulfone mold. Scaffolds were then fabricated by freezing the suspension via cooling from 20°C to -10°C at a constant rate of 1°C/min followed by a temperature hold at -10°C for 2 hours. The frozen suspension was then sublimated at 0°C and 0.2 Torr, resulting in a porous scaffold network.

Mineralized collagen-PLA composites were fabricated by pipetting the precursor suspension into wells, gently lowering the PLA cages into the mold, then adding remaining slurry to cover the cages completely (**Fig. 1B**) (Weisgerber et al., 2016a). Two classes of composites were fabricated to tests described in this manuscript. **Mechanical assays:** Large collagen-PLA composites were fabricated using PLA cages (10 mm dia., 10 mm high) placed into 11.9 mm dia., 10 mm high polysulfone wells with 1.2 mL suspension. ***In vitro* bioactivity assays:**

Smaller collagen-PLA composites, to reduce the number of cells required for *in vitro* experiments, were fabricated using smaller PLA cages (6 mm dia., 3 mm high) placed into 6 mm dia., 3 mm high polysulfone wells with 100  $\mu$ L suspension. Both classes of collagen-PLA composites were designed to have comparable PLA volume fractions (<11%) (**Fig. 1A**).

After fabrication, all scaffolds and composites were sterilized via ethylene oxide treatment for 12 hours utilizing an AN74i Anprolene gas sterilizer (Andersen Sterilizers Inc., Haw River, NC) in sterilization pouches (Ren et al., 2016b; Weisgerber et al., 2015b; Weisgerber et al., 2016b). All subsequent handling steps leading to studies of cell activity were performed in a sterile manner.

### **2.3. ESEM imaging**

Environmental scanning electron microscope was used to examine the integration of the PLA fibers and mineralized collagen scaffold structures in the collagen-PLA composites. Imaging was performed using an FEI Quanta FEG 450 ESEM (FEI, Hillsboro, OR), on composites cut with a razor blade prior to imaging to reveal the internal collagen-PLA microstructure.

### **2.4. Mechanical behavior of scaffold, cage, composites under compression**

Stress-strain curves of the non-hydrated mineralized collagen scaffolds, all PLA cage designs, and all mineralized collagen-PLA composites under compression were generated using an Instron 5943 mechanical tester (Instron, Norwood, MA) using a 100 N load cell under dry conditions. Briefly, samples were compressed to failure at a rate of 2 mm/min with the ultimate stress and strain and Young's Modulus determined from the stress-strain curves using conventional analysis methods for low-density open-cell foam structures such as the collagen scaffolds (Gibson and Ashby, 1997; Harley et al., 2007; Kanungo and Gibson, 2009a, b; Kanungo et al., 2008). While hydrating and carbodiimide crosslinking collagen scaffolds reduces the modulus of the scaffold versus non-hydrated specimens, we have previously shown the

relative effects of scaffold architecture are maintained for dry vs. hydrated specimens and that the performance of non-hydrated and hydrated collagen-fiber composites is largely unaffected by scaffold hydration level due to the dominant influence of the fiber architecture on composite mechanical performance (Harley et al., 2007; Mozdzen et al., 2016; Mozdzen et al., 2017; Weisgerber et al., 2016b).

### ***2.5. Measuring conformal fit via push out testing***

The contribution of shape-fitting PLA fiber designs to the conformal fitting of the mineralized collagen-PLA composite within a cylindrical defect was examined via mechanical push out test (Nganga et al., 2011; Seong et al., 2013) performed using an Instron 5943 mechanical tester (Instron, Norwood, MA). Tests were performed on non-hydrated specimens using a 100 N load cell. Cylindrical mineralized collagen-PLA specimens were compressed radially with forceps, inserted into 10 mm or 9.25 mm dia. cylindrical holes in a Teflon base, then were released, allowing them to expand and fill the hole prior to testing. The 9.25 mm dia. cylindrical defect was the smallest hole the specimens could be press-fit into. The Teflon base plate was clamped on the mechanical tester, with a push out test performed on the specimens using an 8 mm diameter metal rod to push the composites until exit of the bottom of the Teflon base at a rate of 2 mm/min (**Fig. 1C**).

### ***2.6. Hydration and crosslinking of designs***

PLA cages, mineralized collagen scaffolds, and mineralized collagen-PLA composites were all hydrated prior to use with cells. Briefly, samples were soaked for two hours in 100% ethanol, then underwent multiple PBS washes to fully hydrate the scaffold (Weisgerber et al., 2015b). The scaffolds and composites were subsequently crosslinked via carbodiimide chemistry in a PBS solution of 1-ethyl-3-(3-dimethylaminopropyl) carbodiimide hydrochloride (EDC, Sigma-Aldrich) and N-hydroxysulfosuccinimide (NHS, Sigma-Aldrich) at a molar ration of 5:2:1

EDAC:NHS:COOH (carboxylic acid groups on the collagen backbone) (Caliari and Harley, 2011b; Caliari and Harley, 2014; Olde Damink et al., 1996; Veilleux et al., 2004). Scaffold and composites were washed multiple times in sterile PBS, then soaked in cell culture media for 42 hours prior to seeding with cells.

### **2.7. Porcine adipose derived stem cell (pASC) culture and seeding**

Porcine adipose derived stem cells (pASCs, a gift of Dr. M. Wheeler, Department of Animal Science, UIUC, Urbana, IL) were expanded at 37°C and 5% CO<sub>2</sub> in complete mesenchymal stem cell growth media (low glucose DMEM, 10% mesenchymal stem cell fetal bovine serum, and 1% antibiotic-antimycotic) that did not include any osteogenic supplements (Mônaco et al., 2009). pASCs show robust osteogenic capabilities in response to osteogenic media (Bionaz et al., 2015) or in mineralized collagen scaffolds in the absence of osteogenic supplements (Weisgerber et al., 2016a), and were used at passage 4 throughout all experiments here. pASCs were seeded onto PLA cages as well as into collagen scaffolds and collagen-PLA composite using a previously described static-seeding method (Caliari et al., 2012; O'Brien et al., 2005). Briefly, a total of  $7.5 \times 10^4$  pASCs in 40  $\mu$ L of growth media were seeded onto each cage, scaffold, or composite in costar® 24 Well plate ultra-low attachment surface (Corning, Corning, NY). First,  $3.75 \times 10^4$  pASCs (in 20  $\mu$ L of growth media) were seeded on one side of the cylindrical sample and left for 30 min for cells to initiate attachment; cages, scaffolds, and composites were subsequently flipped over and another  $3.75 \times 10^4$  cells (in 20  $\mu$ L of growth media) were seeded on the opposite side. Samples were then incubated for an additional 1.5 hours at 37°C to let cells more fully attach to the specimens. Additional growth media was added to each well, with pASC seeded samples then cultured for the remainder of the experiment (up to 28 days) at 37°C and 5% CO<sub>2</sub> and in the presence of complete mesenchymal cell growth media (replaced every 3 days) that lacked any osteogenic supplements.

### **2.8. Measurement of pASC metabolic activity**

The metabolic activity of pASC seeded constructs (cage, scaffold, composite) was quantified over 28 days (days 1, 4, 7, 14, and 28) using a non-destructive alamarBlue® assay (Caliari and Harley, 2014). Cell seeded samples were incubated in an alamarBlue® solution (Invitrogen, Carlsbad, California) at 37°C under gentle shaking for 2 hours. The fluorescence of the reduced resazurin byproduct, resorufin, by the metabolically active pASCs was measured using a F200 spectrophotometer (Tecan, Mannedorf, Switzerland) at 540(52) nm excitation and 580(20) nm emission. The metabolic activity of each sample is reported as the normalized activity generated using a standard prepared from the initial number of cells seeded onto each construct ( $7.5 \times 10^4$ ).

### **2.9. Measurement of pASC cell number**

The total number of pASCs on the cage, scaffold, and composite at days 1, 7, 14, and 28 was quantified using DNA quantification using methods previously described (Caliari and Harley, 2011a). Samples were rinsed in PBS three times to remove dead or unattached cells, and then placed in a papain solution (Sigma-Aldrich) at 60°C for 24 hours to digest samples and lyse cells. Hoechst 33258 (Invitrogen) was used to fluorescently label double-stranded DNA and was read at an excitation of 360 nm and emission of 465 nm utilizing a fluorescent spectrophotometer (Tecan). Total cells per construct was reported as a normalized value, with background fluorescence first removed for each sample using a blank control construct at each time point, and those results then normalized using a standard generated on day 0 from the initial number of cells seeded onto each construct ( $7.5 \times 10^4$ ) with known cell number to determine cell number in each sample.

### **2.10. Western Blot analysis**

Protein lysates from seeded cage, scaffold, and composites were collected at days 1, 4, 7, and

14 using a mixture of Phosphate Inhibitor Cocktail (Sigma-Aldrich), Phosphatase Inhibitor Cocktails 2 and 3 (Sigma-Aldrich), and a RIPA lysis buffer (Grier et al., 2017). Total protein content was assessed using a Pierce™ BCA Protein Assay Kit (Thermo Fisher Scientific, Waltham, MA) and a Pierce™ Bovine Serum Albumin Standard Pre-Diluted Set (Thermo Fisher Scientific). Western blot analysis was performed using 5 µg of protein lysate per lane, using primary antibodies listed in **Table 1**, followed by a 1:5000 dilution of anti-rabbit HRP-IgG (Cell Signaling Technologies, Danvers, MA). β-actin was used as a loading control throughout. Western blots were imaged using a SuperSignal West Femto Maximum Sensitivity Substrate (Thermo Fisher Scientific) and Image Quant LAS 4010 (GE Healthcare Life Sciences, Little Chalfont, United Kingdom).

### **2.11. RT-PCR analysis**

RNA was extracted from pASC seeded constructs (cage, scaffold, composite) at days 1, 4, 7, and 14 utilizing an RNeasy Plant Mini kit (Qiagen, Valencia, CA) and was reverse transcribed to cDNA utilizing a Bio-Rad S1000 thermal cycler and a QuantiTect Reverse Transcription kit (Qiagen) using previously described methods (Caliari and Harley, 2011a). Real-time PCR reactions were performed in duplicate (10 ng of cDNA) using the QuantiTect SYBR Green PCR kit (Qiagen) or Taqman fast advanced master mix and Taqman gene expression assays (Applied Biosystems, Foster City, CA) Quantstudio™ 7 Flex Real-Time PCR System (Thermo Fisher Scientific), with results normalized to pASC expression profiles from cell-seeded composites at day 0.

Taqman gene expression assays (**Table 2**) are pre-validated by Applied Biosystems. However, RUNX2 was not available in Taqman gene expression assays for porcine cells, so additional primers for SYBR Green analyses were synthesized by Integrated DNA Technologies (Coralville, IA) using sequences previously reported in the literature (**Table 3**), with *GAPDH*

used as a housekeeping gene. Primers for SYBR Green analyses were validated via RT-PCR against multiple concentrations of forward and reverse primer (20uM, 10uM, 5uM, 2.5uM) using pASCs to verify one single melting peak and the lowest CT value. Primer efficiency was then calculated from RT-PCR with the optimal primer concentration against multiple cDNA concentrations (10ng/well, 5ng/well, 2.5ng/well, 1ng/well, 0.5ng/well, 0.1ng/well), with 100% efficiency found if plotting delta CT vs. log(cDNA) led to a straight line (slope < 0.1). In this manner, only *RUNX2* was validated for SYBR Green analysis of porcine cells used in this study. The delta-delta CT method was utilized to generate results, and all results were expressed as fold changes normalized to the day 0 standard.

### **2.12. Micro-CT analysis**

Quantification of new mineral formation in the constructs at day 28 (cage, scaffold, composite) and day 0 unseeded controls was performed via microcomputed tomographic (micro-CT) imaging using the MicroXCT-400 (Zeiss, Oberkochen, Germany). Samples were fixed in 10% formalin and stored at 4°C prior to analysis. Scans were performed using a 1x resolution lens, 40 V, 8 W, with the same binning, exposure time, and source and detector positions. All images had a final pixel size of 15.75 µm, and brightness and contrast were the same for each sample. Total mineral content was analyzed from z-stacks of 2D micro-CT images using a custom Matlab program developed to quantify the fill fraction and mineral intensity in scaffold, composite, and control samples as a function of radial, angular, and depth position (Weisgerber et al., 2018). A value of 215 was set for the threshold of every sample in the program, with a depth of 140. We report the degree of new mineral formation in the scaffold and composite groups along three axes of the cylindrical specimens (depth: 0 – 1 bottom to top; radius: 0 – 1470 center to edge; angle: 0 – 360°) for a volume of interest inside the PLA frame of the composites so as to avoid any contribution of the frame itself on the measurement of mineral formation. A radius of 100 (2mm) was used on the scaffold and composite due to the

interference of PLA struts at a greater radius, and a radius of 120 (2mm) was used for control samples due to their larger size. Results for the mineralized scaffold and mineralized collagen-PLA composite were normalized to the day 0 unseeded scaffold.

### **2.13. Histology of designs**

After micro-CT analysis, samples were rinsed in PBS, embedded in Tissue-Tek ® O.C.T. freezing compound (Sakura Finetek, Netherlands), then stored at -80°C. 14 µm thick histology specimens were cut from frozen block using a motorized Microm HM 550 cryostat (Thermo Fisher Scientific) and placed onto glass slides. Samples were H&E stained using Gill II Hematoxylin solution (Leica, Wetzlar, Germany) and with a Eosin solution made from Eosin Y powder (Fisher Scientific, Pittsburg, PA), and were Alizarin Red stained with a solution made from Alizarin Red S powder (Sigma-Aldrich), and Von Kossa stained using a kit (ab150687, Abcam, Cambridge, UK), then imaged using a NanoZoomer Digital Pathology System (Hamamatsu, Japan). All images taken were analyzed qualitatively.

### **2.14. Statistics**

Statistical analysis utilized OriginPro software (Northampton, MA). Significance was set to  $p < 0.05$ . Data was first tested for normality via the Shapiro-Wilk test, then tested for equal variances between samples with a Browne-Forsythe test. If multiple samples analyzed (2+) were normally distributed and had equal variances, a one-way ANOVA was performed with a tukey post-hoc test. If samples were normally distributed without equal variances, a t-test with a Welch correction was used. If two samples were normally distributed then a t-test was always used. If data was not normally distributed, a Kruskal-Wallis test was performed (Necker, 2010). The power was also checked after running either ANOVA or t-tests, and if found to be less than 0.8 then there was deemed no significance ( $p < 0.05$ ) between samples tested. Outliers were removed using the Grubbs test. The number of samples per experimental group for each type of

assay was informed by previous studies using collagen scaffolds and composites (Caliari and Harley, 2014; Grier et al., 2017; Mozdzen et al., 2016; Weisgerber et al., 2016a; Weisgerber et al., 2016b): compressive tests (n=8), push out tests (n=6), cell number (n=3), metabolic activity (n=6), western blot (n=3), gene expression (n=5), and micro-CT (n=3). . Error bars are reported as mean  $\pm$  standard deviation.

### 3. Results

#### ***3.1. Determining PLA incorporation in mineralized collagen-PLA composites***

ESEM images of both open angled and straight composites architectures showed full incorporation of the PLA into the mineralized collagen scaffold architecture with no evidence of delamination (**Fig. 2**).

#### ***3.2. The compressive strength of the mineralized collagen scaffold is significantly enhanced via the inclusion of PLA reinforcing fibers***

The compressive mechanical behavior of four mineralized collagen-PLA composite designs were chosen to span a range of experimental design parameters. We compared a 0.7 mm dia.

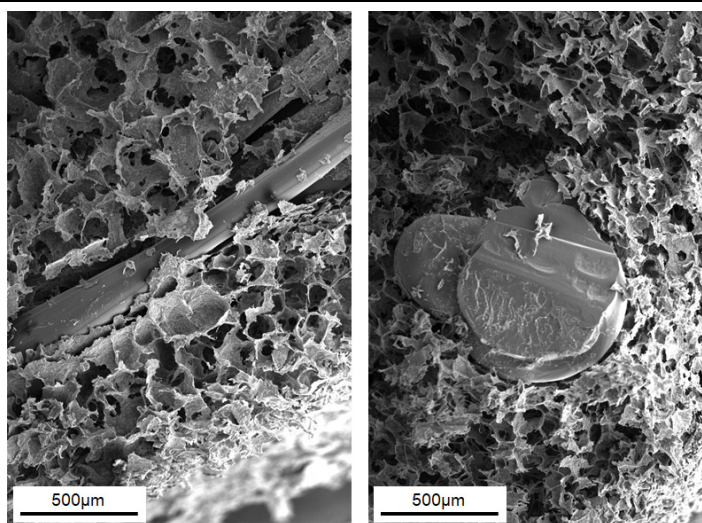


**Figure 2. Environmental Scanning Electron Microscope images of cross-sections of composite designs with 3D printed PLA struts within mineralized collagen scaffold.**

straight cage and composite PLA design with hypothesized highest axial compressive strength to angled composite designs of different fiber diameter (0.7 mm vs. 1.0 mm dia.) and different shape-fitting ability (open vs. closed). For the 0.7 mm dia. PLA fiber variant, we examined the effect of angle of the PLA fibers ('straight' fibers parallel to the direction of compressive loading vs. 'angled' fibers at  $\sim 40.7^\circ$  off the axis of compressive loading (37.9, 40.6, 43.5 $^\circ$ ) with the goal of increasing axial composite compliance). We subsequently examined the effect of the diameter of angle strut (0.7 mm vs. 1 mm) on the open angled design. Lastly, and again using 0.7 mm dia. PLA fiber variants, we examined the effect of removing a section of the circumferential PLA fiber bands at the periphery of the reinforcing cage ('open' vs. 'closed') to enhance the radial compressibility of the composites. We also tested the 0.7 mm dia. straight cage (vs. the 0.7 mm dia. straight composite) as well as the non-reinforced mineralized collagen scaffold (**Fig. 3**). The 0.7 mm straight cage and 0.7 mm straight composite had significantly ( $p < 0.05$ ) higher ultimate stresses and Young's Moduli than all open and closed angled composites, and the scaffold had a significantly ( $p < 0.05$ ) lower ultimate stress and Young's Moduli compared to all other tested designs. No significant difference in ultimate stress and Young's Moduli was found between the 0.7 mm straight composite and the 0.7 mm straight cage. However, increasing the strut diameter of the open angled design from 0.7mm to 1mm led to a significant ( $p < 0.05$ ) increase in ultimate stress.

### ***3.3. Mineralized collagen-PLA composites generated using open fiber designs show conformal fitting and enhanced push-out resistance in a model cylindrical defect***

We subsequently compared the push-out behavior of two open angled mineralized collagen-PLA composites (0.7 mm and 1.0 mm fiber diameter; both originally 11.9 mm in diameter) in 10 mm and 9.25 mm cylindrical channels in a Teflon plate (**Fig. 4**). Both open-angle composite designs could be radially compressed and press-fit into the model defects. The shape-fitting capacity was subsequently assessed as there was increased push-out resistance in smaller

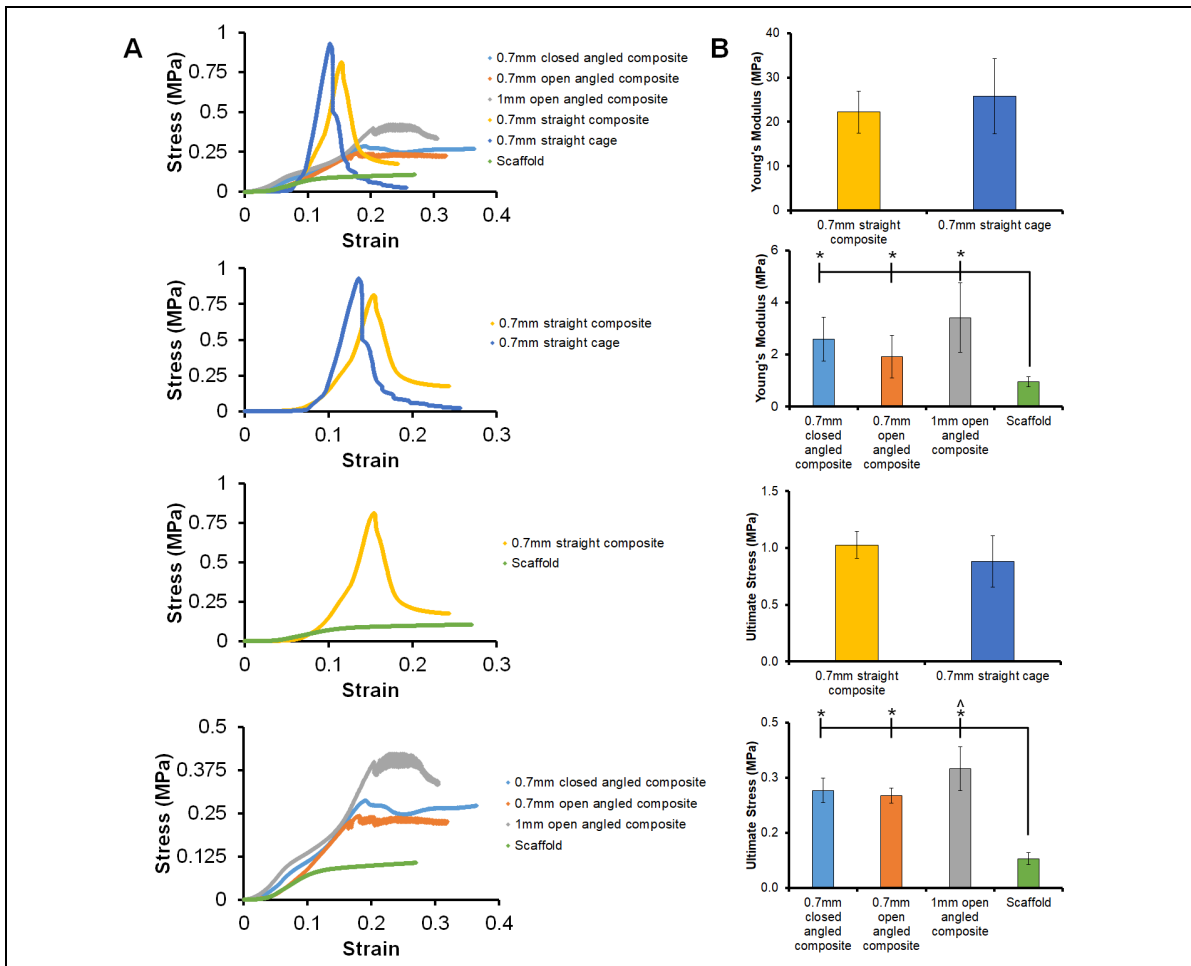
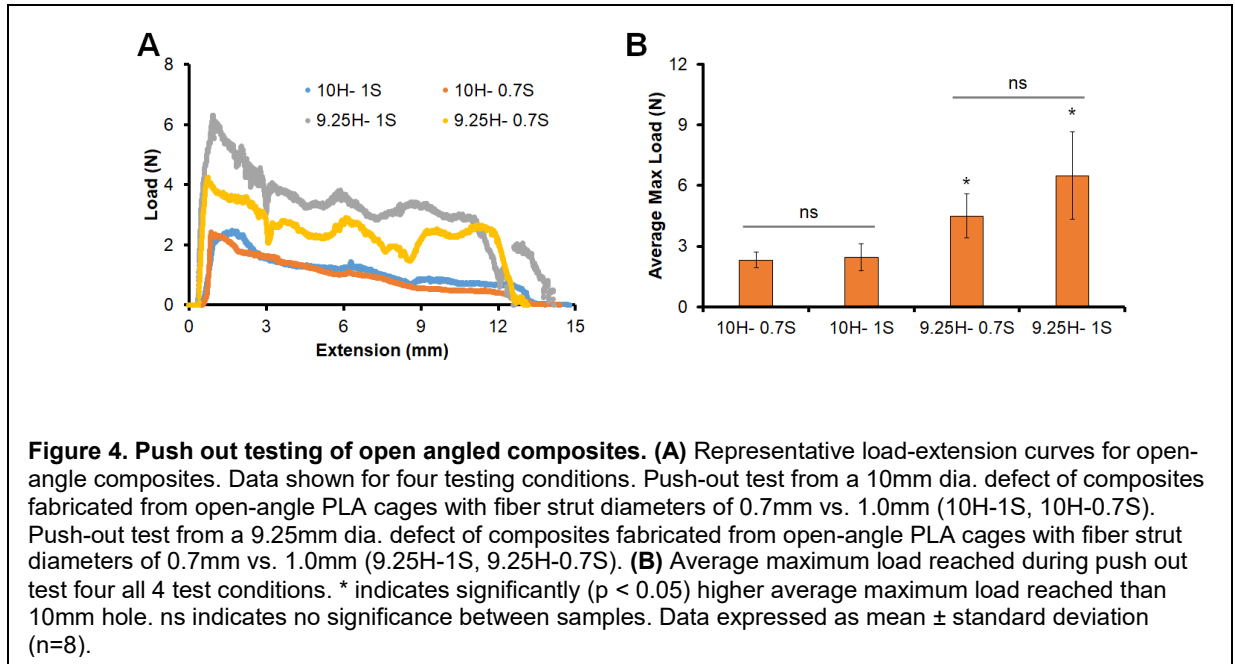


**Figure 3. Mechanical compression testing of PLA cage, scaffold, and various collagen-PLA composite designs. (A)** Representative images of stress-strain curves comparing all experimental conditions, PLA cage vs. collagen-PLA composite, collagen scaffold vs. collagen-PLA composite, and between all composite designs. **(B)** Young's modulus and Ultimate stress for all scaffold, cage, and composite designs. \* indicates significantly ( $p < 0.05$ ) higher value than scaffold. ^ indicates significantly ( $p < 0.05$ ) different Ultimate stress values between groups. Data expressed as mean  $\pm$  standard deviation ( $n=8$ ).

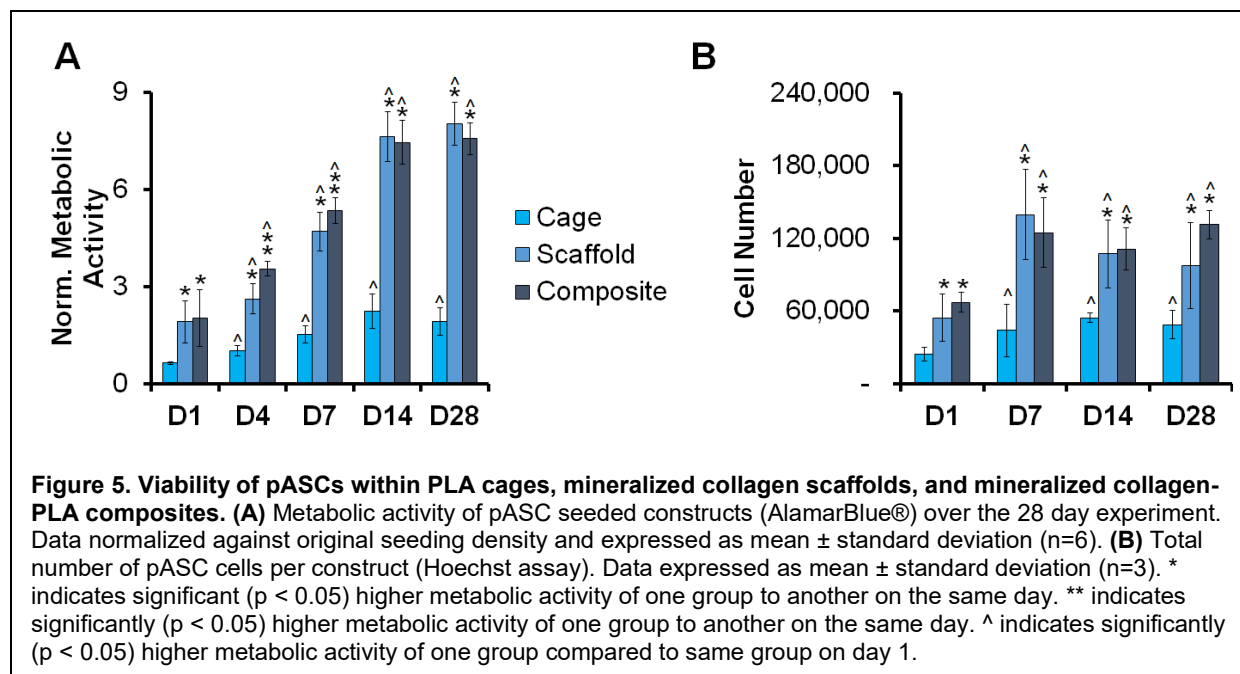
diameter defects, and we observed that both open-angled composite designs demonstrated a significantly ( $p < 0.05$ ) higher maximum load at push-out in the 9.25 mm diameter defect versus the 10 mm diameter defect. Mineralized collagen-PLA composites fabricated using a closed PLA frame design could not be press-fit into the channels (not shown). No significant difference in maximum load was observed between the 0.7 mm vs. 1 mm fiber diameter designs in either the 10 mm or 9.25 mm channels.

### 3.4. Tracing the metabolic activity and proliferation of pASCs



We then evaluated the metabolic activity of porcine ASCs seeded collagen-PLA composites versus the PLA cage and mineralized collagen scaffold alone (**Fig. 5A**). There was a significant ( $p < 0.05$ ) increase in metabolic activity for all samples with time. ASC-seeded PLA cages showed significantly ( $p < 0.05$ ) lower metabolic activity than either the mineralized collagen scaffold or the mineralized collagen-PLA composite. The ASC metabolic activity was largely the same between the scaffold alone and the mineralized collagen-PLA composite, and both scaffold and mineralized collagen-PLA composite showed greater than 3.5-fold expansion in metabolic activity over the course of the experiment

We also examined ASC proliferation by quantifying cell numbers in all groups (**Fig. 5B**). While the total number of cells increased significantly with time (days 7, 14, 28 vs. day 1) for all conditions (PLA cage alone, collagen scaffold, collagen-PLA composite) the effect was largest in the scaffold and collagen-PLA composite groups. Not surprisingly, the PLA cage alone consistently showed significantly ( $p < 0.05$ ) reduced cell number compared to both the collagen scaffold or mineralized collagen-PLA composite.



### 3.5. Evaluating signal transduction and pro-osteogenic signaling

We subsequently examined expression signatures for SMAD1/5/9, AKT, ERK1/2, p38, and SMAD2/3 in the scaffold vs. mineralized collagen-PLA composite to confirm the addition of the PLA cage did not alter the pro-osteogenic signatures previously demonstrated for the mineralized collagen scaffold (**Supp. Fig. 1**). We focused analysis on the collagen scaffold alone versus the collagen-PLA composite as the PLA cage alone group showed significantly reduced cell expansion (and faint  $\beta$ -actin bands, not shown). Faint  $\beta$ -actin bands observed at early timepoints (day 1, 4) are likely due to low cell numbers at early timepoints. Importantly, we observed no appreciable change in the overall signature of SMAD1/5/9, ERK1/2, and SMAD2/3 activity as a result of the inclusion of the PLA-reinforcing cage into the mineralized collagen scaffold (collagen scaffold vs. collagen-PLA composite groups). While largely similar, we observed faster upregulation of AKT activity in the mineralized collagen-PLA composite (significant increase by day 4). Interestingly, while P38 activity decreased significantly ( $p < 0.05$ ) in the collagen scaffold over the course of the 14 day experiment, it increased significantly ( $p < 0.05$ ) in the collagen-PLA composite. Moreover, while the kinetics of the response were

different, both the collagen scaffold and the collagen-PLA composite showed reduction in SMAD2/3 activity over the 14 day experiment.

### 3.6. Gene expression analysis of cage, scaffold, and collagen-PLA composite

We subsequently examined the expression profiles for a suite of genes (*RUNX2*, *BMP2*, *BGLAP*, *Osterix*, *COL1A2*, *MMP9*) associated with osteogenic gene expression and matrix

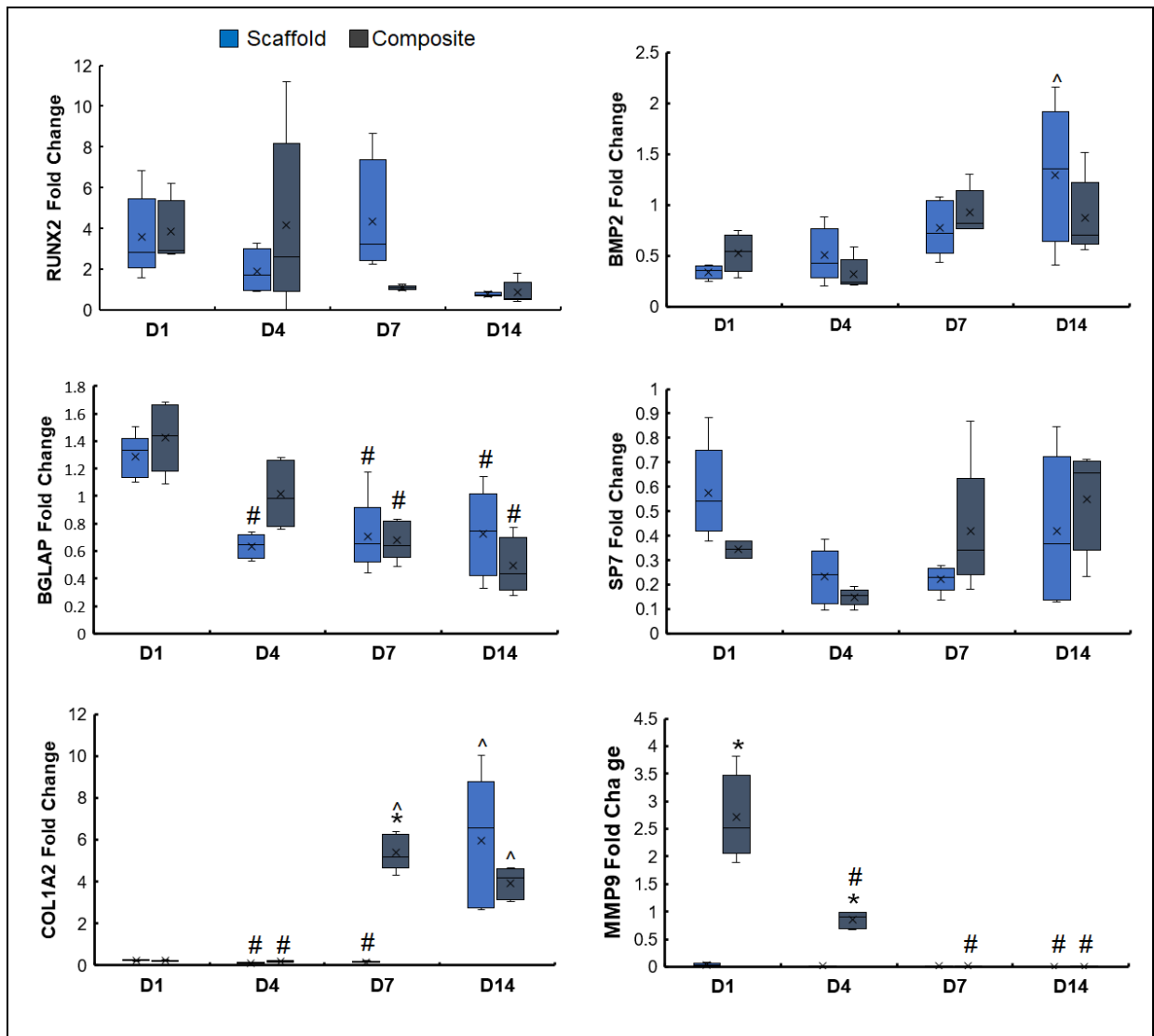
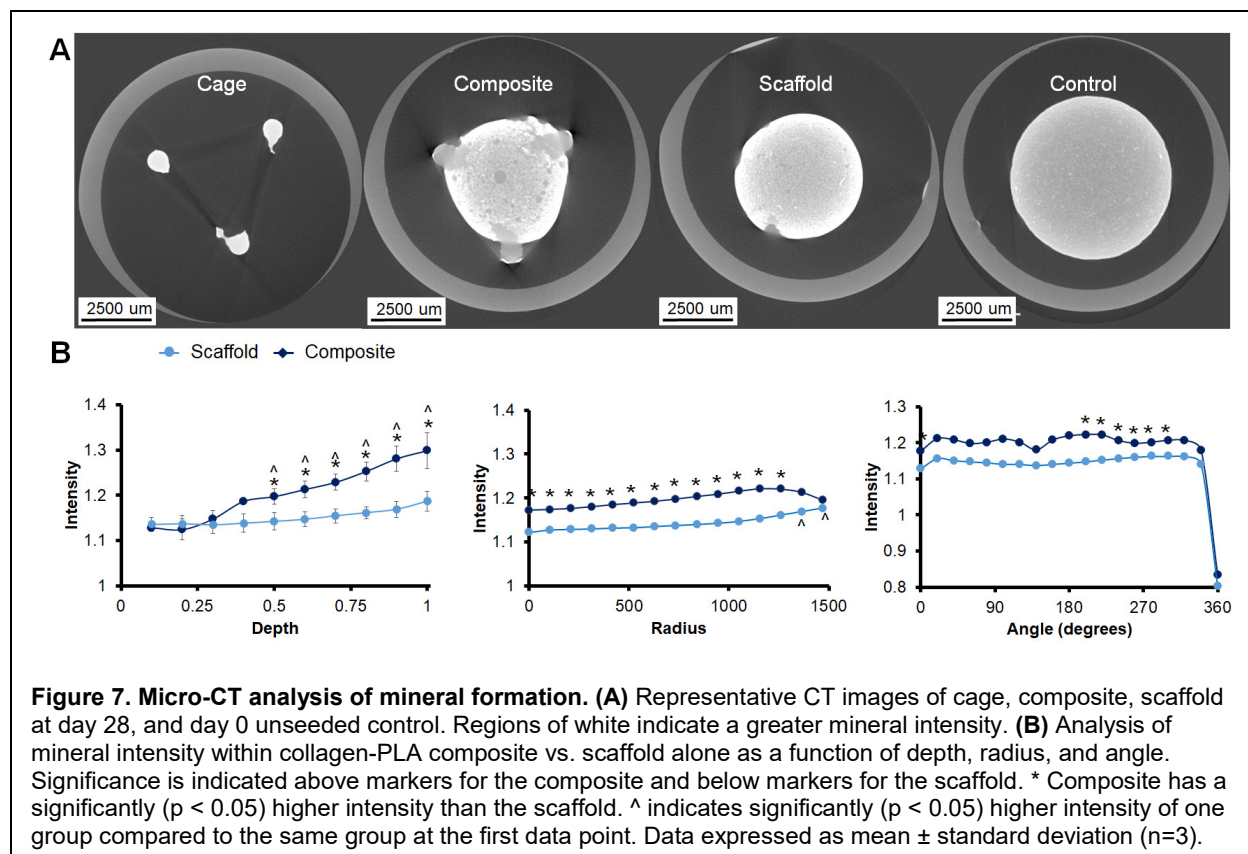


**Figure 6. Comparing osteogenic differentiation profiles after adding PLA reinforcing frame to the mineralized collagen scaffold.** Gene expression profiles of *RUNX2*, *BMP2*, *BGLAP*, *Osterix*, *COL1A2*, and *MMP9* for pASCs within the mineralized collagen scaffold vs. collagen-PLA composite. \* indicates significant ( $p < 0.05$ ) higher gene expression between the two groups on the same day. ^ indicates significantly ( $p < 0.05$ ) higher gene expression of one group compared to the same group on day 1. # indicates significantly ( $p < 0.05$ ) lower gene expression of one group compared to the same group on day 1. Data expressed as mean  $\pm$  standard deviation ( $n=5$ ).

remodeling previously benchmarked in our mineralized collagen scaffold (Ren et al., 2016a; Ren et al., 2016b; Ren et al., 2016c; Weisgerber et al., 2016a). Inclusion of the PLA reinforcing frame did not appreciably alter osteogenic signature of the mineralized scaffold (**Fig. 6**). There was no significant ( $p < 0.05$ ) differences in *RUNX2* expression levels between scaffold and collagen-PLA composite groups across all timepoints, with *RUNX2* upregulated at days 1, 4, and 7 in both groups. *BMP2* expression was downregulated at early timepoints (day 1 and 4) but upregulated by day 14, however, with only the scaffold showing significantly increased ( $p < 0.05$ ) expression over the experiment. Osteocalcin (*BGLAP*), upregulated in both the scaffold and collagen-PLA composite at day 1 showed decreased expression over later timepoints. There was no significant ( $p < 0.05$ ) difference among days and groups fold change of Osterix (*SP7*), which was downregulated at all timepoints. Interestingly, while *COL1A2* was downregulated at early timepoints we observed a marked, significant rise in expression at later timepoints, with the collagen-PLA composite showing the fastest increase in expression. While expression of *MMP9* was largely absent in the mineralized collagen scaffold, the collagen-PLA composite showed significantly ( $p < 0.05$ ) greater fold change of *MMP9* at early timepoints (days 1 and 4).

### **3.7. Micro-CT analysis of cage, scaffold, and mineralized collagen-PLA composite**

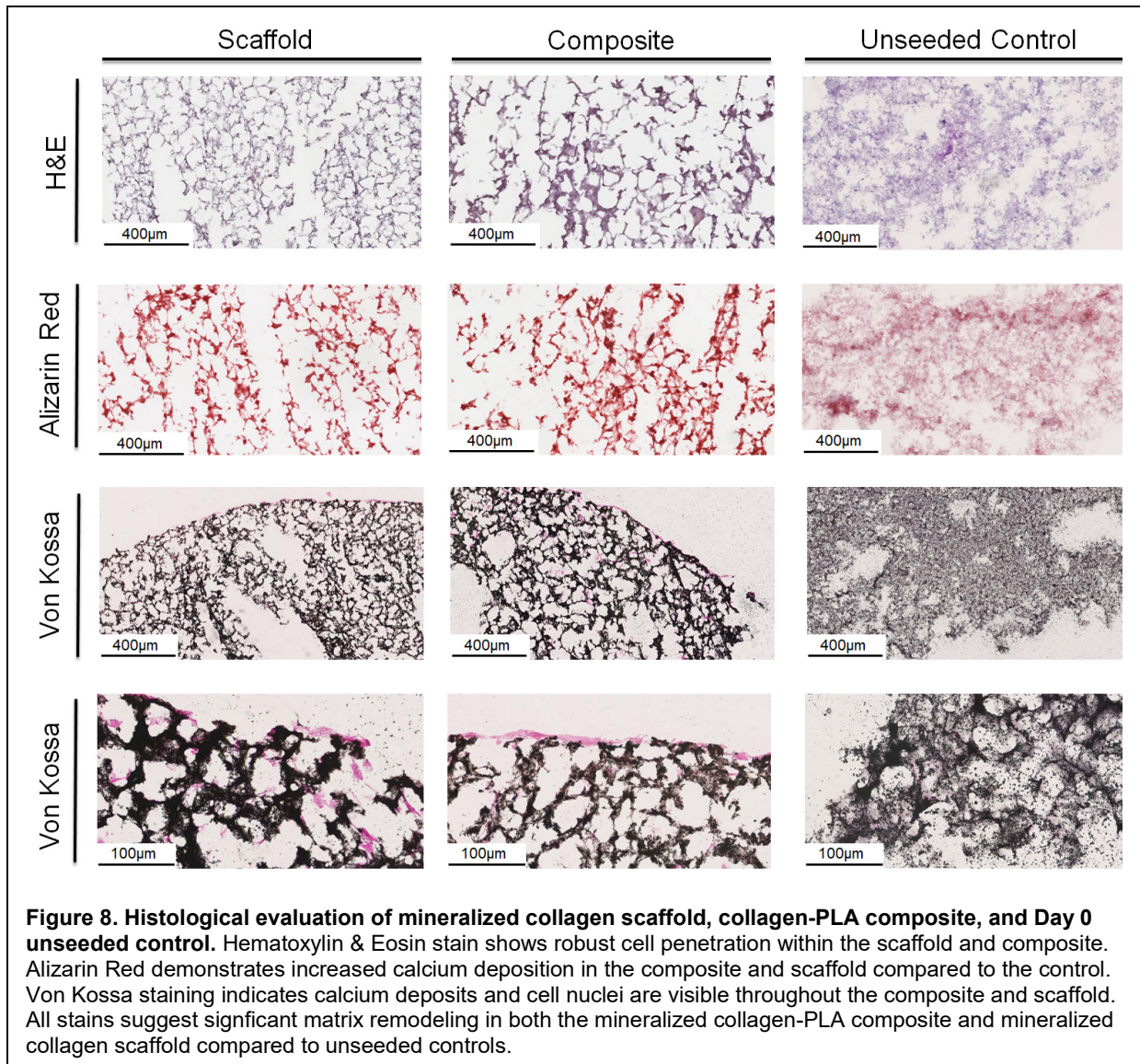
We subsequently performed micro-CT analysis on ASC-seeded constructs at 28 days of culture to quantify the extent of new mineral formation on the surface of the PLA cages as well as within the mineralized collagen scaffolds and mineralized collagen-PLA composites (**Fig. 7**). Not surprising given the stiff PLA, there was some degree of mineralization on the surface of the PLA cage as observed qualitatively with intense white CT images. Overall, the mineralized collagen-PLA composite showed increased mineral formation compared to the mineralized collagen scaffold alone. Looking at the distribution of mineral through the sample depth, the composite showed significantly ( $p < 0.05$ ) higher mineral content towards the top of the



specimens. Examining radial patterns of mineral formation, the mineralized collagen-PLA composite showed significantly ( $p < 0.05$ ) higher micro-CT intensity than the scaffold alone. We also examined mineral formation as a function of angular position around the specimens, finding all specimens showed largely angularly symmetrical mineral formation.

### 3.8. Histological evaluation of scaffold and collagen-PLA composite

We then performed histological evaluation of matrix remodeling and mineral formation via Hematoxylin and Eosin, Alizarin Red staining, and Von Kossa staining (Fig. 8). H & E stains showed good cellular distribution within the scaffold and mineralized collagen-PLA composites. Both scaffolds and composites showed strong Alizarin Red staining at day 28 of culture, with no visible differences between scaffold and composite, and a stronger red than the day 0 control. Von Kossa staining indicated nuclear red stained cells mostly at the edge of the scaffold and mineralized collagen-composite but some cells are visible within the center of the constructs.



Notably, the unseeded control scaffolds and composites show reduced remodeling and mineral formation compared to both the cell-seeded scaffold and mineralized collagen-composite.

#### 4. Discussion

In this study, we describe the development, mechanical testing, and profiling of the *in vitro* bioactivity of a shape-fitting mineralized collagen-PLA composite for applications in CMF defect regeneration. Here, a significant challenge to improving the quality and speed of craniomaxillofacial bone regeneration are competing design requirements for a biomaterial

platform: *porosity* required for cell recruitment and adequate biotransport; *mechanical strength* that is significantly reduced by the inclusion of pores; shape-fitting to improve conformal contact and osseointegration between the implant and the defect. The latter is particularly important in the context of CMF bone defects, where developmental, post-oncologic, and high-energy impacts can result in a wide range of defect morphologies and irregular defect geometries. Our efforts here are built upon our recent development of a class of mineralized-collagen scaffolds that promote osteogenic differentiation of human and rabbit marrow MSCs as well as porcine adipose-derived stem cells in the absence of osteogenic supplements (BMP-2, osteogenic media) (Caliari and Harley, 2014; Weisgerber et al., 2015b). While exogenous BMP-2 can enhance the effect, the mineralized collagen scaffold *natively instructs osteogenesis* (Caliari and Harley, 2014; Lee et al., 2015; Ren et al., 2015; Ren et al., 2016b; Ren et al., 2016c; Weisgerber et al., 2015b). These mineralized scaffolds promote activation of canonical (SMAD1/5/8) (Ren et al., 2015) and SMAD-independent (ERK1/2, AKT, p38 MAPK) BMP receptor signaling pathways (Ren et al., 2016c) leading to robust mineral formation *in vitro* and enhanced bone regeneration *in vivo* (Weisgerber et al., 2018). However, a significant challenge for the scaffold is the porosity (>85%) that support high cell bioactivity significantly reduces scaffold mechanical strength. To address significant challenges associated with clinical translation of these collagen scaffolds for musculoskeletal tissue engineering applications, we are exploring the integration of reinforcing structures created via 3D-printing into the scaffold. Recently we have added polycaprolactone cages to increase the compressive strength of mineralized collagen scaffolds (Weisgerber et al., 2016a) and sinusoidally-crimped PLA fibers to increase the tensile strength of collagen scaffolds for tendon repair (Mozdzen et al., 2016; Mozdzen et al., 2017). However, a unique need for CMF repair is not only mechanical reinforcement but also improved shape-fitting capacity to improve initial osseointegration into irregular defects. Here, we address this need via a unique composite biomaterial design.

Herein we describe inclusion of a low volume fraction (~10% v/v) PLA reinforcement frame into the mineralized collagen scaffold to form a collagen-PLA composite. Notably, the collagen-PLA composite shows enhanced and customizable compressive strength via modification of PLA fiber diameter and orientation (**Fig. 3**). These findings are consistent with recent results from our lab integrating polymeric fibers structures fabricated via 3D printing into collagen scaffolds to increase compressive or tensile properties (Mozdzen et al., 2016; Mozdzen et al., 2017; Weisgerber et al., 2016a) and is consistent with a larger attempt at forming bioactive nano-scale or micro-scale composites for tissue engineering applications (Arce et al., 2016; Sethu et al., 2017; Xing et al., 2017; Yang et al., 2015). A critical advance associated with this work is demonstrating an approach to render the composite shape-fitting. Poor osseointegration into the surrounding mandibular bone is a key contributing factor to poor healing (Lan Levensgood et al., 2010; Wise et al., 2010; Zhang et al., 2014b), suggesting that improving conformal fitting between the micro-scale pore architecture of the collagen scaffold and the wound margins is critical. Push-out tests in model cylindrical defects of decreasing diameter demonstrated that the selective removal of circumferential fiber segments could yield a composite that was deformable radially yet retained sufficient spring-back capacity to increase the required push-out force (**Fig. 4**). Increasing the strut diameter of the open angled design from 0.7 mm to 1 mm increased ultimate stress, suggesting that increasing the diameter of PLA struts further may increase the compressive strength of the open angled design. However, the low volume fraction of PLA in this first-generation composite (~10% v/v) suggests increasing PLA volume fraction may be a useful design consideration. Regardless, the addition of even small volume fractions (~10% v/v) of polymeric mechanical reinforcement are sufficient to increase composite mechanical strength and address the current translational limitation of the mineralized collagen scaffold (compressive moduli < 1MPa) (Weisgerber et al., 2016a).

In addition to examining the changes in mechanical performance of the mineralized collagen-

PLA composite, we also compared the bioactivity of porcine adipose stem cells in the mineralized collagen-PLA composite versus the mineralized collagen scaffold alone to assess any consequences of incorporating the PLA frame. The composition of native bone has long motivated efforts to create mineralized collagen biomaterials (David et al., 2015; Harley et al., 2010a; Kanungo et al., 2008; Kruger et al., 2011). Indeed, recent efforts in our lab have identified a nanocrystallite mineralized collagen scaffold (Caliari and Harley, 2014; Harley et al., 2010a; Lee et al., 2015; Weisgerber et al., 2015b; Weisgerber et al., 2013) that natively instructs osteogenic differentiation of human and rabbit marrow MSCs as well as porcine adipose derived stem cells in the absence of osteogenic supplements (Caliari and Harley, 2014; Weisgerber et al., 2015b) via activation of canonical BMP receptor signaling pathways (Ren et al., 2016c; Zhou et al., 2017). We also demonstrated this mineralized collagen scaffold variant promotes rapid bone regeneration in rat and rabbit calvarial defects as well as porcine mandible defects, finding the scaffold alone (without exogenous MSCs or BMP2) promotes rapid bone in-fill (Lee et al., 2015; Ren et al., 2016b; Weisgerber et al., 2018). In this manuscript, we established that PLA frame could be incorporated into the collagen scaffold during lyophilization (**Fig. 2**), and that the addition of PLA to form the composite did not adversely affect the ability of the mineralized collagen scaffold to support adipose derived stem cell viability and proliferation (**Fig. 5**). Notably, while metabolic activity and cell number increased steadily in the scaffold and composite, the relatively low surface area of the PLA cage alone did not support comparable cell viability, suggesting the PLA frame alone is not sufficient to maintain cell growth and proliferation.

Gene and protein expression patterns within the scaffold and collagen-PLA composite suggested that both promoted osteogenic differentiation and functional mineral formation *in vitro*. Signal transduction pathways suggest the collagen-PLA composite provides a supportive environment for ASC osteogenic differentiation. Notably, SMAD1/5/9, essential in early activation of BMP receptor pathways in mineralized collagen scaffolds (Weisgerber et al.,

2016a), activity was near 100% expression throughout the experiment. Further, we observed increased activity at later timepoints for AKT and p38, both of which are involved in osteoblast differentiation and bone formation (Matsushita et al., 2009; Thouverey and Caverzasio, 2015). SMAD2/3, which can work with or against BMP signaling depending on the differentiation stage (Song et al., 2009), was active throughout the experiment in both the scaffold and collagen-PLA composite. Analysis of gene expression also suggested the inclusion of the PLA reinforcing frame did not significantly alter ASC activity. *RUNX2*, a major transcription factor regulating osteogenic differentiation from mesenchymal stem cells, was upregulated throughout days 1 through 7, indicating osteogenic lineage commitment of pASC (Dalle Carbonare et al., 2012). BMP is an essential element of osteogenic commitment *in vivo* and *in vitro* (James, 2013), with our results confirming *BMP2* was upregulated at later timepoints, suggesting osteogenesis and bone formation was continuing. Further, *BGLAP* (osteocalcin) was upregulated at day 1 and downregulated at later timepoints while *Osterix*, a bone specific transcription factor that regulates late stages of bone formation (Hayrapetyan et al., 2015), was downregulated across all timepoints in the scaffold and composite. *COL1A2*, a marker for the type I collagen alpha 2 chain, an important structural element of bone, was upregulated at day 7 and 14 collagen-PLA composites while *MMP9* was upregulated at early timepoints in the collagen-PLA composite, suggesting early stages of matrix remodeling (Hayrapetyan et al., 2015; James, 2013). Critically, there were minimal differences in gene expression and protein activity between the scaffold and collagen-PLA composite across all days, strongly suggesting the addition of PLA reinforcement frame to the mineralized collagen scaffold did not negatively impact differentiation of osteoblasts and mineralization of the construct.

While analysis of bone regeneration requires *in vivo* assessment, we employed a series of histology and three-dimensional imaging approaches to quantify cell-mediated matrix remodeling and new mineral synthesis, finding inclusion of the PLA reinforcing frame in the

PLA-collagen composite does not negatively influence in vitro metrics of ASC activity. Notably, Alizarin Red and Von Kossa analyses of mineralized collagen scaffold and composites after 28 days in culture demonstrated increased definition of mineral deposits compared to unseeded controls. Subsequent analysis of mineralization patterns via Micro-CT suggested that the presence of the PLA reinforcing frame not only did not reduce mineral formation, but may have an effect of augmenting new mineral formation (**Fig. 7**). Here, we applied an algorithm previously developed to quantify new bone infill into cylindrical scaffold specimens in all 3-axes of a cylindrical coordinate system (depth, radial, angular) (Weisgerber et al., 2018), finding the general trend of increased mineral content in the collagen-PLA composites. Ongoing efforts are employing cell-tracing algorithms to examine the kinetics of stem cell penetration into the composite as well as to explore additional fiber morphologies to facilitate conformal fitting of more complex craniomaxillofacial defect geometries. And while beyond the scope of this work which had the goal to validate the use of three-dimensional printing to generate PLA-reinforced collagen scaffolds that have enhanced compressive strength and shape-fitting capacity, future work will test the osseointegration and regenerative capacity of these composites using a porcine mandibular defect model that we have recently described for testing non-shape fitting implant designs (Weisgerber et al., 2018).

## **5. Conclusions**

We describe the design, fabrication, and testing of a conformal fitting mineralized collagen-PLA composite for CMF defect repair applications. The composite demonstrated similar mineralization, cell viability, and osteogenesis to the mineralized collagen alone, which had previously demonstrated excellent biocompatibility and osteogenesis. Further, we demonstrate a library of PLA reinforcement designs to: increase compressive strength of the collagen scaffold, provide radial compression and spring-back to facilitate shape-fitting within a cylindrical defect; or both. The ability to increase close contact between the biomaterial implant and the

host bone is particularly important for improving cell recruitment and subsequent osseointegration between host and implant.

### **Acknowledgements**

This work was supported by the Office of the Assistant Secretary of Defense for Health Affairs Broad Agency Announcement for Extramural Medical Research through the Award No. W81XWH-16-1-0566. Opinions, interpretations, conclusions and recommendations are those of the authors and are not necessarily endorsed by the Department of Defense. The authors would like to acknowledge the Carl R. Woese Institute for Genomic Biology for assistance with Western blot analysis, Kingsley Boateng for help with Nanozoomer training, and Derek Milner for assistance with histology. The authors would like to acknowledge the Illinois Makerlab and Vishal Sachdev for use of 3D printers and assistance printing PLA reinforcements. This research was carried out in part at the Imaging Technology Group within the Beckman Institute for Advanced Science and Technology at the University of Illinois at Urbana-Champaign; the authors would like to thank Leilei Yin for assistance with Micro-CT, and Scott Robinson and Cate Wallace for assistance with ESEM. The authors would also like to acknowledge the Roy J. Carver Biotechnology Center and assistance with RT-PCR from Tatsiana Akraiko and Mark Band.

## Tables

**Table 1.** Antibodies used for Western Blots

<b>Protein</b>	<b>Blocking</b>	<b>Primary antibody</b>	<b>Secondary antibody</b>
β-actin (45 kDa)	5% dry milk	1:1000 in 5% dry milk (Cell Signaling Technologies, Rabbit mAB, 4967L)	1:5000 in TBST, Anti- rabbit IgG, HRP linked antibody (Cell Signaling Technologies, 7074S)
SMAD1/5/9 (52-60 kDa)	5% dry milk	1:1000 in 5% dry milk (Abcam, Rabbit mAB, ab66737)	
p-SMAD1/5/9 (60 kDa)	5% dry milk	1:1000 in 5% dry milk (Cell Signaling Technologies, Rabbit mAB, 13820S)	
SMAD2/3 (52-60 kDa)	5% dry milk	1:1000 in 5% dry milk (Cell Signaling Technologies, Rabbit mAB, 8828S)	
p-SMAD2/3 (52-60 kDa)	5% dry milk	1:1000 in 5% dry milk (Cell Signaling Technologies, Rabbit mAB, 8685S)	
ERK1/2 (42-44 kDa)	5% dry milk	1:1000 in 5% dry milk (Cell Signaling Technologies, Rabbit mAB, 9102S)	
p-ERK1/2 (44-42 kDa)	5% dry milk	1:1000 in 5% dry milk (Cell Signaling Technologies, Rabbit mAB, 9101S)	
p38 (40 kDa)	5% dry milk	1:1000 in 5% dry milk (Cell Signaling Technologies, Rabbit mAB, 8690S)	
p-p38 (43 kDa)	5% dry milk	1:1000 in 5% dry milk (Cell Signaling Technologies, Rabbit mAB, 9215S)	
AKT (60 kDa)	5% dry milk	1:1000 in 5% dry milk (Cell Signaling Technologies, Rabbit mAB, 9272S)	
p-AKT (60 kDa)	5% dry milk	1:1000 in 5% dry milk (Cell Signaling Technologies, Rabbit mAB, 4060S)	

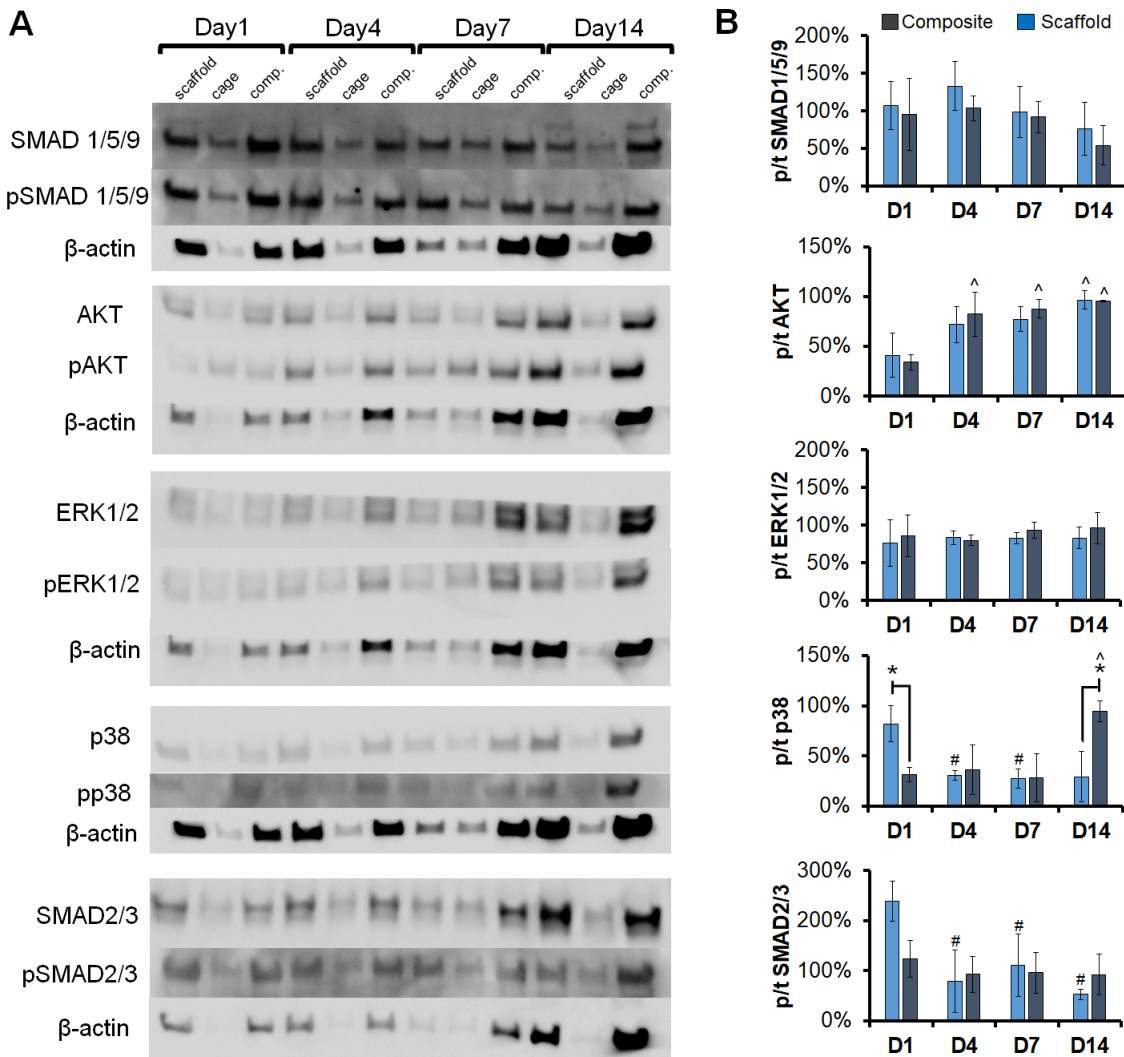
**Table 2.** Primers used for TAQMAN gene expression analyses.

<b>Gene</b>	<b>Catalog Number</b>
<i>GAPDH</i>	Ss03375629_u1
<i>COL1A2</i>	Ss03375009_u1
<i>BGLAP</i>	Ss03373655_s1
<i>BMP2</i>	Ss03373798_g1
<i>Osterix</i> (LOC404701)	Ss03373734_s1
<i>MMP9</i>	Ss03392100_m1

**Table 3.** Primers used for SYBR Green gene expression analyses.

<b>Gene</b>	<b>Primer Sequence (5'-xxx-3')</b>	<b>Citation</b>
<i>GAPDH</i>	Forward: GGACCTCTGGGTATGGCTTTC Reverse: TGG TAA CAT CAA TAC GAT TTC TGA	(Nygard et al., 2007)
<i>RUNX2</i>	Forward: CTC AGT GAT TTA GGG CGC ATT Reverse: AGG GGT AAG ACT GGT CAT AGG	(Lee et al., 2016)

## Supplementary Figures



**Supplemental Figure 1. Levels of phosphorylated to total SMAD1/5/9, AKT, ERK1/2, p38, SMAD2/3. (A)** Representative Western Blots (day 1, 4, 7, 14) with B-actin controls. Mineralized collagen scaffold (*scaffold*), PLA cage alone (*cage*), mineralized-collagen composite (*comp.*).

**(B)** Quantitative comparison of phosphorylated to total protein activity. \* indicates significantly ( $p < 0.05$ ) higher activity of one group to another within the same day. ^ indicates significantly ( $p < 0.05$ ) higher activity of one Day group compared to the same group on day 1. # indicates significantly ( $p < 0.05$ ) lower activity of one group compared to the same group on day 1. Data expressed as mean  $\pm$  standard deviation ( $n=3$ ).

## Supplemental Tables

**Supplementary Table 1.** Young's modulus under unconfined compression of mineralized collagen scaffold alone, PLA cage alone, and a series of collagen-PLA composites. Data presented as mean  $\pm$  standard deviation (n= 8 samples/group).

<b>Name</b>	<b>E*, MPa</b>
Scaffold	0.95 $\pm$ 0.19
0.7mm straight cage	25.80 $\pm$ 8.46
0.7mm straight composite	22.22 $\pm$ 4.73
0.7mm closed angle composite	2.59 $\pm$ 0.85
0.7mm open angle composite	1.91 $\pm$ 0.83
1mm open angle composite	3.41 $\pm$ 1.33

## References

- Al-Munajjed, A.A., Plunkett, N.A., Gleeson, J.P., Weber, T., Jungreuthmayer, C., Levingstone, T., Hammer, J., O'Brien, F.J., 2009. Development of a biomimetic collagen-hydroxyapatite scaffold for bone tissue engineering using a SBF immersion technique. *J Biomed Mater Res B Appl Biomater*.
- Arce, J.E., Arce, A.E., Aguilar, Y., Yate, L., Moya, S., Rincón, C., Gutiérrez, O., 2016. Calcium phosphate–calcium titanate composite coatings for orthopedic applications. *Ceramics International* 42, 10322-10331.
- Bionaz, M., Monaco, E., Wheeler, M.B., 2015. Transcription adaptation during in vitro adipogenesis and osteogenesis of porcine mesenchymal stem cells: dynamics of pathways, biological processes, up-stream regulators, and gene networks. *PLoS ONE* 10, e0137644.
- Bose, S., Roy, M., Bandyopadhyay, A., 2012. Recent advances in bone tissue engineering scaffolds. *Trends Biotechnol* 30, 546-554.
- Caliari, S.R., Harley, B.A., 2011a. The effect of anisotropic collagen-GAG scaffolds and growth factor supplementation on tendon cell recruitment, alignment, and metabolic activity. *Biomaterials* 32, 5330-5340.
- Caliari, S.R., Harley, B.A.C., 2011b. The effect of anisotropic collagen-GAG scaffolds and growth factor supplementation on tendon cell recruitment, alignment, and metabolic activity. *Biomaterials* 32, 5330-5340.
- Caliari, S.R., Harley, B.A.C., 2014. Structural and biochemical modification of a collagen scaffold to selectively enhance MSC tenogenic, chondrogenic, and osteogenic differentiation. *Advanced healthcare materials* 3, 1086-1096.
- Caliari, S.R., Weisgerber, D.W., Ramirez, M.A., Kelkhoff, D.O., Harley, B.A.C., 2012. The influence of collagen-glycosaminoglycan scaffold relative density and microstructural anisotropy on tenocyte bioactivity and transcriptomic stability. *J Mech Behav Biomed Mater* 11, 27-40.
- Cunniffe, G.M., Dickson, G.R., Partap, S., Stanton, K.T., O'Brien, F.J., 2010. Development and characterisation of a collagen nano-hydroxyapatite composite scaffold for bone tissue engineering. *J Mater Sci Mater Med* 21, 2293-2298.
- Curtin, C.M., Cunniffe, G.M., Lyons, F.G., Bessho, K., Dickson, G.R., Duffy, G.P., O'Brien, F.J., 2012. Innovative collagen nano-hydroxyapatite scaffolds offer a highly efficient non-viral gene delivery platform for stem cell-mediated bone formation. *Adv Mater* 24, 749-754.
- Dalle Carbonare, L., Innamorati, G., Valenti, M.T., 2012. Transcription factor Runx2 and its application to bone tissue engineering. *Stem Cell Rev* 8, 891-897.
- David, F., Levingstone, T.J., Schneeweiss, W., de Swarte, M., Jahns, H., Gleeson, J.P., O'Brien, F.J., 2015. Enhanced bone healing using collagen–hydroxyapatite scaffold implantation in the treatment of a large multiloculated mandibular aneurysmal bone cyst in a thoroughbred filly. *Journal of Tissue Engineering and Regenerative Medicine*, n/a-n/a.
- Depeyre, A., Touzet-Roumazielle, S., Lauwers, L., Raoul, G., Ferri, J., 2016. Retrospective evaluation of 211 patients with maxillofacial reconstruction using parietal bone graft for implants insertion. *J Craniomaxillofac Surg* 44, 1162-1169.
- Donzelli, E., Salvade, A., Mimo, P., Vigano, M., Morrone, M., Papagna, R., Carini, F., Zaopo, A., Miloso, M., Baldoni, M., Tredici, G., 2007. Mesenchymal stem cells cultured on a collagen scaffold: In vitro osteogenic differentiation. *Arch Oral Biol* 52, 64-73.
- Elsalanty, M.E., Genecov, D.G., 2009. Bone grafts in craniofacial surgery. *Craniofacial trauma & reconstruction* 2, 125-134.
- Farrell, E., Byrne, E.M., Fischer, J., O'Brien, F.J., O'Connell, B.C., Prendergast, P.J., Campbell,

- V.A., 2007. A comparison of the osteogenic potential of adult rat mesenchymal stem cells cultured in 2-D and on 3-D collagen glycosaminoglycan scaffolds. *Technol Health Care* 15, 19-31.
- Farrell, E., O'Brien, F.J., Doyle, P., Fischer, J., Yannas, I., Harley, B.A., O'Connell, B., Prendergast, P.J., Campbell, V.A., 2006. A collagen-glycosaminoglycan scaffold supports adult rat mesenchymal stem cell differentiation along osteogenic and chondrogenic routes. *Tissue Eng* 12, 459-468.
- Gibson, L.J., Ashby, M.F., 1997. *Cellular solids: structure and properties*, 2nd ed. Cambridge University Press, Cambridge, U.K.
- Grier, W.K., Moy, A.S., Harley, B.A., 2017. Cyclic tensile strain enhances human mesenchymal stem cell Smad 2/3 activation and tenogenic differentiation in anisotropic collagen-glycosaminoglycan scaffolds. *Eur Cell Mater* 33, 227-239.
- Harley, B.A., Kim, H.D., Zaman, M.H., Yannas, I.V., Lauffenburger, D.A., Gibson, L.J., 2008. Microarchitecture of three-dimensional scaffolds influences cell migration behavior via junction interactions. *Biophys J* 95, 4013-4024.
- Harley, B.A., Leung, J.H., Silva, E.C., Gibson, L.J., 2007. Mechanical characterization of collagen-glycosaminoglycan scaffolds. *Acta Biomater* 3, 463-474.
- Harley, B.A., Lynn, A.K., Wissner-Gross, Z., Bonfield, W., Yannas, I.V., Gibson, L.J., 2010a. Design of a multiphase osteochondral scaffold II: fabrication of a mineralized collagen-GAG scaffold. *J Biomed Mater Res A* 92, 1066-1077.
- Harley, B.A., Lynn, A.K., Wissner-Gross, Z., Bonfield, W., Yannas, I.V., Gibson, L.J., 2010b. Design of a multiphase osteochondral scaffold. II. Fabrication of a mineralized collagen-glycosaminoglycan scaffold. *J Biomed Mater Res A* 92, 1066-1077.
- Hayrapetyan, A., Jansen, J.A., van den Beucken, J.J., 2015. Signaling pathways involved in osteogenesis and their application for bone regenerative medicine. *Tissue Eng Part B Rev* 21, 75-87.
- James, A.W., 2013. Review of Signaling Pathways Governing MSC Osteogenic and Adipogenic Differentiation. *Scientifica (Cairo)* 2013, 684736.
- Kanungo, B.P., Gibson, L.J., 2009a. Density-property relationships in collagen-glycosaminoglycan scaffolds. *Acta Biomater* 6, 344-353.
- Kanungo, B.P., Gibson, L.J., 2009b. Density-property relationships in mineralized collagen-glycosaminoglycan scaffolds. *Acta Biomater* 5, 1006-1018.
- Kanungo, B.P., Silva, E., Van Vliet, K., Gibson, L.J., 2008. Characterization of mineralized collagen-glycosaminoglycan scaffolds for bone regeneration. *Acta Biomater* 4, 490-503.
- Kruger, E.A., Im, D.D., Bischoff, D.S., Pereira, C.T., Huang, W., Rudkin, G.H., Yamaguchi, D.T., Miller, T.A., 2011. In vitro mineralization of human mesenchymal stem cells on three-dimensional type I collagen versus PLGA scaffolds: a comparative analysis. *Plast Reconstr Surg* 127, 2301-2311.
- Lan Levengood, S.K., Polak, S.J., Wheeler, M.B., Maki, A.J., Clark, S.G., Jamison, R.D., Wagoner Johnson, A.J., 2010. Multiscale osteointegration as a new paradigm for the design of calcium phosphate scaffolds for bone regeneration. *Biomaterials* 31, 3552-3563.
- Lee, H.Y., Chae, H.J., Park, S.Y., Kim, J.H., 2016. Porcine placenta hydrolysates enhance osteoblast differentiation through their antioxidant activity and effects on ER stress. *BMC Complement Altern Med* 16, 291.
- Lee, J.C., Pereira, C.T., Ren, X., Huang, W., Weisgerber, D.W., Yamaguchi, D.T., Harley, B.A.C., Miller, T.A., 2015. Optimizing collagen scaffolds for bone engineering: effects of crosslinking and mineral content on structural contraction and osteogenesis. *J Craniofac Surg*

26, 1992-1996.

Matsushita, T., Chan, Y.Y., Kawanami, A., Balmes, G., Landreth, G.E., Murakami, S., 2009. Extracellular signal-regulated kinase 1 (ERK1) and ERK2 play essential roles in osteoblast differentiation and in supporting osteoclastogenesis. *Mol Cell Biol* 29, 5843-5857.

Mônaco, E., Lima, A.S., Bionaz, M., Maki, A., Wilson, S.M., Hurley, W.L., Wheeler, M.B., 2009. Morphological and transcriptomic comparison of adipose and bone marrow derived porcine stem cells. *Open Tiss. Eng. Regen. Med. J* 2.

Mozdzen, L.C., Rodgers, R., Banks, J.M., Bailey, R.C., Harley, B.A.C., 2016. Increasing the strength and bioactivity of collagen scaffolds using customizable arrays of 3D-printed polymer fibers. *Acta Biomater* 15, 25-33.

Mozdzen, L.C., Vucetic, A., Harley, B.A.C., 2017. Modifying the strength and strain concentration profile within collagen scaffolds using customizable arrays of poly-lactic acid fibers. *J Mech Behav Biomed Mater* 66, 28-36.

Murphy, C.M., Haugh, M.G., O'Brien, F.J., 2010. The effect of mean pore size on cell attachment, proliferation and migration in collagen-glycosaminoglycan scaffolds for bone tissue engineering. *Biomaterials* 31, 461-466.

Naderi, H., Matin, M.M., Bahrami, A.R., 2011. Review paper: critical issues in tissue engineering: biomaterials, cell sources, angiogenesis, and drug delivery systems. *J Biomater Appl* 26, 383-417.

Nail, L.N., Zhang, D., Reinhard, J.L., Grunlan, M.A., 2015. Fabrication of a Bioactive, PCL-based "Self-fitting" Shape Memory Polymer Scaffold. *J Vis Exp*, e52981.

Necker, R.L.O.a.L., 2010. *An Introduction to Statistical Methods and Data Analysis*, 7 ed. Cengage Learning.

Nganga, S., Yla-Soininmaki, A., Lassila, L.V., Vallittu, P.K., 2011. Interface shear strength and fracture behaviour of porous glass-fibre-reinforced composite implant and bone model material. *J Mech Behav Biomed Mater* 4, 1797-1804.

Nygaard, A.B., Jorgensen, C.B., Cirera, S., Fredholm, M., 2007. Selection of reference genes for gene expression studies in pig tissues using SYBR green qPCR. *BMC Mol Biol* 8, 67.

O'Brien, F.J., Harley, B.A., Yannas, I.V., Gibson, L.J., 2005. The effect of pore size on cell adhesion in collagen-GAG scaffolds. *Biomaterials* 26, 433-441.

Olde Damink, L.H.H., Dijkstra, P.J., van Luyn, M.J.A., Van Wachem, P.B., Nieuwenhuis, P., Feijen, J., 1996. Cross-linking of dermal sheep collagen using a water soluble carbodiimide. *Biomaterials* 17, 765-773.

Ren, X., Bischoff, D., Weisgerber, D.W., Lewis, M.S., Tu, V., Yamaguchi, D.T., Miller, T.A., Harley, B.A., Lee, J.C., 2015. Osteogenesis on nanoparticulate mineralized collagen scaffolds via autogenous activation of the canonical BMP receptor signaling pathway. *Biomaterials* 50, 107-114.

Ren, X., Tu, V., Bischoff, D., Weisgerber, D.W., Lewis, M.S., Yamaguchi, D.T., Miller, T.A., Harley, B.A., Lee, J.C., 2016a. Nanoparticulate mineralized collagen scaffolds induce in vivo bone regeneration independent of progenitor cell loading or exogenous growth factor stimulation. *Biomaterials* 89, 67-78.

Ren, X., Tu, V., Bischoff, D., Weisgerber, D.W., Lewis, M.S., Yamaguchi, D.T., Miller, T.A., Harley, B.A.C., Lee, J.C., 2016b. Nanoparticulate mineralized collagen scaffolds induce in vivo bone regeneration independent of progenitor cell loading or exogenous growth factor stimulation. *Biomaterials* 89, 67-78.

Ren, X., Weisgerber, D.W., Bischoff, D., Lewis, M.S., Reid, R.R., He, T.-c., Yamaguchi, D.T., Miller, T.A., Harley, B.A.C., Lee, J.C., 2016c. Nanoparticulate mineralized collagen scaffolds

and BMP-9 induce a long term bone cartilage construct in human mesenchymal stem cells. *Advanced healthcare materials* 5, 1821-1830.

Seong, W.-J., Grami, S., Jeong, S.C., Conrad, H.J., Hodges, J.S., 2013. Comparison of push-in versus pull-out tests on bone-implant interfaces of rabbit tibia dental implant healing model. *Clin Implant Dent Relat Res* 15, 460-469.

Sethu, S.N., Namashivayam, S., Devendran, S., Nagarajan, S., Tsai, W.B., Narashiman, S., Ramachandran, M., Ambigapathi, M., 2017. Nanoceramics on osteoblast proliferation and differentiation in bone tissue engineering. *Int J Biol Macromol* 98, 67-74.

Song, B., Estrada, K.D., Lyons, K.M., 2009. Smad signaling in skeletal development and regeneration. *Cytokine Growth Factor Rev* 20, 379-388.

Spicer, P.P., Kretlow, J.D., Young, S., Jansen, J.A., Kasper, F.K., Mikos, A.G., 2012. Evaluation of bone regeneration using the rat critical size calvarial defect. *Nat Protoc* 7, 1918-1929.

Thompson, E.M., Matsiko, A., Farrell, E., Kelly, D.J., O'Brien, F.J., 2015. Recapitulating endochondral ossification: a promising route to in vivo bone regeneration. *J Tissue Eng Regen Med* 9, 889-902.

Thouverey, C., Caverzasio, J., 2015. Focus on the p38 MAPK signaling pathway in bone development and maintenance. *Bonekey Rep* 4, 711.

Tierney, C.M., Jaasma, M.J., O'Brien, F.J., 2008. Osteoblast activity on collagen-GAG scaffolds is affected by collagen and GAG concentrations. *J Biomed Mater Res A*.

Veilleux, N.H., Yannas, I.V., Spector, M., 2004. Effect of passage number and collagen type on the proliferative, biosynthetic, and contractile activity of adult canine articular chondrocytes in type I and II collagen-glycosaminoglycan matrices in vitro. *Tissue Eng* 10, 119-127.

Weisgerber, D.W., Caliarì, S.R., Harley, B.A., 2015a. Mineralized collagen scaffolds induce hMSC osteogenesis and matrix remodeling. *Biomater Sci* 3, 533-542.

Weisgerber, D.W., Caliarì, S.R., Harley, B.A.C., 2015b. Mineralized collagen scaffolds induce hMSC osteogenesis and matrix remodeling. *Biomater Sci* 3, 533-542.

Weisgerber, D.W., Erning, K., Flanagan, C., Hollister, S.J., Harley, B.A.C., 2016a. Evaluation of multi-scale mineralized collagen-polycaprolactone composites for bone tissue engineering. *J Mech Behav Biomed Mater* 61, 318-327.

Weisgerber, D.W., Erning, K., Flanagan, C.L., Hollister, S.J., Harley, B.A., 2016b. Evaluation of multi-scale mineralized collagen-polycaprolactone composites for bone tissue engineering. *J Mech Behav Biomed Mater* 61, 318-327.

Weisgerber, D.W., Kelkhoff, D.O., Caliarì, S.R., Harley, B.A.C., 2013. The impact of discrete compartments of a multi-compartment collagen-GAG scaffold on overall construct biophysical properties. *J Mech Behav Biomed Mater* 28, 26-36.

Weisgerber, D.W., Milner, D.J., Lopez-Lake, H., Rubessa, M., Lotti, S., Polkoff, K., Hortensius, R.A., Flanagan, C.L., Hollister, S.J., Wheeler, M.B., Harley, B.A.C., 2018. A mineralized collagen-polycaprolactone composite promotes healing of a porcine mandibular ramus defect. *Tissue Eng Part A* 24, 943-954.

Wise, J.K., Sena, K., Vranizan, K., Pollock, J.F., Healy, K.E., Hughes, W.F., Sumner, D.R., Viridi, A.S., 2010. Temporal gene expression profiling during rat femoral marrow ablation-induced intramembranous bone regeneration. *PLoS One* 5.

Xing, J., Mei, T., Luo, K., Li, Z., Yang, A., Li, Z., Xie, Z., Zhang, Z., Dong, S., Hou, T., Xu, J., Luo, F., 2017. A nano-scaled and multi-layered recombinant fibronectin/cadherin chimera composite selectively concentrates osteogenesis-related cells and factors to aid bone repair. *Acta Biomater* 53, 470-482.

Yang, Y., Michalczyk, C., Singer, F., Virtanen, S., Boccaccini, A.R., 2015. In vitro study of

polycaprolactone/bioactive glass composite coatings on corrosion and bioactivity of pure Mg. *Applied Surface Science* 355, 832-841.

Zhang, D., George, O.J., Petersen, K.M., Jimenez-Vergara, A.C., Hahn, M.S., Grunlan, M.A., 2014a. A bioactive "self-fitting" shape memory polymer scaffold with potential to treat cranio-maxillo facial bone defects. *Acta Biomater* 10, 4597-4605.

Zhang, D., George, O.J., Petersen, K.M., Jimenez-Vergara, A.C., Hahn, M.S., Grunlan, M.A., 2014b. A bioactive "self-fitting" shape memory polymer scaffold with potential to treat cranio-maxillo facial bone defects. *Acta Biomaterialia* 10, 4597-4605.

Zhou, Q., Ren, X., Bischoff, D., Weisgerber, D.W., Yamaguchi, D.T., Miller, T.A., Harley, B.A.C., Lee, J.C., 2017. Nonmineralized and mineralized collagen scaffolds induce differential osteogenic signaling pathways in human mesenchymal stem cells. *Advanced healthcare materials* 6, 1700641.

## Supplementary Information

### **Shape-fitting collagen-PLA composite promotes osteogenic differentiation of porcine adipose stem cells**

**Marley J. Dewey<sup>1</sup>, Eileen M. Johnson<sup>2</sup>, Daniel W. Weisgerber<sup>1</sup>, Matthew B. Wheeler<sup>2,4</sup>,  
Brendan A.C. Harley<sup>2,3,4</sup>**

<sup>1</sup> Dept. of Materials Science and Engineering

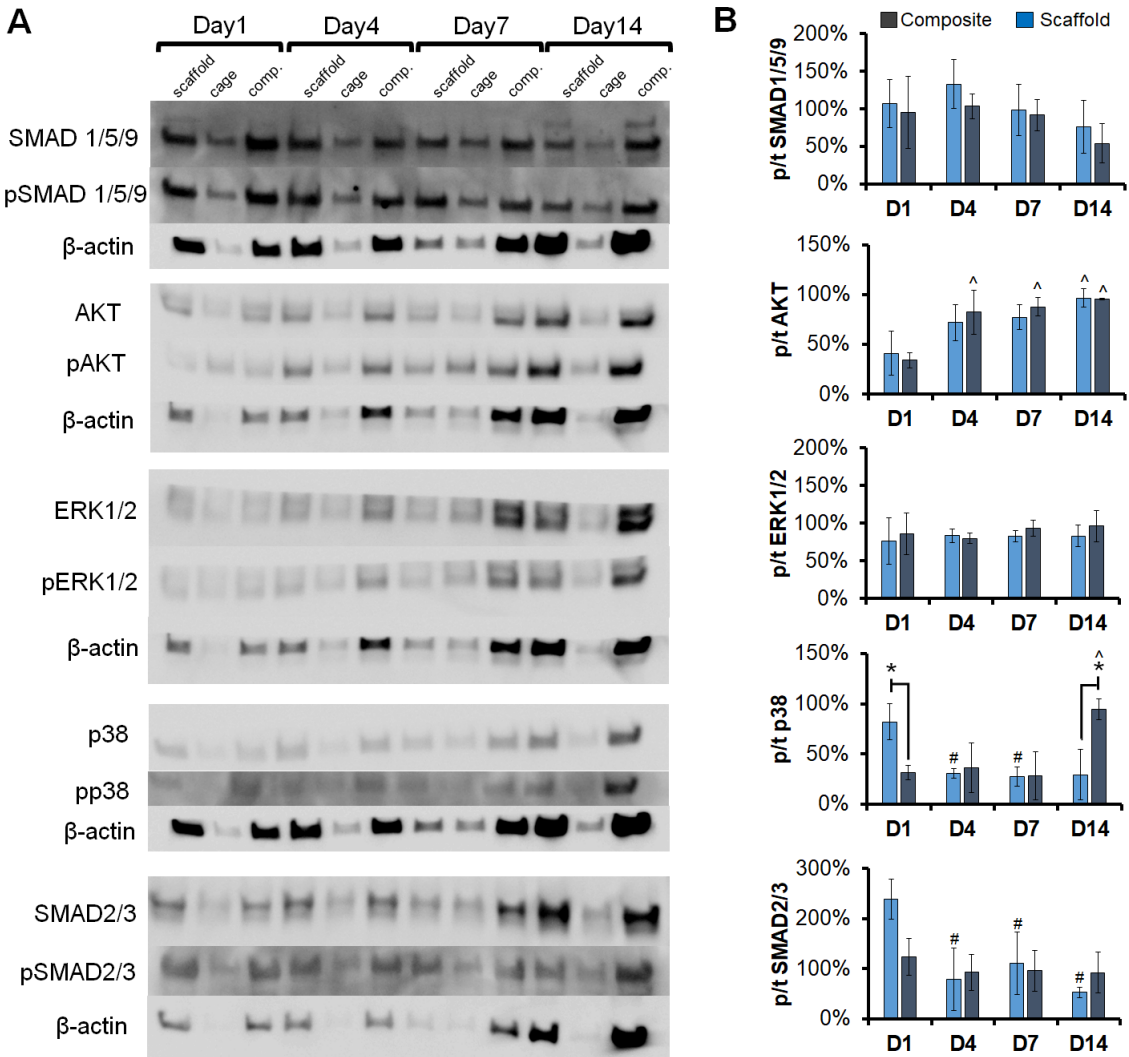
<sup>2</sup> Dept. of Bioengineering

<sup>3</sup> Dept. of Chemical and Biomolecular Engineering

<sup>4</sup> Carl R. Woese Institute for Genomic Biology

University of Illinois at Urbana-Champaign  
Urbana, IL 61801

Supplementary Figures



**Supplemental Figure 1. Levels of phosphorylated to total SMAD1/5/9, AKT, ERK1/2, p38, SMAD2/3. (A)** Representative Western Blots (day 1, 4, 7, 14) with B-actin controls. Mineralized collagen scaffold (*scaffold*), PLA cage alone (*cage*), mineralized-collagen composite (*comp.*). **(B)** Quantitative comparison of phosphorylated to total protein activity. \* indicates significantly ( $p < 0.05$ ) higher activity of one group to another within the same day. ^ indicates significantly ( $p < 0.05$ ) higher activity of one group compared to the same group on day 1. # indicates significantly ( $p < 0.05$ ) lower activity of one group compared to the same group on day 1. Data expressed as mean  $\pm$  standard deviation (n=3).

## Supplemental Tables

**Supplementary Table 1.** Young's modulus under unconfined compression of mineralized collagen scaffold alone, PLA cage alone, and a series of collagen-PLA composites. Data presented as mean  $\pm$  standard deviation (n= 8 samples/group).

Name	E*, MPa
Scaffold	0.95 $\pm$ 0.19
0.7mm straight cage	25.80 $\pm$ 8.46
0.7mm straight composite	22.22 $\pm$ 4.73
0.7mm closed angle composite	2.59 $\pm$ 0.85
0.7mm open angle composite	1.91 $\pm$ 0.83
1mm open angle composite	3.41 $\pm$ 1.33